ACIBADEM MEHMET ALİ AYDINLAR UNIVERSITY
INSTITUTE OF HEALTH SCIENCES

# DETERMINATION OF THE BIOLOGICAL AND FUNCTIONAL PROPERTIES OF MONOCLONAL ANTIBODY IN IgG STRUCTURE DEVELOPED FOR PHARMACEUTICAL USE

ZEYNEP ZÜLFİYE YILDIRIM KELEŞ

Ph.D. THESIS

DEPARTMENT OF MEDICAL BIOTECHNOLOGY

SUPERVISOR
Prof. Dr. Özge Can

ISTANBUL-2023

ACIBADEM MEHMET ALİ AYDINLAR UNIVERSITY
INSTITUTE OF HEALTH SCIENCES

# DETERMINATION OF THE BIOLOGICAL AND FUNCTIONAL PROPERTIES OF MONOCLONAL ANTIBODY IN IgG STRUCTURE DEVELOPED FOR PHARMACEUTICAL USE

ZEYNEP ZÜLFİYE YILDIRIM KELEŞ

Ph.D. THESIS

DEPARTMENT OF MEDICAL BIOTECHNOLOGY

SUPERVISOR
Prof. Dr. Özge Can

ISTANBUL-2023

| | |
|---|---|
| Department: | Medical Biotechnology |
| Program: | Medical Biotechnology Doctoral Program |
| Thesis Title: | Determination of the Biological and Functional Properties of Monoclonal Antibody in IgG Structure Developed for Pharmaceutical Use |
| Student's name and Surname: | Zeynep Zülfiye Yıldırım Keleş |
| Date of Defence: | 20 / 06 / 2023 |

This is to certify that I have examined this copy of Ph.D thesis. I have found that she/he prepared after fulfilling the specified requirements in the associated legislations before the final examining committee, whose signatures are below.

| | |
|---|---|
| Jury Member | Prof. Dr., Tanıl Kocagöz |
| (Head of the Defense) | Acıbadem Mehmet Ali Aydınlar University |
| Jury Member | Prof. Dr., Özge Can |
| (Thesis Supervisor) | Acıbadem Mehmet Ali Aydınlar University |
| Jury Member | Asst. Prof., Dr. Özgül Gök |
| | Acıbadem Mehmet Ali Aydınlar University |
| Jury Member | Prof. Dr., Gizem Dinler Doğanay |
| | İstanbul Technical University |
| Jury Member | Prof. Dr., Demet Cansaran Duman |
| | Ankara University |

## DECLARATION

I declare that this thesis work is my own work, I had no unethical behavior at any stages from the planning to the writing of the thesis, I obtained all the information in this thesis in accordance with academic and ethical rules, I cited all the information and comments that were not obtained with this thesis work, and I provided resources in the list of references. I also declare that there was no violation of any patents and copyrights during the study and writing of this thesis.

Date: 20.06.2023

Zeynep Zülfiye Yıldırım Keleş

## PREFACE AND ACKNOWLEDGEMENT

First and foremost, I would like to thank my supervisor Prof. Dr. Özge Can, for assisting me in bringing this work to life by encouraging, helping, and always guiding me. His immense knowledge and plentiful experience have encouraged me in all the time of my academic research and daily life. It was an honor to be his student. Thank you for everything.

I would like to express my most profound appreciation to Mr. Tunç Turgut for allowing me to proceed as a Ph.D. student and conduct my experiments. I would like to thank Ms. Ayfer Gültekin for her motivation and encouragement of the study. Also, special thanks to Mr. Kaya Turgut for allowing me to develop myself in the biotechnological area. He has given me the basic principle of producing the best quality and accessible medicines.

I would like to thank my colleagues Ahmet Emin Atik, Gülipek Güven, Berna Somuncu, Tuğçe Ertüzün, and all QC Team members who has supported and motivated me during this period.

Special thanks to my best friend, Cansu Akın Levi, for being with me during my undergraduate, graduate, and doctoral studies. I consider myself lucky to have her by my side.

Last but by no means least, I would like to thank my dear mother, Willy van Dijk, and my sister Azize Cahide Yıldırım, who has encouraged me in all of my pursuits, inspired me to follow my dreams and was always there for me. I also thank my father, Cahit Yıldırım. I would also like to thank my wonderful husband, Murat Keleş, who supported me the most during this thesis and encouraged me in every decision. I could not have undertaken this journey without him. I owe every success I have achieved to my family's love and support.

# TABLE OF CONTENTS

**DECLARATION** ..... iii

**PREFACE AND ACKNOWLEDGEMENT** ..... iv

**TABLE OF CONTENTS** ..... v

**LIST OF ABBREVIATIONS AND SYMBOLS** ..... vii

**LIST OF FIGURES** ..... ix

**LIST OF TABLES** ..... xi

**ÖZET** ..... 1

**ABSTRACT** ..... 2

**1 INTRODUCTION AND AIM** ..... 3

**2 BACKGROUND** ..... 5

**2.1 General Concept of Antibodies** ..... 5
**2.2 History of Biopharmaceuticals** ..... 8
**2.3 Definition of Biosimilars** ..... 11
**2.4 Quality Analysis of mAbs** ..... 12
**2.4.1 Physicochemical attributes** ..... 13
**2.4.2 Functional attributes** ..... 14
**2.4.3 Stress studies** ..... 16
**2.4.4 Anti TNFα monoclonal antibody** ..... 18

**3 MATERIALS AND METHODS** ..... 21

**3.1 Materials and Equipment** ..... 21
**3.1.1 Sample descriptions** ..... 21
**3.1.2 Equipment details** ..... 22
**3.2 Methods** ..... 22
**3.2.1 MS/MS analysis** ..... 22
**3.2.2 SPR analysis** ..... 24
**3.2.3 Cell-based assay** ..... 31
**3.2.4 Stress conditions** ..... 33
**3.2.5 Statistical analysis** ..... 33

**4 RESULTS** ..... 34

**4.1 Comparability Study Results** ..... 34
**4.1.1 MS/MS analysis** ..... 34
**4.1.2 SPR analysis** ..... 35
**4.1.3 Cell-based Assay** ..... 50

**4.2 Stress Analysis ..... 56**
**4.2.1 Evaluation of MS/MS data under stress ..... 57**
**4.2.2 Evaluation of SPR data under stress ..... 60**
**4.2.3 Evaluation of Cell-based assay data under stress ..... 65**

**5 DISCUSSION ..... 66**

**6 CONCLUSION ..... 71**

**7 REFERENCES ..... 73**

**8 APPENDIX ..... 79**

**APPENDIX 1: Antigen and Antibody Binding Kinetic Data ..... 79**
**APPENDIX 2: FcγRI and Antibody Binding Kinetic Data ..... 82**
**APPENDIX 3: FcγRIII and Antibody Binding Kinetic Data ..... 84**
**APPENDIX 4: FcRn and Antibody Binding Affinity Data ..... 86**

**9 CURRICULUM VITAE ..... 88**

# LIST OF ABBREVIATIONS AND SYMBOLS

| | |
|---|---|
| **ADCC** | Antibody-Dependent Cellular Cytotoxicity |
| **ADCP** | Antibody-Dependent Cell-Mediated Phagocytosis |
| **ATP** | Adenosine Triphosphate |
| **α** | Alpha |
| **BS** | Biosimilar Sample |
| **CD** | Circular Dichroism |
| **CDC** | Complement-Dependent Cytotoxicity |
| **CDR** | Complementarity-Determining Region |
| **CE-SDS** | Capillary Electrophoresis-Sodium Dodecyl Sulfate |
| **CHMP** | Committee for Medicinal Products for Human Use |
| **CHO** | Chinese Hamster Ovary |
| **CQA** | Critical Quality Attributes |
| **DMSO** | Dimethyl Sulfoxide |
| **DP** | Drug Product |
| **DRS** | Drug Reference Standard |
| **DS** | Drug Substance |
| **EDC** | 1-Ethyl-3-(3-Dimethylaminopropyl)-Carbodiimide |
| **EDTA** | Ethylenediamine Tetraacetic Acid |
| **ELISA** | Enzyme-Linked Immunosorbent Assay |
| **EMA** | European Medicines Agency |
| **Fab** | Fragment Antigen-Binding |
| **Fc** | Fragment Crystallizable Region |
| **FcγR** | Fcγ Receptor |
| **FDA** | US Food and Drug Administration |
| **FT-IR** | Fourier Transformed İnfrared |
| **γ** | Gamma |
| **H** | Heavy Chain |

| | |
|---|---|
| **IBD** | Inflammatory Bowel Disease |
| **ICH** | International Conference of Harmonization |
| **Ig** | Immunoglobulin |
| **IgG** | Immunoglobulin G |
| **kDa** | Kilodalton |
| **L** | Light Chain |
| **LC-MS** | Liquid Chromatography-Tandem Mass Spectrometry |
| **mAb** | Monoclonal Antibody |
| **MoA** | Mechanisms of Action |
| **MTT** | 3-(4,5-Dimethylthiazol-2-Yl)-2,5-Diphenyltetrazolium Bromide |
| **NHS** | N-Hydroxysuccinimide |
| **PD** | Pharmacodynamics |
| **pI** | Isoelectric Point |
| **PK** | Pharmacokinetics |
| **PTM** | Post-Translational Modification |
| **RP** | Reference Product |
| **SEC-HPLC** | Size-Exclusion Chromatography – High-Performance Liquid Chromatography |
| **SPR** | Surface Plasmon Resonance |
| **WHO** | World Health Organization |

# LIST OF FIGURES

Figure 1. Schematic structure of a human IgG antibody ..... 7
Figure 2. Monoclonal antibodies production by hybridoma technology ..... 8
Figure 3. Process of antibody humanization ..... 9
Figure 4. Recombinant DNA technology ..... 9
Figure 5. Stress factors to which a biotherapeutic could be exposed..... 17
Figure 6. Adalimumab Functional Attributes ..... 18
Figure 7. Published Adalimumab Amino Acid Sequence: Light Chain ..... 19
Figure 8. Published Adalimumab Amino Acid Sequence: Heavy Chain ..... 19
Figure 9. The sequence coverage map of the biosimilar..... 34
Figure 10. A-The chemistry behind immobilization of ligands by amine coupling method. B-A typical sensorgram of a ligand immobilization using amine coupling. 35
Figure 11. Protein AG immobilization sensorgram ..... 36
Figure 12. Protein AG immobilization results ..... 36
Figure 13. Anti-His antibody immobilization sensorgram ..... 37
Figure 14. Anti-His antibody immobilization results ..... 37
Figure 15. Assay Design for Protein A/G capture approach..... 38
Figure 16. Antigen-antibody binding sensorgrams..... 39
Figure 17. Antigen-antibody binding sensorgrams with 1:1 binding fit (A: Biosimilar, B: Reference) ..... 40
Figure 18. Relative binding to sTNFα ..... 41
Figure 19. Biotinylated TNFα and antibody binding sensorgrams..... 42
Figure 20. FcγRI and antibody binding sensorgrams ..... 43
Figure 21. FcγRI and antibody binding sensorgrams with 1:1 binding fit (A: Biosimilar, B: Reference)..... 44
Figure 22. Relative binding to FcγRI (%)..... 45
Figure 23. FcγRIIIa and antibody binding sensorgrams ..... 46
Figure 24. FcγRIIIa and antibody binding sensorgrams with a two-state binding model (A: Biosimilar, B: Reference) ..... 47
Figure 25. Relative binding to FcγRIIIa (%) ..... 48

Figure 26. A: Sensorgram of Adalimumab binding to FcRn. B: Affinity graph of adalimumab binding to FcRn ..... 49
Figure 27. Relative binding to FcRn ..... 50
Figure 28. Neutralizing of human TNF-α induced cytotoxicity on L929 cells..... 51
Figure 29. Relative potency results of cytotoxicity on L929 cells..... 52
Figure 30. Neutralizing of human TNF-α induced apoptosis in U937 cells ..... 53
Figure 31. Relative potency results of cytotoxicity on U937 cells ..... 54
Figure 32. Relative potency results of ADCC assay..... 55
Figure 33. EC50 results of ADCC assay..... 56
Figure 34. Comparison of MS/MS spectra for modified and unmodified peptide A: T19 T39 peptide B: T39 peptide ..... 59
Figure 35. Oxidation profiles of Met256 and M493 under increasing H2O2 concentration ..... 60
Figure 36. FcγRIa and oxidative stressed antibody binding sensorgrams for biosimilar ..... 61
Figure 37. FcγRIa and oxidative stressed antibody binding sensorgrams for the reference product..... 61
Figure 38. FcγRIIIa and oxidative stressed antibody binding sensorgrams for biosimilar ..... 63
Figure 39. FcγRIIIa and oxidative stressed antibody binding sensorgrams for the reference product..... 63

# LIST OF TABLES

Table 1. Main functions of immunoglobulins and their structures ..... 6
Table 2. The top five monoclonal antibody drugs in 2018 on the global market ..... 10
Table 3. Solutions for immobilization of ligands by amine coupling..... 25
Table 4. The ligand immobilization method details..... 26
Table 5. Antigen antibody binding method details ..... 27
Table 6. Biotin TNF Capture and binding analysis method details ..... 28
Table 7. FcgRI and FcgRIIIa binding method details..... 29
Table 8. Antibody and antigen incubation details..... 30
Table 9. Stress Conditions ..... 33
Table 10. Antigen and Antibody Binding Kinetic Data..... 42
Table 11. FcγRIa binding with mAb and antigen binding kinetic data ..... 48
Table 12. FcγRIIIa binding with mAb and antigen binding kinetic data..... 49
Table 13. Comparison of Average $EC_{50}$ and relative potency for L929 cell line ..... 51
Table 14. EC50 and Relative Potency Results..... 53
Table 15. ADCC activity results ..... 55
Table 16. ADCC activity results from reporter gene bioassay ..... 56
Table 17. Methionine Oxidation Level for Biosimilar Sample..... 58
Table 18. Methionine Oxidation Level for Reference Product..... 58
Table 19. Oxidation stress results for FcɣRI binding with mAb ..... 62
Table 20. Oxidation stress results for FcɣRIIIa binding with mAb..... 64
Table 21 ADCC activity results from reporter gene bioassay under stress ..... 65

# ÖZET

**Farmasötik Kullanım İçin Geliştirilen IgG Yapısındaki Monoklonal Antikorun Biyolojik ve Fonksiyonel Özelliklerinin Belirlenmesi**

Biyobenzer bir antikor, kalite, biyolojik aktivite, güvenlik ve etkililik açısından halihazırda pazarlama onayı almış bir referans biyolojik ürüne oldukça benzeyen terapötik bir biyoteknolojik üründür. Biyobenzerlerin onaylanması için, referans ürüne benzerliklerini kanıtlamak amacıyla analitik, fonksiyonel ve klinik araştırmaların karşılaştırılmasına yönelik titiz bir süreçten geçmesi gerekir. Karmaşık moleküler yapı ve üretim teknikleri nedeniyle geliştirme sırasında yapı ve işlevde küçük farklılıklar beklenebilir. Fonksiyonel veya klinik aktiviteyi değiştiren herhangi bir yapısal varyasyon olmamalıdır. Fonksiyonel aktivitede biyobenzer ve referans ürünün benzerliklerini göstermek için kapsamlı bir değerlendirme yapılmıştır. Fonksiyonel benzerlik değerlendirmesi, çözünür tümör nekroz faktörü-α (sTNFα) ve Fcgamma reseptörlerine (FcγRIa, FcγRIIIa) ve neonatal Fc reseptörüne (FcRn) bağlanma kinetiklerinin test edilmesini içermiştir. Ayrıca TNFα kaynaklı hücre ölümünün nötralizasyonu, transmembran TNFα'ya nispi bağlanma ve antikora bağlı hücre aracılı sitotoksisite aktivitesi karşılaştırıldı. Oksidatif stres etkileri, peptit haritalama, bağlanma kinetiği ve biyobenzer ve referans ürünler için hücre bazlı tahlil analizi ile araştırıldı. Biyobenzerliği kanıtlamak için gereken verilerin toplamının önemli bir unsuru, fonksiyonel aktivitedeki benzerliktir. Veriler, değerlendirilen fonksiyonel aktiviteler açısından biyobenzerin referans ürüne oldukça benzer olduğunu göstermektedir. Biyobenzer için gösterilen fonksiyonel benzerlik, adalimumabın bilinen etki mekanizmalarını kapsamlı bir şekilde değerlendirerek, biyobenzer ve referans ürünlerin klinik olarak benzer olabileceği sonucunu desteklemektedir.

**Anahtar Sözcükler:** Monoklonal Antikor, Biyobenzer, Fonksiyonel Analiz, Oksidatif Stres, anti-TNF-α.

# ABSTRACT

**Determination of the Biological and Functional Properties of Monoclonal Antibody in IgG Structure Developed for Pharmaceutical Use**

A biosimilar antibody is a therapeutic biotechnological product, highly similar to a reference biological product, which has already been given marketing approval in terms of quality, biological activity, safety, and efficacy. For approval, biosimilars must undergo a rigorous process of comparing analytical, functional, and clinical investigations to prove their resemblance to the reference product. Minor differences in structure and function may be expected during the development due to the complicated molecular structure and production techniques. There shouldn't be any structural variations that alter functional or clinical activity. A thorough evaluation was conducted to demonstrate biosimilar and reference product similarities in functional activity. The functional similarity assessment included testing of binding kinetics to soluble tumor necrosis factor-α (sTNFα) and Fcgamma receptors (FcγRIa, FcγRIIIa) and neonatal Fc receptor (FcRn). Also, the neutralization of TNFα-induced cell death, relative binding to transmembrane TNFa, and antibody-dependent cell-mediated cytotoxicity activity were compared. The oxidative stress effects were investigated with peptide mapping, binding kinetics, and cell-based assay analysis for biosimilar and reference products. A crucial element of the totality of data needed to prove biosimilarity is the similarity in functional activity. The data demonstrate that the biosimilar is highly similar to the reference product for evaluated functional activities. The functional similarity demonstrated for biosimilar comprehensively assesses the known mechanisms of action of adalimumab, supporting the conclusion that biosimilar and reference products are likely to be clinically similar.



**Keywords:** Monoclonal Antibody, Biosimilar, Functional Analysis, Oxidative Stress, anti-TNF-α

# 1 INTRODUCTION AND AIM

Antibodies are considered the most effective components of the human immune system, and many studies have been conducted on the structure and function of them. When we look at the history of antibodies, Muramomab was the first licensed therapeutic monoclonal antibody in 1986. Then Abciximab and Rituximab were licensed in 1994 and 1997, respectively (1).

Nowadays, most top-selling medications are biologics, quickly overtaking other therapies as the dominant group. Since its commercial debut three decades ago, monoclonal antibodies (mAbs) have proven to be the most efficient and secure biological therapeutic class (2). They are used to treat a wide range of disorders. Treatment of severe illnesses such autoimmune, cancer and cardiovascular has been made possible by therapeutic molecules. The increased use of mAbs therapeutically has resulted in a significant increase in costs for healthcare providers (3).

Biotechnological products are distinguished by their physicochemical and biological structures. The industrial manufacture of therapeutic biotechnological products requires considerable effort in both processes and analyses. By the functional analyzes, which are performed in addition to the classical analytical methods, the reliability of the produced molecule is increased. Each biotechnological product requires its own method and process optimization (4,5).

Due to the high commercial value of therapeutic mAbs, the development of biosimilar products has been enabled after the expiration of the patent period. The biosimilar products are being developed with different cell lines and processes and licensed with different regulatory expectations (6).

The quality profiles of biosimilar and original mAbs are highly dependent on process conditions and physicochemical and functional critical quality characteristics. Since the new cell line and process are used for biosimilar mAbs, the similarity of the

products must be demonstrated by comparative analysis in terms of quality, safety, and efficacy (7).

This thesis aims to develop suitable functional analysis methods for antibody binding analysis, such as antigen-antibody binding and FcγR-antibody binding. These methods were used to compare the anti-TNFα antibody biosimilar with the reference product, which is a therapeutic mAb. Surface plasmon resonance (SPR) and cell-based analyzes are used for biological functional analysis. Also, the biosimilar and reference products were compared with these methods under oxidation stress conditions.

# 2 BACKGROUND

## 2.1 General Concept of Antibodies

Antibodies, also known as immunoglobulins (Ig), are utilized in research and industry to bind molecules. They serve two primary functions in nature: bind and eliminate antigens like bacteria or viruses individually and enable communication through attaching to proteins and cell activation by cell-surface receptors (8). Numerous body fluids contain antibodies, including saliva, intestinal contents, urine, tears, and respiratory system secretions (9). The highest concentration and types of antibodies can be found in the blood serum.

The immunoglobulins are structured as a Y-shaped glycoprotein. They have two heavy chains (H) and two light chains (L); disulfide bonds hold them together. The antibodies have different variable regions, the part that binds to the antigens, and the constant areas do not change. Unique antigens are recognized fragment antigen-binding (Fab) at the variable region (10). The variable region domain can be subdivided into a complementarity-determining region (CDR) which binds antigen directly. The antibody is essential in activating the immune system through interaction with cell surface receptors, called fragment crystallizable region (Fc). Depending on the subclasses of an antibody, this region has two heavy chains consisting of two or three constant domains. In the Fc region, *N*-linked glycosylation is critical in the mAb effector function (11).

Immunoglobulins are divided into five major classes based on their amino acid sequences on the heavy chain, namely IgM, IgG, IgA, IgD, and IgE (8,10). The general structure and function details are given below in Table 1.

Table 1. Main functions of immunoglobulins and their structures

| Ig Class | Function | Structure |
|---|---|---|
| **IgA** | Molecular weight: 320,000 Da<br>H-chain type: alpha<br>Percent of total immunoglobulin: 15%<br>Distribution: intravascular and secretions<br>Function: protect mucus membranes from microorganisms | 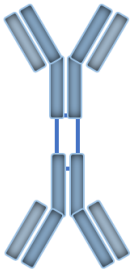 |
| **IgD** | Molecular weight: 180,000 Da<br>H-chain type: delta<br>Serum concentration: 0 to 0.4 mg/mL<br>Percent of total immunoglobulin: 1%<br>Distribution: lymphocyte surface<br>Function: Controls lymphocyte activation or suppression. | 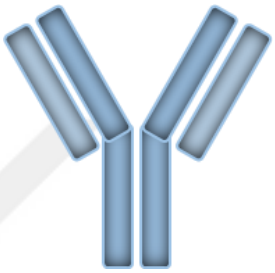 |
| **IgE** | Molecular weight: 200,000 Da<br>H-chain type: epsilon<br>Serum concentration: 10 to 400 ng/mL<br>Percent of total immunoglobulin: 0.002%<br>Distribution: basophils and mast cells in saliva and nasal secretions<br>Function: protect against parasites | 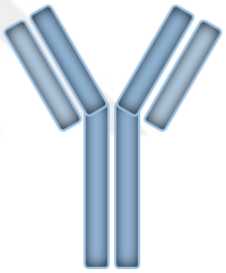 |
| **IgG** | Molecular weight: 150,000 Da<br>H-chain type: gamma<br>Serum concentration: 10 to 16 mg/mL<br>Percent of total immunoglobulin: 75%<br>Distribution: intra- and extravascular<br>Function: secondary response | 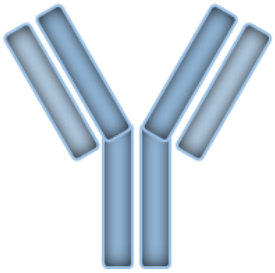 |

Table 1. Main functions of immunoglobulins and their structures (continue)

| Ig Class | Function | Structure |
|---|---|---|
| **IgM** | Molecular weight: 900,000 Da<br>H-chain type: mu<br>Serum concentration: 0.5 to 2 mg/mL<br>Percent of total immunoglobulin: 10%<br>Distribution: mostly intravascular<br>Function: primary response | 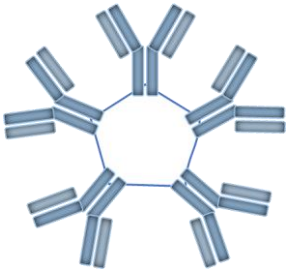 |

Immunoglobulin G (IgG) is the predominant Ig class and enables phagocytosis (monocytes, macrophages, and neutrophils) or antibody-dependent cellular cytotoxicity (ADCC) (monocytes, macrophages, and lymphocytes) or to effect feedback control on antibody synthesis (B and T lymphocytes), it binds to cell surface receptors on many different types of cells (12). It is the only type of Ig that can cross the placenta in humans (12,13). IgG consists of two identical light chains (LC, ~25 kDa each) and two heavy chains (HC, ~50 kDa each), connected by interchain disulfide bonds (10).

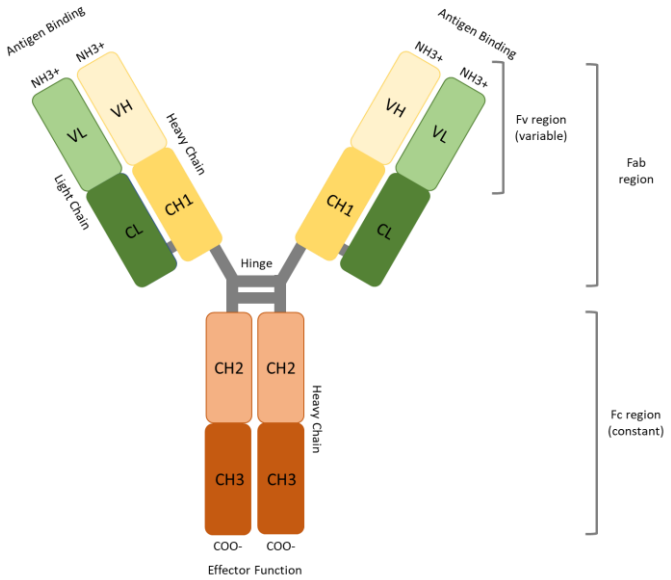


Figure 1. Schematic structure of a human IgG antibody

The general concept of Ig is shown in Figure 1. IgG has four subclasses: IgG1, IgG2, IgG3, and IgG4. These subclasses are associated with the different sizes of the hinge region, position of interchain disulfide bonds, and molecular weight that affect their binding to molecules, receptors, and functionality (14).

## 2.2 History of Biopharmaceuticals

Georges Köhler and Cesar Milstein discovered the modern era of antibody research and discovery in 1975. The first therapeutic mAb was made using the hybridoma technology (15). This technology is very efficient and critical in raising mAbs against antigens of interest. The conventional method for hybridoma technology is immunizing the mouse with the antigen of interest. Spleen cells of the immunized mouse are fused with B-lymphocytes, producing antibodies that bind to the injected antigen and myeloma cells. After a high antibody titer, myeloma cells generate hybridomas to produce mAbs (16,17) (Figure 2). Also, the development of immunotherapy with hybridoma technology allowed for specific targeting of antigens both *in vitro* and *in vivo*.

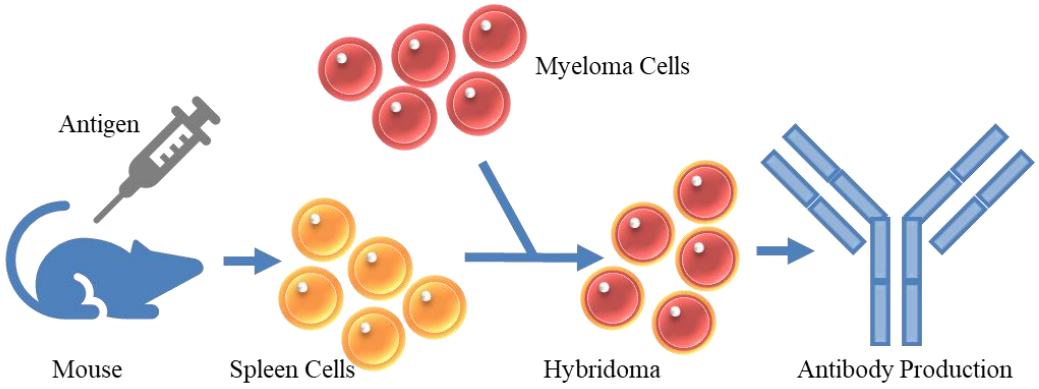


Figure 2. Monoclonal antibodies production by hybridoma technology

Genetic engineering has been used to develop chimeric antibodies, which have human constant domains and mouse variable domains to maintain the specificity and to decrease the immunogenicity against mouse antibodies. Humanized antibodies were created by grafting the CDRs from a mouse antibody onto a human variable and

constant regions (18). Later, fully human antibodies were discovered and produced (19,20) (Figure 3).

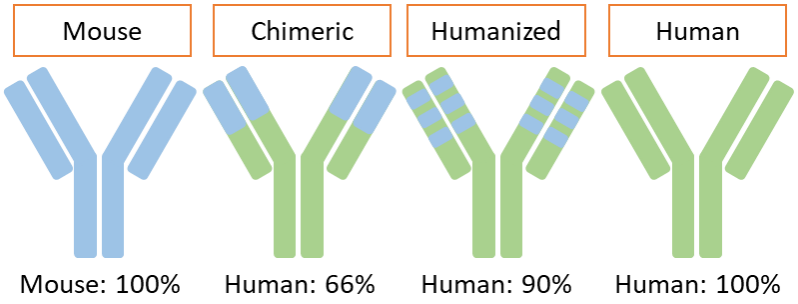


Figure 3. Process of antibody humanization

Recombinant mAbs are executed successfully in vitro using recombinant DNA technology. This technique allows the production of mAbs with high specificity and reproducibility (2) (Figure 4). One of the most commonly used platforms for expressing recombinant monoclonal antibodies is the Chinese hamster ovary (CHO) cell culture. Due to larger densities of viable cells and extended culture viability, the volumetric efficiency of commercial CHO cell cultures has risen significantly in recent decades (21,22).

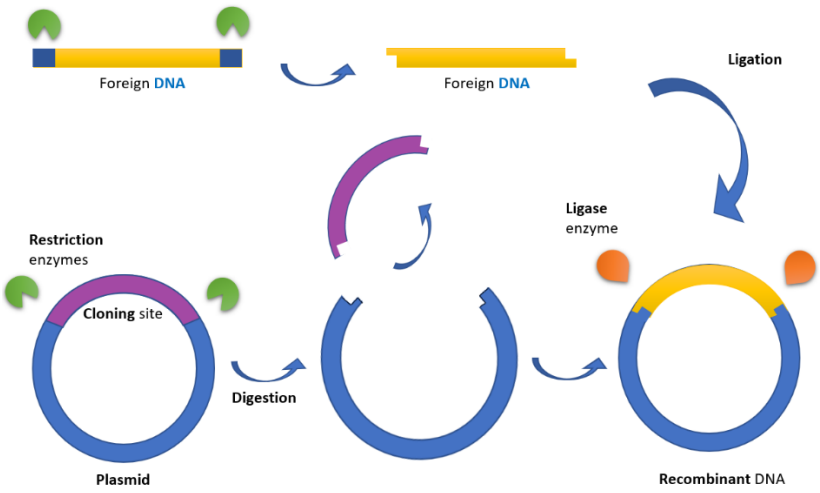


Figure 4. Recombinant DNA technology

The interest in enhancing the drug development process to more quickly and reliably advance antibody lead candidates to the clinic continues to grow. As a result of the increasing number of approved antibody therapeutics, including those that have revolutionized the treatment of human disorders ranging from cancer to autoimmune and infectious diseases (3). Characterization is essential to evaluate the properties of antibodies during early antibody discovery and development stages. With this fact in mind, it is possible to eliminate candidates with poor stability, specificity, solubility, aggregation, viscosity, pharmacokinetics, and immunogenicity features (4,5,23). In particular, developing innovative methods to analyze critical molecular properties at the antibody discovery and process development stage is critical.

The global therapeutic mAbs market is increasing with the development of new mAbs and supporting the growth in this market. The first FDA-approved therapeutic mAb, muromonab, was released in 1986 (3). According to Monoclonal Antibodies Global Market Report, the global mAb therapeutics market has estimated to be US $ 188.18 billion in 2022. The growth rate of the global biopharmaceutical mAbs market is 11.5%, with an estimated value of US$ 292.22 billion in 2026. This growth rate is also covered by the recovery of the trajectory of COVID-19 (24). The top five mAb-drug based in the global market is shown in Table 2 (1).

Table 2. The top five monoclonal antibody drugs in 2018 on the global market

| **Name** | **Trade Name** | **Drug Class & Indication** |
|---|---|---|
| Humira | Adalimumab | TNF Inhibitor<br>Rheumatoid arthritis |
| Opdivo | Nivolumab | Anti PD-1<br>Melanoma |
| Keytruda | Pembrolizumab | Anti PD-1<br>Melanoma |
| Herceptin | Trastuzumab | Anti HER2<br>Breast cancer |
| Avastin | Bevacizumab | VEGF Inhibitor<br>Colorectal cancer |

## 2.3 Definition of Biosimilars

A biosimilar antibody is a therapeutic biotechnological product highly similar to a reference biological product, also known as an originator or innovator product, which has already been given marketing approval. While often made by a different company, biosimilars are intended to have the same clinical efficacy and safety profile as reference medicine. With the introduction of biosimilar products to the market, it is predicted that the quality and prices of these products will shape the market (3,6). Because they can give comparable therapeutic advantages to the reference product at a lower cost, biosimilars are created to offer more inexpensive options for patients and healthcare systems. The appearance of biosimilars on the market has resulted in affordable biological treatments for patients and thus increased access to otherwise expensive therapies (6).

Generic medications, produced chemically and with the same active components as their reference medicines, are distinct from biosimilars. Contrarily, biosimilars are enormous, complex molecules made from living cells that may change slightly from the reference product regarding their molecular structure. Despite these variations, biosimilars must undergo a rigorous process of comparing analytical, functional, and clinical investigations to prove their resemblance to the reference product (25).

In biosimilar development processes, the companies are expected to produce, formulate, and administer the same approved originator reference without access to proprietary manufacturing information. A high degree of similarity between the biosimilar and the reference product must be established during the development stages. According to the comparability analysis, shorter clinical studies are targeted for biosimilars compared to new therapeutic antibodies (7,26,27). The proposed biosimilar must be equivalent to the original reference regarding its structure, function, animal toxicity, human pharmacokinetics (PK), human pharmacodynamics (PD), clinical safety, immunogenicity, and effectiveness. The biosimilars are utilized in the same manner as the reference product and frequently have identical indications authorized for them (26,27).

Several therapeutic fields, including oncology, rheumatology, gastroenterology, and dermatology, have already authorized biosimilars (3,6,24). The primary worldwide organizations that oversee the use and sales of pharmaceuticals are the US Food and Drug Administration (FDA), the European Medicines Agency (EMA), and the Committee for Medicinal Products for Human Use (CHMP). Regulatory worldwide also accept World Health Organization (WHO) and International Conference of Harmonization (ICH) rules. These organizations have issued technical guidelines for the research, development, and evaluation of biosimilars to meet the fast development of biosimilars (6,7,26,28).

### 2.4 Quality Analysis of mAbs

In the production of a biopharmaceutical mAb, the activity, immunogenicity, and efficacy are controlled within predefined analytical specifications. Developing and evaluating biosimilars aims to ensure that a proposed biosimilar candidate and its reference product have comparable quality attributes before the clinical studies (7).

Critical quality attributes (CQA) are an essential first step in developing biopharmaceuticals. It includes physical, chemical, biological, and microbiological properties to ensure the desired quality. The biosimilar should be within the CQA limit range. For this reason, biosimilar candidates go through many physicochemical, microbiological, and functional analyses and clinical trials. The goal is always to improve the safety and efficacy of the biopharmaceutical mAbs (29).

Glycoforms, charge, cysteine-related, oxidized, size, and low-level point-mutation variations are some of the heterogeneous isoforms of mAbs. A considerable number of quality attributes, some CQAs may be produced by the complexity of the mAbs (30,31). The most crucial similarity is that the reference product's amino acid sequence should be identical to the biosimilar product. The post-translational modifications (PTM), which may have distinct profiles, must be in the reference product's quality range. These PTMs include terminal amino acid variants, charge variants, oligosaccharide profiles, etc.(5,26,32).

### 2.4.1 Physicochemical attributes

Physicochemical analysis is focused on the molecular structure of mAbs like, size, aggregation, heterogeneity, and glycosylation. To analyze the structure of mAbs, there are many methods for physicochemical methods. State-of-the-art analytical instruments can monitor protein quality from various perspectives (29,31).

The primary structure analyses use electrospray ionisation-mass spectrometry (ESI-MS) and liquid chromatography-mass spectrometry (LC-MS) methods. These methods utilizes the molecular mass and molecular heterogeneity of the intact mAb. For peptide mapping, the LC-MS approach is used. Peptide mapping is also an important technique that provides primary sequence information of the mAbs and the identification as well as quantitation of PTMs like glycosylation, deamidation, N-/C-terminal modifications, and oxidation after enzymatic digestion (33,34).

Size exclusion chromatography (SEC) and capillary electrophoresis-sodium dodecyl sulfate (CE-SDS) are the most commonly used methods in the literature and industry for monitoring and quantifying product-related impurity levels. These tests are used during drug release analysis and stability studies to analyze aggregation and fragmentation of mAbs (34,35). High molecular weight (HMW) species (HMW) like aggregates can be determined using SEC. However, CE-SDS can measure low molecular weight (LMW) species like fragments, more accurately under denaturing conditions (35,36). Another product-related impurity could be defined as the charge variants. Cation exchange chromatography (CEX) or capillary isoelectric focusing (cIEF) methods can be used to analyze these charge variants (37).

Circular dichroism (CD) and Fourier-transformed infrared (FT-IR) methods monitor the secondary structure. The percentage of α-helix and β-sheet can be determined with these two methods. The main aim of the CD analysis is to determine whether the mAb is folded or not. FT-IR is used to obtain information about the vibrational states of atoms in mAbs (38).

In the higher-order structure, HDX-MS (hydrogen deuterium exchange mass spectrometry) and IM-MS (ion mobility mass spectrometry) methods are used. Specially, HDX-MS is used for obtaining information on mAb-mAb or mAb-ligand interaction sites and allosteric effects (39).

### 2.4.2 Functional attributes

The development of biosimilars depends heavily on functional analysis. It requires a thorough analysis of the degree to which the reference biologic and the biosimilar are similar in efficacy, safety, and mechanism of action (40). The functional analyses are conducted during pre-clinical *in-vitro* studies and before entering clinical trials (41). The following are some essential components of functional analysis in the development of biosimilars (42,43):

1. **Ligand-binding assays:** Ligand-binding assays evaluate the specificity and binding affinity of the target protein or receptor of the antibody. This analysis aims to determine whether biosimilar and reference products interact with the target similarly.

2. **Cell-based assays:** Cell-based assays evaluate the impact of biosimilar and reference product functions on cellular functions. These assays could measure cytokine production, cell proliferation, or other distinct biological reactions related to the biosimilar's mechanism of action.

3. **Receptor-mediated signaling pathway analysis:** Biosimilar and the reference product are evaluated to ensure the similarity of the activation or inhibition of the relevant signaling pathways. This analysis helps to show that the biosimilar exerts its therapeutic effect in the same ways as the reference product.

A ligand binding assay measures the interaction or binding between the antibody and target protein or receptors. These could be antigen-antibody binding or antibody receptor bindings. The most popular in vitro methods are enzyme-linked

immunosorbent assay (ELISA) and surface plasmon resonance (SPR). With the ELISA technique, two primary forms can be used to evaluate the binding ability. The first one is the classical direct and sandwich ELISA where the binding of two molecules is measured with a labeled ligand. The other one is competitive ELISA, where the target protein competes with a labeled protein. In such an ELISA assay, the fluorescent or radioactive tag is typically used with single or various concentrations of a labeled ligand. With the SPR technique, the real-time interaction of antibodies and target proteins can be monitored without any labels. When the ligand binds together, the change in the refractive index can be measured with a particular optical biosensor, and the association and dissociation kinetics can be determined. During the characterization, the binding assay can be utilized in addition to the cell-based assay if the therapeutic antibody's expected mechanism of action involves binding activity to a particular ligand (5,44).

Cell-based assays allow the understanding of the mechanism of action of the antibody. Due to the target molecule variety, many cell lines can be used to evaluate the cellular response. Cell-based assays are commonly used for cytotoxicity testing to determine the antibody's biological activity. Four types of cell-based assays model are founded, namely cell migration assays, cell signaling assays, cell proliferation/inhibition assays, and binding and competitive assays (45). A cell migration assay is used to measure the chemotactic capability of cells. By using antibodies, disease processes such as metastasis, inflammation, and tumor cell migration can be observed (46). Cell signaling assays, also called signaling pathway assays, is helped to understand the reactions of cells with the usage of various internal and external stimulations. Cell proliferation/inhibition assays are a simple approach to quantifying the number of cells that survive antibody treatment. Compounds such as 3-(4,5-dimethylthiazol-2-yl)-2,5-diphenyltetrazolium bromide (MTT) turn into a colored one, quantifying metabolic activity. Another approach is adenosine triphosphate (ATP) to maintain only at high levels in metabolically active cells (47).

Receptor-mediated signaling pathway analysis allows the understanding of the activation or inhibition of the relevant signaling pathways in the presence of the

antibody. Generally, antibody-dependent cell-mediated cytotoxicity (ADCC), complement-dependent cytotoxicity (CDC), and antibody-dependent cell-mediated phagocytosis (ADCP) activity of the antibodies is measured. ADCC is an immune defense mechanism in which an effector cell of the immune system actively lyses a target cell to which an antibody has bound. Several therapeutic monoclonal antibodies have been designed to harness the immune system and mediate ADCC, CDC, or ADCP as a clinical mechanism of action. To measure the biological activity of these molecules, *in vitro* assays are required (5). As part of the humoral response, ADCC and ADCP activity plays a pivotal role in preventing infections and disease by destroying virus-infected or diseased cells. Different immune system cells (leukocytes) can mediate ADCC as effector cells; these include Natural Killer (NK) cells, monocytes, macrophages, neutrophils, and eosinophils cells (48,49). Cell death can be induced by activation of Fcγ receptors (FcγR) in ADCC and ADCP (50). CDC activity is initiated by the C1q protein binding to the Fc part of an antibody bound to the target cell. This activates the complement cascade, and the target cell gets attacked with the membrane attack complex, which lysis the cell (51). FcγR activation and C1q binding are Fc mediate mechanisms of action.

### 2.4.3 Stress studies

The long-term stability for mAb is critical for the usage of mAb-drug based. Long-term stability behavior with stress conditions helped to determine the shelf-life of a mAb drug. Antibody is exposed to many stress conditions that can result in physical and chemical modifications. These modifications may affect the safety and quality of the mAb-drug based. For example, chemical changes in amino acid residues might disrupt chemical and physical stability due to changes in the overall protein structure. Stress conditions are given in Figure 5 (52);

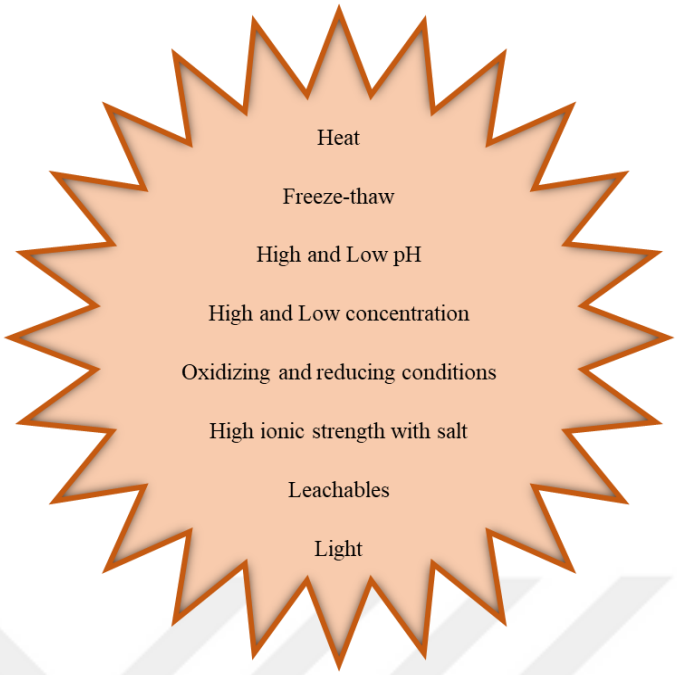


Figure 5. Stress factors to which a biotherapeutic could be exposed

Antibodies come into contact with oxidizing elements such as free radicals, dissolved oxygen, and atmospheric oxygen during manufacturing and storage. The most oxidative amino acid is methionine (Met), and the major byproduct of its oxidation with oxidizing agents like hydrogen peroxide is methionine sulfoxide (53,54). Methionine (Met), tryptophan (Trp), and tyrosine (Tyr) residues may also been oxidized during manufacturing processes such as production, purification, formulation, and storage procedures (55,56). The place where the oxidation occurs dramatically affects how it turns out and might cause conformational changes that result in the development of soluble and insoluble aggregates (55). Antibody binding to Fc receptors and antigens, mAb stability, and half-life of the mAbs in the body are all impacted by oxidation on the CDR. The immunogenicity of Met residues can also rise as a result of oxidation (54,56). For this reason, monitoring oxidation is essential for antibody quality control assays.

### 2.4.4 Anti TNFα monoclonal antibody

Adalimumab is a completely human monoclonal antibody against TNFα and belongs to the immunoglobulin isotype G subclass 1 (IgG1) family (57). As a host expression system, the CHO cell line is used. This antibody has disulfide linkages within and among chains involving 32 cysteine residues. *N*-linked glycans are present on the Asn301 residue in the Fc region of HCs (58). While L only has 214 amino acids, H has 451 amino acid residues. The functional activities of the Fab and Fc regions in Adalimumab are summarized below in Figure 6 (59).

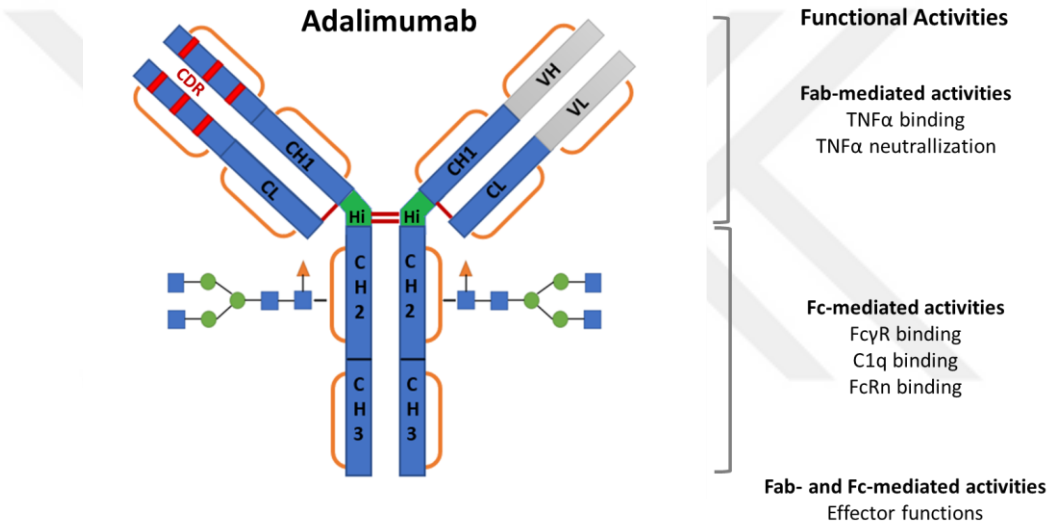


Figure 6. Adalimumab Functional Attributes

The primary amino-acid sequence of the adalimumab molecule subunits is reported in the following figures (Figure 7 and Figure 8).

**Light Chain (LC)**

```
        10          20          30          40          50          60
DIQMTQSPSS LSASVGDRVT ITCRASQGIR NYLAWYQQKP GKAPKLLIYA ASTLQSGVPS

        70          80          90         100         110         120
RFSGSGSGTD FTLTISSLQP EDVATYYCQR YNRAPYTFGQ GTKVEIKRTV AAPSVFIFPP

       130         140         150         160         170         180
SDEQLKSGTA SVVCLLNNFY PREAKVQWKV DNALQSGNSQ ESVTEQDSKD STYSLSSTLT

       190         200         210
LSKADYEKHK VYACEVTHQG LSSPVTKSFN RGEC
```

Figure 7. Published Adalimumab Amino Acid Sequence: Light Chain

**Heavy Chain (HC)**

```
        10          20          30          40          50          60
EVQLVESGGG LVQPGRSLRL SCAASGFTFD DYAMHWVRQA PGKGLEWVSA ITWNSGHIDY

        70          80          90         100         110         120
ADSVEGRFTI SRDNAKNSLY LQMNSLRAED TAVYYCAKVS YLSTASSLDY WGQGTLVTVS

       130         140         150         160         170         180
SASTKGPSVF PLAPSSKSTS GGTAALGCLV KDYFPEPVTV SWNSGALTSG VHTFPAVLQS

       190         200         210         220         230         240
SGLYSLSSVV TVPSSSLGTQ TYICNVNHKP SNTKVDKKVE PKSCDKTHTC PPCPAPELLG

       250         260         270         280         290         300
GPSVFLFPPK PKDTLMISRT PEVTCVVVDV SHEDPEVKFN WYVDGVEVHN AKTKPREEQY

       310         320         330         340         350         360
NSTYRVVSVL TVLHQDWLNG KEYKCKVSNK ALPAPIEKTI SKAKGQPREP QVYTLPPSRD

       370         380         390         400         410         420
ELTKNQVSLT CLVKGFYPSD IAVEWESNGQ PENNYKTTPP VLDSDGSFFL YSKLTVDKSR

       430         440         450
WQQGNVFSCS VMHEALHNHY TQKSLSLSPG K
```

Figure 8. Published Adalimumab Amino Acid Sequence: Heavy Chain

The beginning and persistence of autoimmune disorders may be influenced by dysregulation of TNF activity, which may also mediate harmful consequences. An extra rise in proinflammatory cytokines, enhanced T cell survival, inhibition of regulatory macrophages, endothelial cell dysfunction, and tissue deterioration may result from overexpression of this soluble protein. The TNF-induced pro-inflammatory activities seen in disease states are caused by systemic TNFα overexpression,

particularly in all autoimmune illnesses for which Humira® is authorized. Adalimumab's Fab domain has been demonstrated to bind to TNFα antigens with high specificity and affinity (60–62). Adalimumab has been approved for the following indications; Rheumatoid arthritis, Ankylosing spondylitis, Crohn's disease, Ulcerative colitis, Hidradenitis suppurativa, Juvenile idiopathic arthritis, Plaque psoriasis, Psoriatic arthritis, Uveitis (60). Crohn's disease and ulcerative colitis are also called inflammatory bowel diseases (IBD).

# 3 MATERIALS AND METHODS

This thesis consists of two parts. The first part is the functional comparability study, and the second one is the stress study. In these studies, the samples were analyzed using the same analytical techniques under the same experimental conditions to compare the reference product and developed biosimilar candidate.

## 3.1 Materials and Equipment

### 3.1.1 Sample descriptions

The biosimilar anti-TNF-α mAb was manufactured at Turgut İlaçları A.Ş. (İstanbul, Turkey) from CHO cell culture and purified as a drug substance using affinity chromatography and two more standard chromatographic methods, and a final TFF step. The drug substance was formulated in 6.16 mg/mL NaCI, 0.86 mg/mL monobasic sodium phosphate dihydrate, 1.53 mg/mL dibasic sodium phosphate dihydrate, 0.342 mg/mL sodium citrate dihydrate, 1.30 mg/mL citric acid monohydrate, 12.0 mg/mL mannitol, 1 mg/mL polysorbate 80 and pH 5.2. Aliquoted biosimilar drug substances were stored at ≤-65°C for further use

The biosimilar and reference products are immunoglobulin G (IgG1) monoclonal antibodies expressed in Chinese hamster ovary (CHO) cells by recombinant DNA technology. Both products have the same active substance along with the same target concentration, and the composition of the formulation buffer is also identical. Reference product batches were purchased from the local pharmacy and stored per the manufacturer's instructions. The aliquots obtained from the drug products were not frozen to avoid freeze-thaw stress and were stored at 5±3°C.

In the analysis, three different biosimilar (BS) and five reference products (RP) lots were used during these analyses. All relative data were compared to the drug reference standard (DRS) sample manufactured during small-scale process development.

### 3.1.2 Equipment details

SPR binding experiments were conducted on a Biacore T200 instrument (Cytiva) with Control Software Version 2.0.1 GxP 2.0.1 and Evaluation Software version 3.0 GxP 2.0.2.

LC–MS/MS peptide mapping analysis was implemented on an ultra-performance liquid chromatography (ACQUITY H-Class Bio UPLC) coupled online to a Xevo G2–XS QTOF hybrid mass spectrometer (Waters Corporation). The instrument was equipped with an ESI source operating with $MS^E$ functionality in positive and sensitivity ion modes. MS and MS/MS spectra were acquired in the mass range of *m/z* 50 – 2000 with a scan time of 0.5 sec. System control, data acquisition, and data analysis were made using UNIFI™ software version 1.9.4.

Spectramax i3X multi-mode microplate reader (Molecular Devices) was used as a luminometer for cell-based assay analysis. The system control, data acquisition, and analysis were made using Softmax Pro software version 7.1.1.

## 3.2 Methods

### 3.2.1 MS/MS analysis

100 µg of biosimilar and reference products were denatured in 30 µL of 8M Guanidine-HCl (cat#G9284, Sigma-Aldrich) solution and vortexed well. The reduction of disulfide bonds was performed with 1 µL of 500 mM DTT (cat#43815, Sigma-Aldrich) for 30 min at 57°C, followed by an alkylation step with 5 µL of 300 mM iodoacetamide (cat#I6125, Sigma-Aldrich) for 30 min at room temperature in darkness. The alkylation reaction was quenched by adding 5 µL of DTT solution. Samples were then buffer exchanged by passage through polyacrylamide desalting columns (cat#89849, Thermo Scientific) into an ammonium bicarbonate buffer (cat#A6141, Sigma-Aldrich), pH 8, for tryptic digestion. To the eluate, 10 µL of *Rapi*Gest™ SF surfactant (cat#186001861, Waters) was added to make a final

concentration of 0.1% to increase the efficiency of the enzyme. Trypsin (cat#V5111, Promega) was added at 1:25 (w/w) (enzyme/protein) and incubated at 37°C for 45 min. The digestion was terminated by lowering the pH by adding 2 µL of 50% Trifluoroacetic Acid (TFA) (cat#1081780050, Sigma-Aldrich). The final solution was centrifuged at 18,000xg for 15 min at 10°C to remove insoluble material, and the supernatant was loaded into autosampler vials for analysis. 45 µL of each sample was injected per analysis. The eluted peptides were then monitored by UV absorbance at 214 nm and identified with MS/MS. An appropriate volume of the initial mobile phase mixture was used for the blank. Carbamidomethyl of cysteine (Cys, C) was considered as a fixed modification during data evaluation. The following modifications were set as variables during the data evaluation.

- Methionine (Met, M) and tryptophan (Trp, W) oxidation
- Asparagine (Asn, N) deamidation
- C-terminal lysine (Lys, K) truncation
- N-terminal pyroglutamic acid (pE) formation

Before analysis, the instrument was calibrated externally with sodium iodide (cat#409286, Sigma-Aldrich) solution (2 µg/µL). Leucine enkephaline solution (cat#186006013, Waters) (*m/z* 556.2766) with a 200 ng/mL concentration was continuously infused at a 10 µL/min flow rate during data acquisition to check mass accuracy. The following ESI settings were used: capillary voltage, 1 kV; cone voltage, 25 V; source temperature, 100 °C; desolvation temperature, 350 °C; sampling cone gas flow, 50 L/h; desolvation gas flow, 800 L/h.

The mobile phases A, B, and C are composed of ultra-pure water, acetonitrile (cat#100029, Merck), and 1.0% trifluoroacetic acid solution, respectively. During the analysis, the autosampler and column temperatures were held at 10°C and 40°C, respectively. The flow rate of the mobile phases was set to 250 µL/min. Tryptic digests were separated with a 90 min run incorporating a 70-minute gradient of 5-60% acetonitrile before introduction into the MS.

Identification of the separated peptides is based on the data acquired in the mass spectrometry, using an accurate mass comparison of the detected ions with the calculated masses of the peptides expected from theoretical tryptic digestion of the target mAb. In addition to the comparison of the accurate masses, MS/MS dimension confirms the peptide sequence. The post-translational modifications (PTMs) on the individual peptide were confirmed by detailed MS/MS spectra analysis.

For Glu-C digestion, the same sample preparation steps were followed as described above (such as denaturation, reduction, and alkylation). Samples were then buffer exchanged by passage through polyacrylamide desalting columns into a histidine monohydrochloride buffer (cat#H5659, Sigma), pH 6 for Glu-C digestions. The Glu-C (cat#V1651, Promega) enzyme was added to a final enzyme-to-substrate ratio of 1:50 (w/w). Digestion proceeded for approximately 18 hours (overnight digestion) at 37°C before being terminated by adding 2 µL of 50% TFA solution. The final solution was centrifuged at 18,000xg for 15 min at 10°C to remove insoluble material, and the supernatant was loaded into autosampler vials for analysis. 45 µL of each sample was injected per analysis. The eluted peptides were then monitored by UV absorbance at 214 nm and identified with MS/MS.

### 3.2.2 SPR analysis

In all SPR analyses, the data were collected at 10 Hz. Sample compartment and analysis temperatures were set to 12°C and 25°C, respectively. All sensorgrams were double-referenced using evaluation software by subtracting data from the reference flow cell and then subtracting a blank cycle where the buffer was injected instead of the protein sample.

A relative binding kinetic value (($KD_{DRS}/KD_{Sample}$) × 100) was calculated using the KD value. In all experiments, the sample set's beginning and end was a DRS sample. The DRS sample relative KD result must be between 80-120%. This parameter was considered as system suitability for SPR analysis. If the analysis had more than 5

samples, one more DRS sample was added in the middle of the sample set. The relative KD results were compared for biosimilar and reference products similarity assessment.

All running buffers were prepared freshly using ultrapure water (Milli-Q) and filtered with 0.2 µm polyethersulfone membrane. HBS-EP+ Buffer (10mM HEPES, 0.15M NaCl, 3mM EDTA, and 0.05% v/v Surfactant P20, pH 7.4) (cat# BR100669, Cytiva), and PBS-P+ (Phosphate buffered saline containing 2% DMSO) (cat#28995084 Cytiva) were used as running buffer.

Series S Sensor Chip CM5 (cat # BR100530, Cytiva) chips and amine coupling kit (cat # BR100050, Cytiva) were used to immobilizing a ligand with the amine coupling method. Reagents for amine coupling available in the amine coupling kit are given below in Table 3.

Table 3. Solutions for immobilization of ligands by amine coupling

| | |
|---|---|
| **EDC** | 0.4 M of 1-ethyl-3-(3-dimethylaminopropyl)-carbodiimide in Milli-Q™ water |
| **NHS** | 0.1 M of N-hydroxysuccinimide in Milli-Q water |
| **Ethanolamine** | 1 M ethanolamine-HCl, pH 8.5 |

EDC and NHS were mixed in a 1:1 ratio (v/v) for surface activation and injected onto the chip surface at a 10 µL/min flow rate for 420 seconds. After surface activation was complete, the ligand was injected. After immobilization, 1 M ethanolamine HCl pH 8.5 was injected onto the sensor surface for 420 seconds at a 5 µL/min flow rate to deactivate excess reactive groups. The difference between the final response unit and the initial buffer baseline determined the total amount of immobilized ligands.

The ligands used for immobilization, the concentration, and the flow rate/time details are given below in Table 4. Reference and test flow cells were immobilized at the same time

Table 4. The ligand immobilization method details

| Ligand | Concentration | Immobilization Buffer | Target Immobilization |
|---|---|---|---|
| Protein A/G | 50 µg/mL | 10mM Sodium acetate pH 4.0 | 1200RU |
| Anti-His Antibody | 30 µg/mL | 10mM Sodium acetate pH 4.5 | 7000RU |

Recombinant Protein A/G (cat#77679, Thermo Scientific) was reconstituted with sterile D-PBS (cat#14190144, Gibco) and glycerol (cat#G5516, Sigma-Aldrich) to 0.5mg/mL and the aliquots were stored at ≤-65°C before immobilization. The anti-his antibody and immobilization buffer were used from His Capture kit (cat# 28995056, Cytiva).

#### 3.2.2.1 Antigen binding analysis

Antigen-antibody binding was analyzed in two different SPR methodologies. First, the antibody was captured with Protein AG, and the antigen binding was sent over to determine the binding kinetics. Second, the antigen was captured on the surface of the chip, and the antibody was sent over to determine the binding kinetics.

##### 3.2.2.1.1 Protein AG capture method

Recombinant human soluble TNFα Protein (cat#210-TA-100/CF, R&D Systems) was reconstituted with sterile D-PBS (cat#14190144, Gibco) to 0.1mg/mL, and the aliquots were stored at ≤-65°C before analysis.

The antibody samples were captured by the Protein AG on the chip surface in the test flow cell. The antibody concentration was adjusted to 2.5 µM with 1x HBS-EP+ to achieve a 50-100 RU capture level. Different TNFα concentrations were prepared in 1x HBS-EP+ running buffer (20 - 2.5 nM). The TNFα dilutions were injected over the antibody-captured surface and reference flow cell. For regeneration, 10 mM glycine-HCl at pH 1.5 was injected. The method details for antigen and antibody are below in Table 5.Table 5. Antigen antibody binding method details

Table 5. Antigen antibody binding method details

| | | |
|---|---|---|
| **Capture** | Capture Solution | Antibody |
| | Contact Time | 5 s |
| | Flow rate | 30 µL/min |
| | Flow Path | Test flow cell |
| **Sample** | Antigen concentration | 20 nM<br>10 nM<br>5 nM<br>2.5 nM |
| | Contact Time | 300s |
| | Flow rate | 50 µL/min |
| | Dissociation time | 2400s |
| | Flow Path | Both |
| **Regeneration** | Regeneration Solution | Glycine-HCl pH 1.5 |
| | Contact Time | 80s |
| | Flow rate | 30 µL/min |
| | Flow Path | Both |

#### 3.2.2.1.2 Biotin TNF capture method

The Biotin CAPture Kit (cat# 28920234, Cytiva), including Sensor Chip CAP, Biotin CAPture reagent, and regeneration solutions, were used for biotin TNF capture analysis. PBS-P+ Buffer 10x (0.2M phosphate buffer with 27 mM KCl, 1.37 M NaCl, and 0.5% Surfactant P20 (Tween 20) were from Cytivia. Biotinylated TNFα (Cat# TNA-H82E3, Acro) were solubilized and aliquoted to a concentration of 0.250 mg/mL with sterile water according to the manufacturer's instructions and stored at ≤-65°C.

Reversible biotin capture was used to bind the antibody and the receptor to this compound to set up the same binding type. Upon injection of the biotin capture reagent, biotinylated TNFα (1µg/mL) was captured on the surface of the sensor chip. Different antibody concentrations were prepared and analyzed in the single-cycle kinetic method. The analysis method details are given below in Table 6.

Table 6. Biotin TNF Capture and binding analysis method details

| Cycle Steps | Chemical | Contact Time (s) | Dissociation Time (s) | Flow rate (µL/min) |
|---|---|---|---|---|
| 1. Capture | Biotin CAP Reagent | 120 | - | 2 |
| 2. Capture | Biotinylated TNF-α | 60 | - | 2 |
| Sample | IgG | 90 | 900 | 30 |
| Regeneration | Regeneration solution 1&2 | 120 | - | 30 |
| Extra Regeneration | %30 Acetonitrile 0.25 M NaOH | 30 | - | 30 |

### 3.2.2.2 Fc gamma receptors and antibodies binding analysis

Anti-His Antibody immobilized CM5 chips were used in this assay. FcγRI (CD64 Human Recombinant Protein with His-tag (cat# 10256-H08H, Sino Biologicals) and FcγRIIIa (CD16a Human Recombinant Protein with His-tag (158 Val) (Cat# 10389-H08H, Sino Biologicals) were solubilized and aliquoted to a concentration of 0.250 mg/mL with sterile water according to the manufacturer's instructions and stored at ≤-65°C.

His-tagged FcγRI was captured by the anti-histidine antibody on the chip surface in the test flow cell. The concentration of FcγRI was adjusted to 1 µg/mL to achieve a capture level of around 50-100 RU. Different antibody concentrations were prepared in PBS-P+ running buffer. The antibody samples were injected over the Fc gamma receptor captured surface and reference flow cell. For regeneration, 10 mM glycine-HCl at pH 1.5 was injected.

His-tagged FcγRIIIa was captured by the anti-histidine antibody on the chip surface in the test flow cell. The concentration of FcγRIIIa was adjusted to 0.5 µg/mL to achieve a capture level of around 10-30 RU. After His-tag FcγRIIIa capture step, a stabilization period of 600 seconds was performed to stabilize the baseline response unit. Different antibody concentrations were prepared in PBS-P+ running buffer. The antibody samples were injected over the Fc gamma receptor captured surface and

reference flow cell. For regeneration, 10 mM glycine-HCl at pH 1.5. The method details for FcγRI and FcγRIII are given below in Table 7.

Table 7. FcgRI and FcgRIIIa binding method details

| | | | |
|---|---|---|---|
| **Capture** | Capture Solution | His-tag FcγRI | His-tag FcγRIIIa |
| | Contact Time | 45 s | 30 s |
| | Flow rate | 5 µl/min | |
| | Flow Path | Second | |
| **Sample** | Sample concentration | 128 nM<br>32 nM<br>8 nM<br>2 nM | 2000 nM<br>500 nM<br>125 nM<br>31.5 nM |
| | Contact Time | 60s | |
| | Flow rate | 30 µL/min | |
| | Dissociation time | 600s | |
| | Flow Path | Both | |
| **Regeneration** | Regeneration Solution | Glycine-HCl pH 1.5 | |
| | Contact Time | 30s | |
| | Flow rate | 30 µL/min | |
| | Flow Path | Both | |

The binding kinetics, $k_{on}$ (1/Ms), $k_{off}$ (1/s), and KD (M), were calculated from global fittings using a 1:1 kinetics binding model on the evaluation software. The KD value was calculated from the two-state binding model on the evaluation software regarding two different off-rate appearances.

To understand the effect of the antigen in FcγR binding the antibody was first incubated with Recombinant Human TNF-α Protein (cat#210-TA-100/CF, R&D Systems) at different conditions. The conditions are given below in Table 8. After incubation of antigen and mAb, the Anti-His Antibody immobilized CM5 chips were used in this assay, and the same method for FcγR was followed for analysis. In sample preparation, the antibody was diluted in PBS-P+ according to the antibody concentration, and the antigen concentration was not included.

Table 8. Antibody and antigen incubation details

| | Antibody Concentration | TNFα Concentration | Temperature | Time |
|---|---|---|---|---|
| FcγRI | 256 nM<br>64 nM<br>16 nM<br>4 nM | 256 nM<br>64 nM<br>16 nM<br>4 nM | 25°C | 1 hour |
| | | | 37°C | 1 hour |
| FcγRIIIa | 4000 nM<br>1000 nM<br>250 nM<br>62.5 nM | 4000 nM<br>1000 nM<br>250 nM<br>62.5 nM | 25°C | 1 hour |
| | | | 37°C | 1 hour |

### 3.2.2.3 FcRn binding analysis

The KD value for adalimumab binding to FcRn was determined using surface plasmon resonance (SPR) in a single-cycle assay format. The Biotin CAPture Kit (cat# 28920234, Cytiva), including Sensor Chip CAP, Biotin CAPture reagent, and regeneration solutions, were used for FcRn binding analysis. Sensor Chip CAP is built on a carboxymethylated dextran matrix to which an ss-DNA molecule is pre-immobilized. Biotin CAPture Reagent consists of streptavidin conjugated with the complementary ss-DNA molecule and hybridized to the surface of the sensor chip. The reagent and sensor chip were used according to the manufacturer's instructions, and a running buffer at pH 6.0 was prepared in-house (20 mM phosphate, 150 mM NaCl, 0.05% P20). Recombinant extracellular domains of FcRn expressed with C-terminal biotinylated human cells (cat# ITF01-0400 Immunitrack) were captured only in active flow cell via Biotin CAPture reagent. Next, several concentrations of antibody (2000-24.7nM) were injected consecutively over reference and active flow cells, applying a single cycle kinetics procedure and adding a 300 s dissociation time after the last antibody injection. Data were double referenced by first subtraction of reference flow cell and then subtraction of blank cycles. The binding of FcRn to adalimumab was measured and fitted using a steady-state affinity binding model. A relative binding affinity was calculated by comparing the values obtained for the reference with the sample.

### 3.2.3 Cell-based assay

#### 3.2.3.1 In vitro TNF-neutralizing activity

TNF neutralizing activity of the biosimilar and reference product was compared with cell-based bioactivity assays. In this assay, mouse fibroblast (L929) cells (cat# CCL-1, ATCC) were used for non-apoptotic cell death, and monocytic (U937) cells (cat# CRL-1593.2, ATCC) were used for apoptotic cell death comparison.

L929 cells were cultured with cDMEM (Dulbecco's Modified Eagle Medium) (cat#31053, Invitrogen) in 96-well culture plates for 5h, then stimulated with TNFα (1 µg/mL) (cat#12/154, NIBSC) and actinomycin D (2 µg/mL) in the presence of dose titration of biosimilar reference products following overnight incubation (22-24h). Cytotoxicity was measured using the ATPlite (cat#6016731, Perkin Elmer), which was added to the cells at the end of incubation. Plates were analyzed for luminescence with a luminometer plate reader. The EC50 was calculated for each sample using sigmoidal dose-response-curve-fitting. Percent viability was calculated based on unstimulated cells and cells stimulated in the absence of added test antibodies.

U937 cells were cultured in RPMI 1640 (cat#1187509, Thermo Fisher Scientific) and seeded at 96-well sterile plates. The cells were stimulated with 3 ng/mL of TNFα (cat#12/154, NIBSC). U937 cells and TNF-α in the presence of a dose titration of biosimilar and reference product. The treatment was carried out at 37ºC for approximately 2 hours. After treatment, Caspase-Glo® 3/7 reagent (cat# G8093, Promega) was added to samples, with additional 60 minutes of room temperature incubation. Luminescence for each sample was measured in the plate reading luminometer (Spectramax), and the results were given as relative luminescence units.

#### 3.2.3.2 ADCC activity

ADCC activity of the biosimilar and reference product was compared with PBMC isolated from human blood and reporter gene bioassay.

The assay was designed with Natural Killer (NK) cells isolated from V/F genotype donors. For this, NK cells were purified from PBMC isolated from fresh human blood samples and used as effector cells for measuring the killing of the target cells overexpressing tm-TNFα as an endpoint of this ADCC pathway activation. CHO cells, engineered to express an uncleavable form of TNFα, were used as target cells. The target cells were seeded at $4x10^4$ cells per mL in a 96-well plate and incubated overnight (18-24h). The PMBC was cultured, and the concentration was adjusted to $2.4x10^6$ cells per mL. The biosimilar and reference products were serially diluted in a Complete Growth medium. The PBMC cells and test material were added to the target cell plate and incubated at 37°C overnight (18-24h). After incubation, the number of dead cells was measured using a luminescent cytotoxicity detection assay (Cyto Tox-Glo Assay (cat# G9290, Promega). The reference standard and test material results were plotted using non-linear regression analysis in a 4-parameter logistic model. Maximum induction and relative potency were measured for all biosimilar and reference products. The relative slope, half-maximal inhibitory concentration ($EC_{50}$) and maximal response were also determined. Two assay plates with triplicates of each sample were analyzed.

For reporter gene bioassay, the mTNF-alpha (+) target test (Cat#BM5013, Svar) and ADCC Effector (V) Assay Ready Cells (Cat#BM5001, Svar) were used as they are ready to use. All cells and samples were prepared in RPMI-1640 (Cat#11875093, Thermo Scientific) medium containing 10%FBS (Cat#10270106, Gibco) and 1%Pen-Strep (Cat#15240062, Gibco). The ADCC effect of the adalimumab antibody has been assessed using a mixture of mTNF-alpha (+) Target Test Ready Cells and ADCC Effector (V) Assay Ready Cells in a ratio of 1:4, respectively. The final concentration of the monoclonal antibody samples was diluted three-fold to range from 500 to 0 ng/mL. 40 µL of effector cells: the target cells mixture was added into the 96-well plate containing 40 µL of antibody samples at indicated serial concentrations (500-0.7 ng/mL). All wells were mixed very carefully with a pipette. Then the plate was incubated in a 37°C, 5% $CO_2$ incubator for 4 hours. The cell viability was detected using Dual-Glo Luciferase Assay System (Cat#E2940, Promega) following the manufacturer's protocol via Spectramax i3x equipment.

### 3.2.4 Stress conditions

The oxidation stress was performed by incubating the samples with different Hydrogen peroxide ($H_2O_2$) (cat# 386790, Merck) concentrations. Samples were diluted with $dH_2O$ to 50mg/mL. After this, the samples were incubated with 1:1 hydrogen peroxide at 25°C for 24 hours. The final sample's hydrogen peroxide concentrations were 0.1%, 0.5%, 1.0%, and 3.0%. The pulled samples were buffer exchanged to ammonium bicarbonate prior to MS/MS analysis. For the other analysis, the samples were not buffer exchanged (Table 9).

Table 9. Stress Conditions

| Condition | Temperature | Time Point | Methods |
|---|---|---|---|
| 0.1% $H_2O_2$ | 25°C | 24 hours | MS/MS, SPR, cell-based |
| 0.5% $H_2O_2$ | 25°C | 24 hours | MS/MS |
| 1.0% $H_2O_2$ | 25°C | 24 hours | MS/MS, SPR, cell-based |
| 3.0% $H_2O_2$ | 25°C | 24 hours | MS/MS |

### 3.2.5 Statistical analysis

The similarity of the biosimilar to the reference product was assessed using statistical equivalence. The similarity was achieved for antigen binding analysis and potency assay when the mean relative result was contained within an equivalence acceptance criterion of ±2 times the standard deviation (SD) of reference lots tested. For the secondary mechanism of action, including FcγR binding, FcRn binding, and ADCC results were considered similar when the mean relative result of the biosimilar fell within the quality range; the quality range was defined as the mean of the reference product tested ±3 times SD. For characterization assays like peptide mapping, the similarity was determined by a qualitative comparison of the results.

# 4 RESULTS

The results obtained from the analysis are summarized under two parts: comparability studies and oxidation stress studies.

## 4.1 Comparability Study Results

In the comparability study, lots of the biosimilar (BS) and reference products (RP) were analyzed in parallel. MS analysis has shown that the amino acid sequence is identical, and SPR analysis has shown that the antigen, FcγR, and FcRn binding kinetics are similar. Cell-based has shown that the antigen-neutralizing activity is similar for the biosimilar and reference products, except for ADCC analysis which concluded that the assay variation was too high.

### 4.1.1 MS/MS analysis

Combining two (or more) peptide mapping data sets enhances the probability of attaining high sequence coverage and improves confidence in amino acid sequence confirmation. In this study, the Glu-C enzyme was selected for orthogonal digestion in addition to trypsin. It was characterized as cleaving C-terminal to glutamic acid, with a lower incidence of peptide bond cleavage C-terminal to aspartic acid in the histidine buffer conditions.

Overall, in combination with two enzymes (trypsin and Glu-C), it was sufficient to obtain full sequence coverage for the biosimilar and reference mAb. The regions with blue labeled showed that 100% sequence coverage was achieved Figure 9.

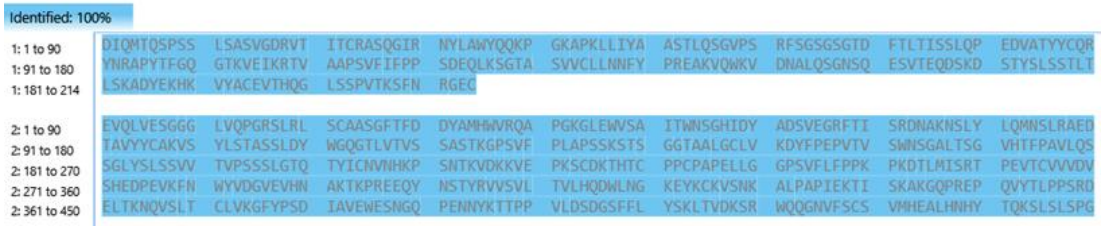


Figure 9. The sequence coverage map of the biosimilar

This has shown that the biosimilar and reference product have the same amino acid sequence.

### 4.1.2 SPR analysis

With the Biacore system, protein-protein interactions can be studied sensitively with the SPR technique. Depending on the purpose of the test to be performed in SPR analysis, the chip to be used, the ligand, and the molecules to be immobilized are selected. The chemistry and typical sensorgram of ligand immobilization by the amine coupling method are given in Figure 10. The target level of immobilization was calculated from the response bound result. The response final result show response unit change after the EDC/NHS, the ligand, and ethanolamine were injected onto the sensor chip.

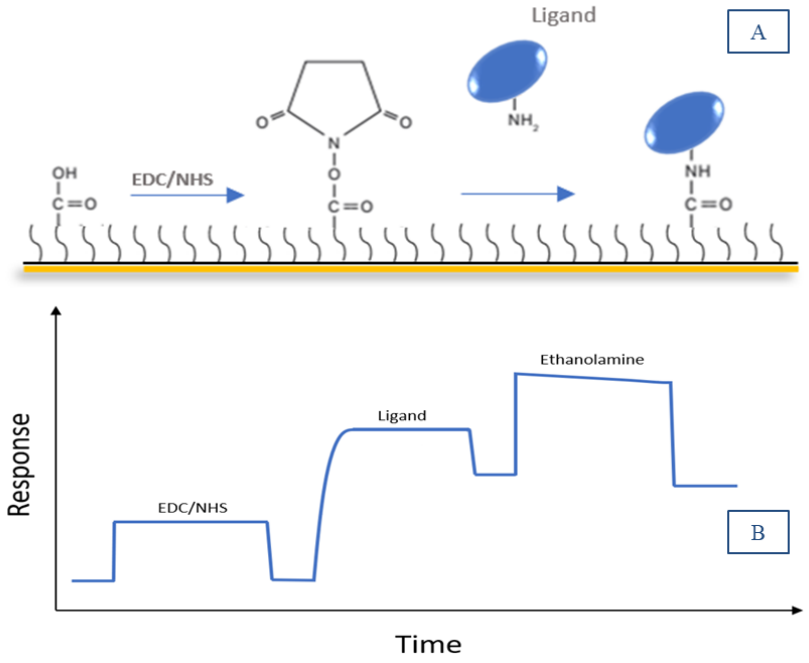


Figure 10. A-The chemistry behind immobilization of ligands by amine coupling method. B-A typical sensorgram of a ligand immobilization using amine coupling.

Series S Sensor Chip CM5 chips and Amine Coupling Kit were used to immobilize Protein AG with the amine coupling method. Recombinant Protein AG was diluted with 10mM sodium acetate pH4.0, giving the best sensor chip interaction.

The immobilization sensorgram and results were given in Figure 11 and Figure 12, respectively. According to the previous experience, a concentration determination step was added before EDC/NHS injection.

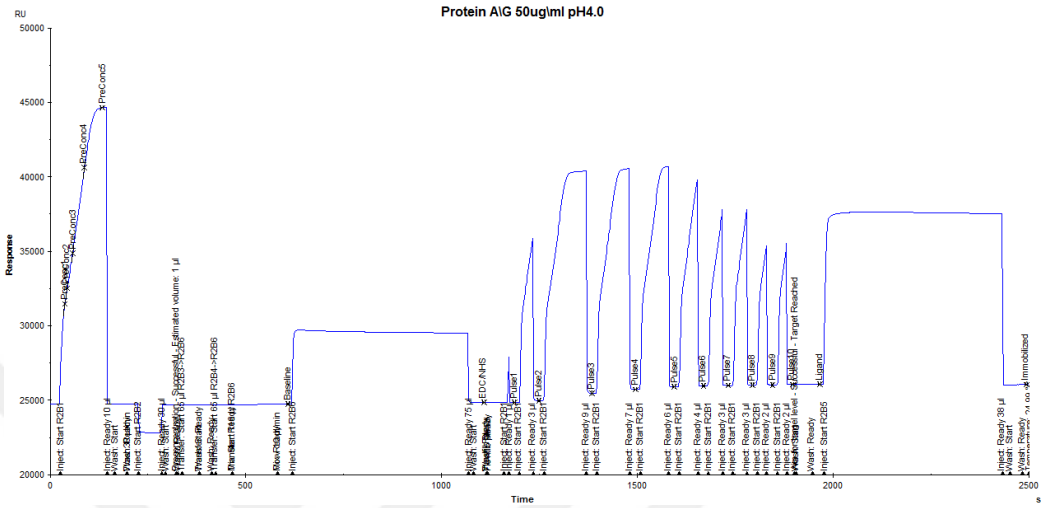


Figure 11. Protein AG immobilization sensorgram

First, the preconcentration determination step injects Protein AG and calculates injection volume according to the given target level. Protein AG immobilization was targeted for 1200RU. After activation of the chip surface with EDC/NHS, many ligand injections were sent to the chip to reach the desired target level. Finally, the chip unbound chip surface was deactivated with ethanolamine, and the final responses were around 1350RU.

**Chip: CM5**
**Flow cells per cycle: 1**

| Flow cell | Procedure | Method | Ligand | Response Bound (RU) | Response Final (RU) | Target Reached |
|---|---|---|---|---|---|---|
| 3 | Target level | Amine Protein AG (Custom) | Protein A\G 50ug\ml pH4.0 | 1203.7 | 1317.2 | Yes |
| 4 | Target level | Amine Protein AG (Custom) | Protein A\G 50ug\ml pH4.0 | 1198.1 | 1377.5 | Yes |

Figure 12. Protein AG immobilization results

Series S Sensor Chip CM5 chips and Amine Coupling Kit were used to immobilizing an anti-His antibody with the amine coupling method. According to the

manufacturer, the recombinant anti-His antibody was diluted with 10 mM sodium acetate pH4.5, which interacts best with the sensor chip. The immobilization sensorgram and results were given in Figure 13 and Figure 14, respectively.

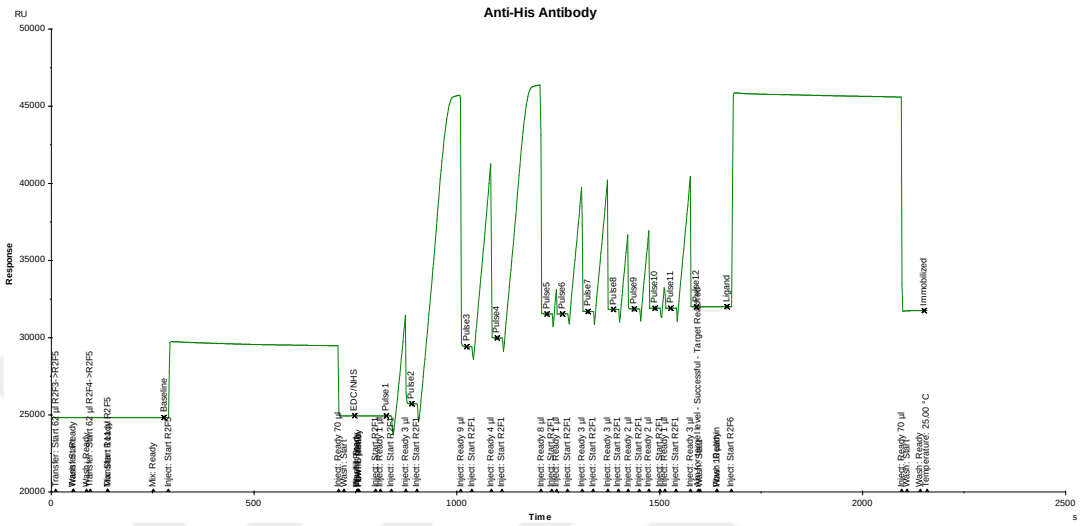


Figure 13. Anti-His antibody immobilization sensorgram

Anti-His antibody immobilization was targeted for 7000RU. After activation of the chip surface with EDC/NHS, many injections of the anti-his antibody were sent to the chip to reach the desired target level. Finally, the unbound chip surface was deactivated with ethanolamine, and the final responses were around 7000RU.

**Chip: CM5**
**Flow cells per cycle: 1**

| Flow cell | Procedure | Method | Ligand | Response Bound (RU) | Response Final (RU) | Target Reached |
|---|---|---|---|---|---|---|
| 1 | Target level | Anti His Antibody (Custom) | Anti-His Antibody | 7139.3 | 7001.8 | Yes |
| 2 | Target level | Anti His Antibody (Custom) | Anti-His Antibody | 7063.2 | 6936.8 | Yes |

Figure 14. Anti-His antibody immobilization results

Adalimumab is highly specific for human TNFα. The primary mechanism of action of adalimumab is to bind to soluble TNFα with high affinity and inhibit its bioactivity. SPR determined the binding kinetics of biosimilar and reference products to soluble human TNFα with a single-cycle kinetics methodology (Figure 15).

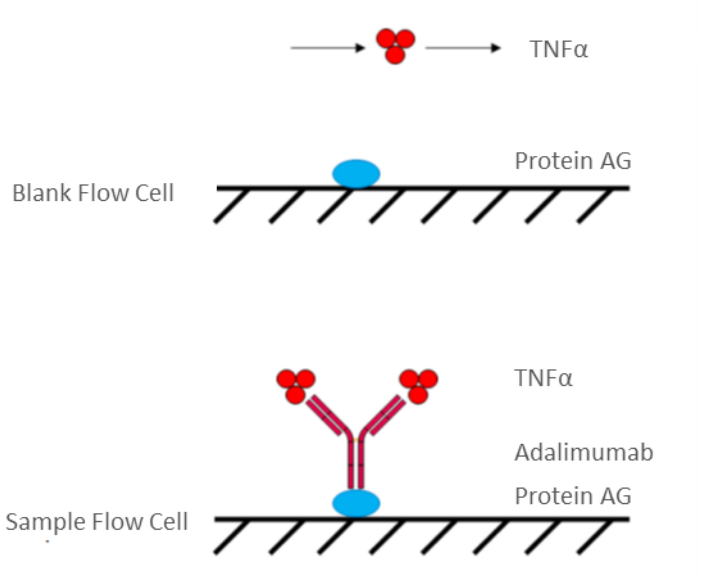


Figure 15. Assay Design for Protein A/G capture approach

IgG-TNFα binding for biosimilar and reference products was measured by several different assay sets. Each experiment set fulfilled the system suitability criteria. Data were double referenced by first subtraction of reference flow cell and then of blank cycles.

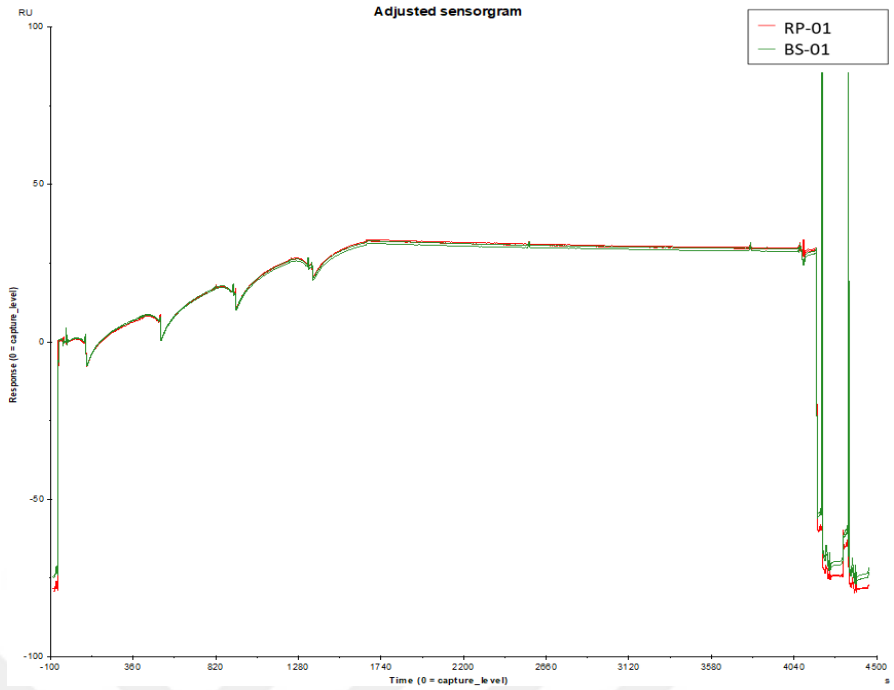


Figure 16. Antigen-antibody binding sensorgrams

The capture level of the antibody on immobilized Protein AG was optimized between 50-100RU, and this parameter was used as system suitability criteria. In the sensorgram given in Figure 16, the x-axis and y-axis were adjusted with the capture level of the antibody. After the capture step, the TNFα was injected into the flow cells. After the regeneration, the sensorgram returns to the values before the capture injections. This shows that the regeneration injection has removed all the molecules but not the Protein AG immobilized on the sensor chip.

From the initial SPR assessments, the KD of the interactions (the equilibrium dissociation constant between mAb and TNFα) was calculated using the 1:1 Binding model (Figure 17).

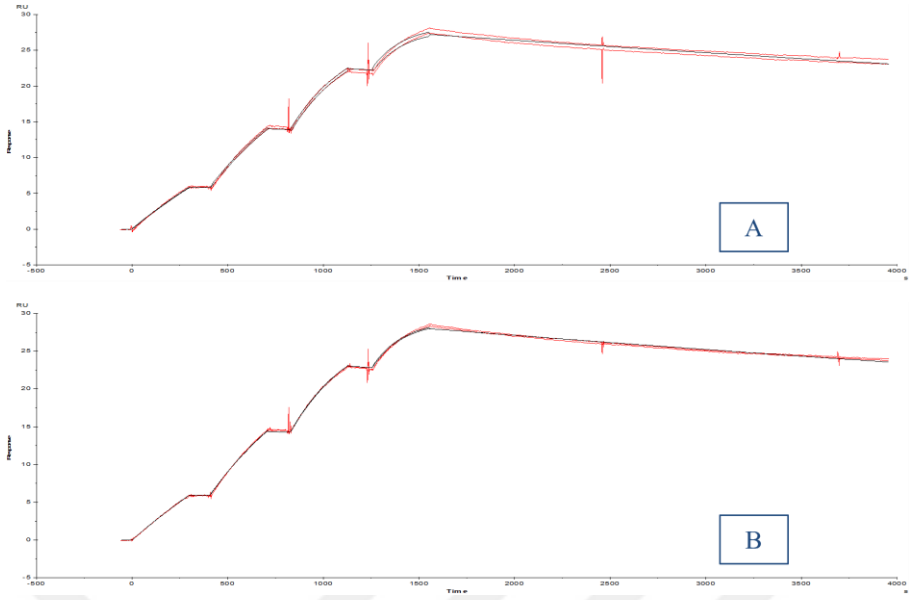


Figure 17. Antigen-antibody binding sensorgrams with 1:1 binding fit (A: Biosimilar, B: Reference)

The biosimilarity was concluded when the ± SD for the difference in means between the biosimilar is contained within an equivalence acceptance criterion (EAC) of ± 2 times the SD of the dataset for the reference product lots tested. The quality range limits were 85.6% to 111.3% relative binding in Figure 18. The biosimilar batches resulted between these quality ranges.

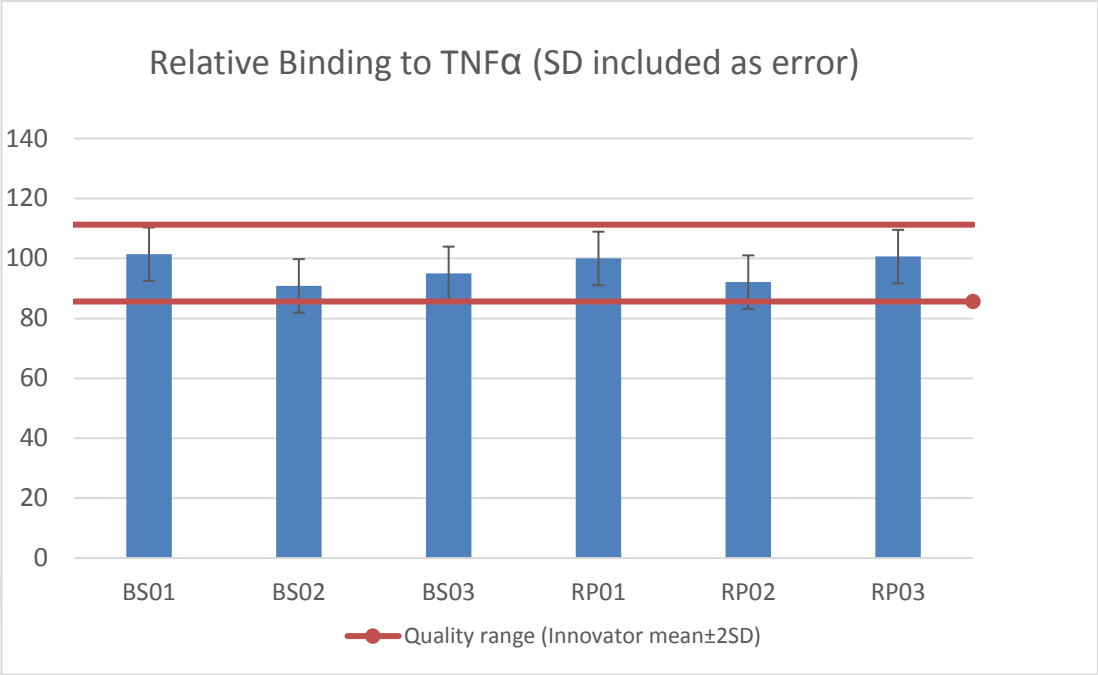


Figure 18. Relative binding to sTNFα

#### 4.1.2.1 Biotin TNF capture analysis

A biotin capture approach was developed to compare the biosimilar and reference products antigen binding kinetics. With analysis, the Protein AG binding was eliminated. In Figure 19, the x-axis and y-axis were adjusted with the capture level of biotinylated TNFα.

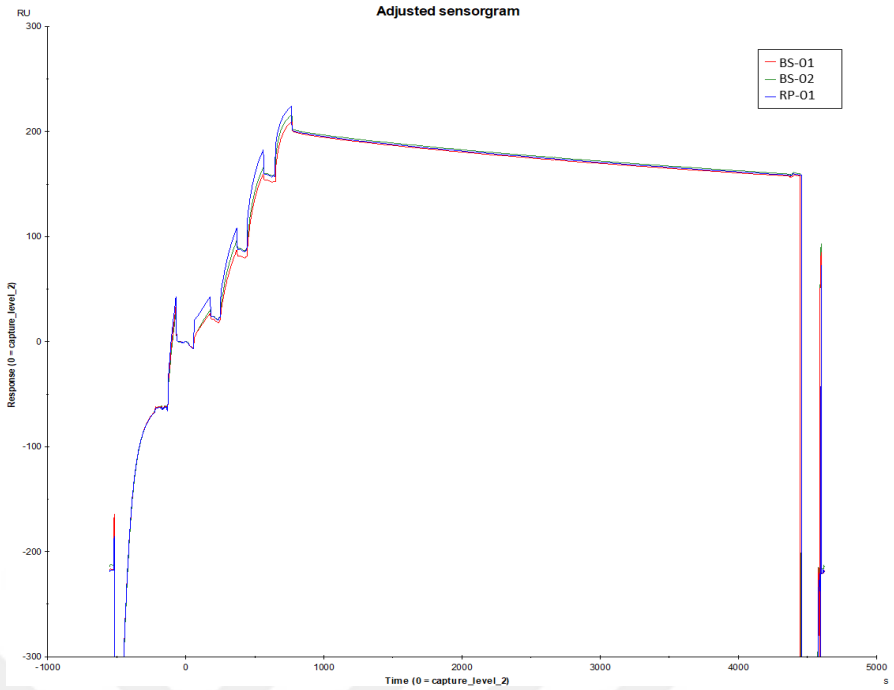


Figure 19. Biotinylated TNFα and antibody binding sensorgrams

From the initial SPR assessments, the KD of the interactions (the equilibrium dissociation constant between mAb and TNFα) was calculated using the 1:1 Binding model. The binding kinetics of the biosimilar and refence product gave similar results (Table 10).

Table 10. Antigen and Antibody Binding Kinetic Data

| Sample ID | ka (1/Ms) | kd (1/s) | KD (M) | Rmax (RU) | U-value |
|---|---|---|---|---|---|
| **BS01** | 1,96E+05 | 6,43E-05 | 3,29E-10 | 193,3 | 2 |
| **BS02** | 2,37E+05 | 6,15E-05 | 2,60E-10 | 195,3 | 2 |
| **RP01** | 2,52E+05 | 6,10E-05 | 2,42E-10 | 196,3 | 2 |

### 4.1.2.2 FcgR binding results

Relative binding to human FcγR was determined by SPR with single-cycle kinetics methodology. Antibody binding to FcγR results in cytokine release, cell activation, apoptosis, and ADCC. All mAb-FcγR interaction experiments were performed using an anti-His antibody immobilized CM5 chip. Recombinant

extracellular domains of FcγR expressed with C-terminal His-tags in human/HEK293 cells were captured in active flow cell only.

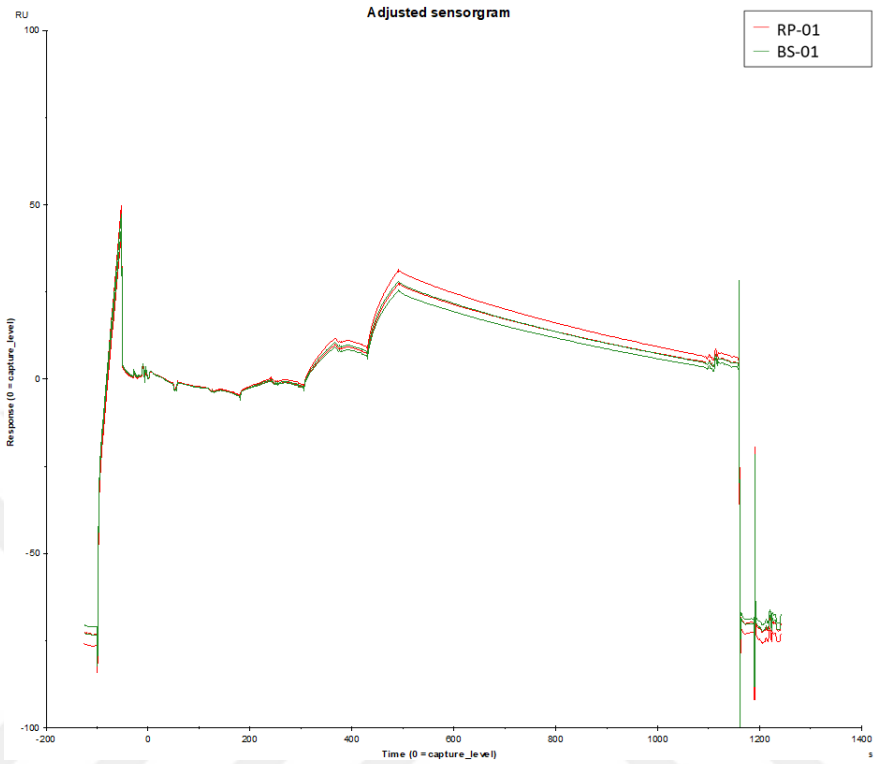


Figure 20. FcγRI and antibody binding sensorgrams

The high-affinity FcγR that binds monomeric IgG is FcγRI. In Figure 20, the x-axis and y-axis were adjusted with the capture level of FcγRI. After the capture step, the antibodies were injected into the flow cells. After the regeneration, the sensorgram returns to the values before the capture injections. This shows that the regeneration injection has removed all the molecules but not the anti-His antibody immobilized on the sensor chip. Data were double-referenced. The KD of the interactions was calculated using the 1:1 Binding Model (Figure 21).

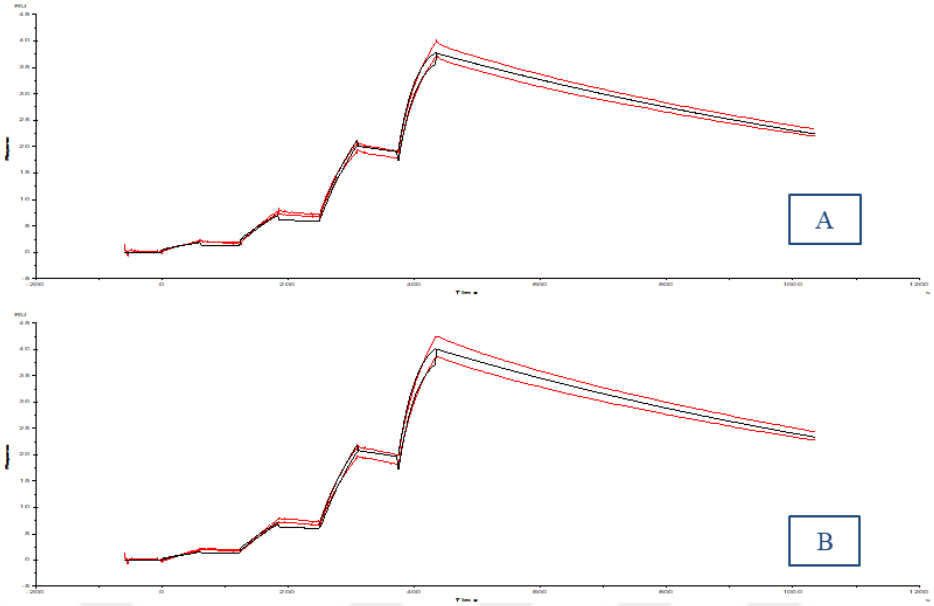


Figure 21. FcγRI and antibody binding sensorgrams with 1:1 binding fit (A: Biosimilar, B: Reference)

The capture level of the FcγRI on immobilized anti-His antibody was optimized between 50-100RU, and this parameter was used as system suitability criteria. The relative KD results were used to compare biosimilar and the reference product.

The biosimilarity was concluded when the ± SD for the difference in means between the biosimilar is contained within an EAC of ± 3 times the SD of the dataset for the reference product lots tested. The quality range limits were 45.9% to 132.4% relative binding, as given in Figure 22. The biosimilar batches resulted between these quality ranges.

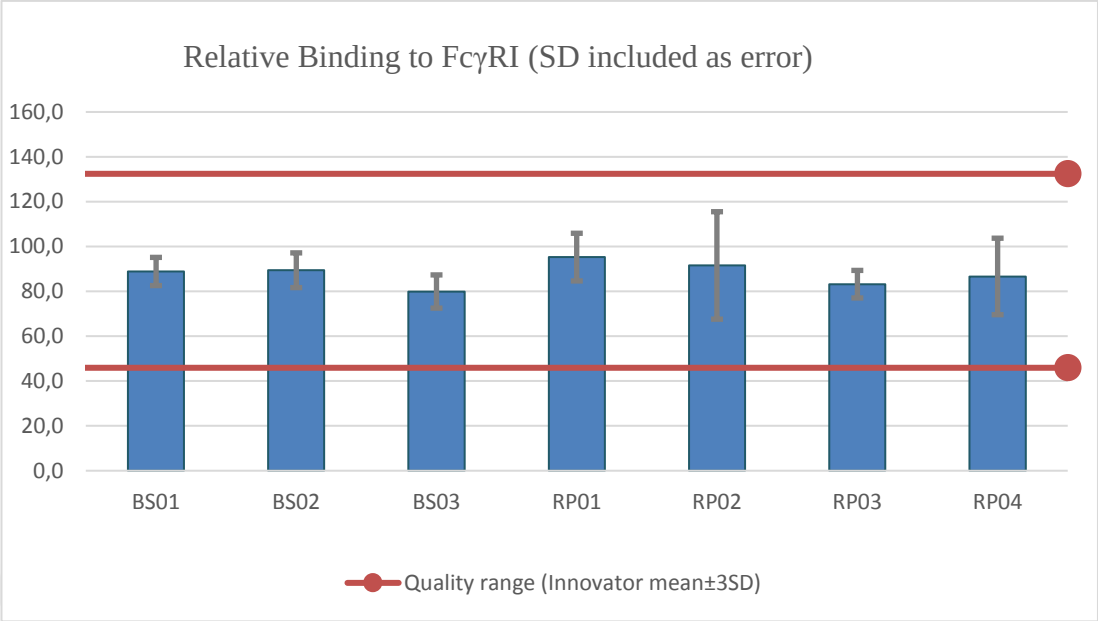


Figure 22. Relative binding to FcγRI (%)

FcγRIIIa is a receptor expressed on natural killer cells and involved in the induction of ADCC. This receptor has two allotypes, FcγRIIIa (158V) and FcγRIIIa (158F). The high-affinity allotype FcγRIIIa (158V) was captured on the anti-His antibody immobilized chip, mAb was injected in increasing concentrations over reference and active flow cells, and a single cycle kinetics procedure was applied.

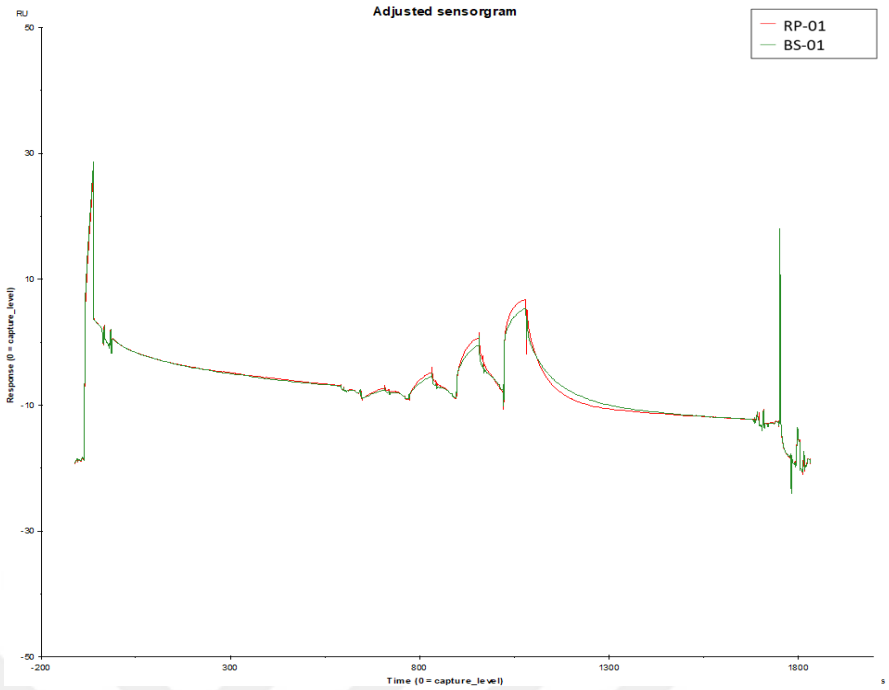


Figure 23. FcγRIIIa and antibody binding sensorgrams

In Figure 23, the x-axis and y-axis were adjusted with the capture level of FcγRIIIa. In the experiment, after the capture of FcγRIIIa, a stabilization period was added because of the decrease in the response level. After the stabilization period, the antibodies were injected into the flow cells. After the regeneration, the sensorgram returns to the values before the capture injections. This shows that the regeneration injection has removed all the molecules but not the anti-His antibody immobilized on the sensor chip.

Data collected from the experiment were double-referenced, and for the antibody and FcγRIIIa binding two-state binding model was fitted to generate the kinetic data (Figure 24), because the biphasic dissociation characteristics of the antibody two-state binding model had fitted better to the sensorgrams.

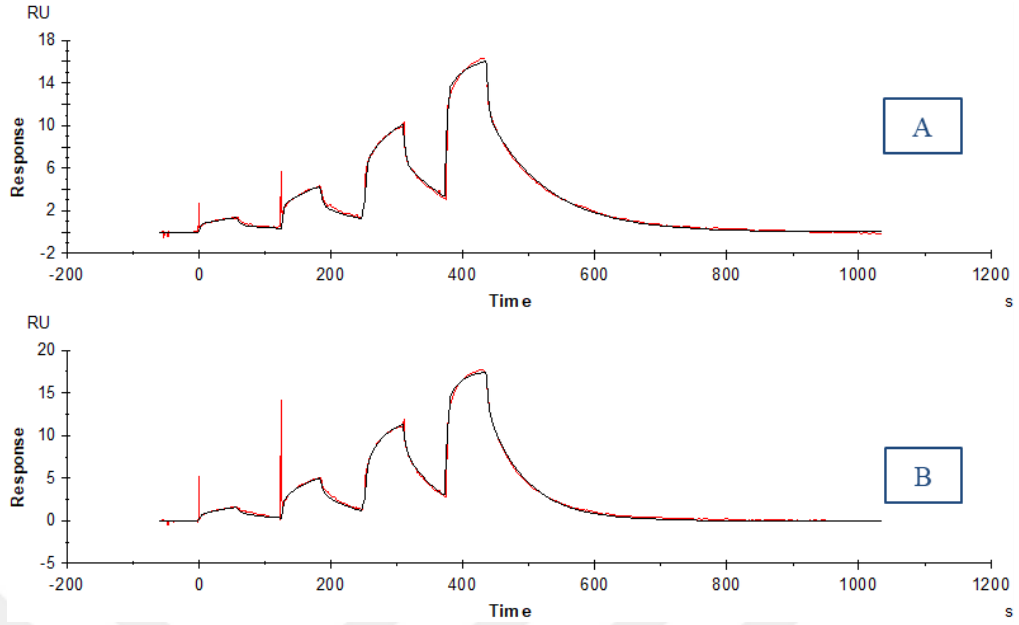


Figure 24. FcγRIIIa and antibody binding sensorgrams with a two-state binding model (A: Biosimilar, B: Reference)

For FcγRIIIa binding, a two-state binding model was used to calculate the kinetic data. Since the U-value score is a property of 1:1 binding, it was impossible to compare the U-value for this analysis. For this reason, only Chi2 scores could be compared.

The biosimilarity was concluded when the ± SD for the difference in means between the biosimilar is contained within an EAC of ± 3 times the SD of the dataset for the reference product lots tested. The quality range limits were 99.2% to 136.5% relative potency, as depicted in Figure 25. The biosimilar batches resulted between these quality ranges.

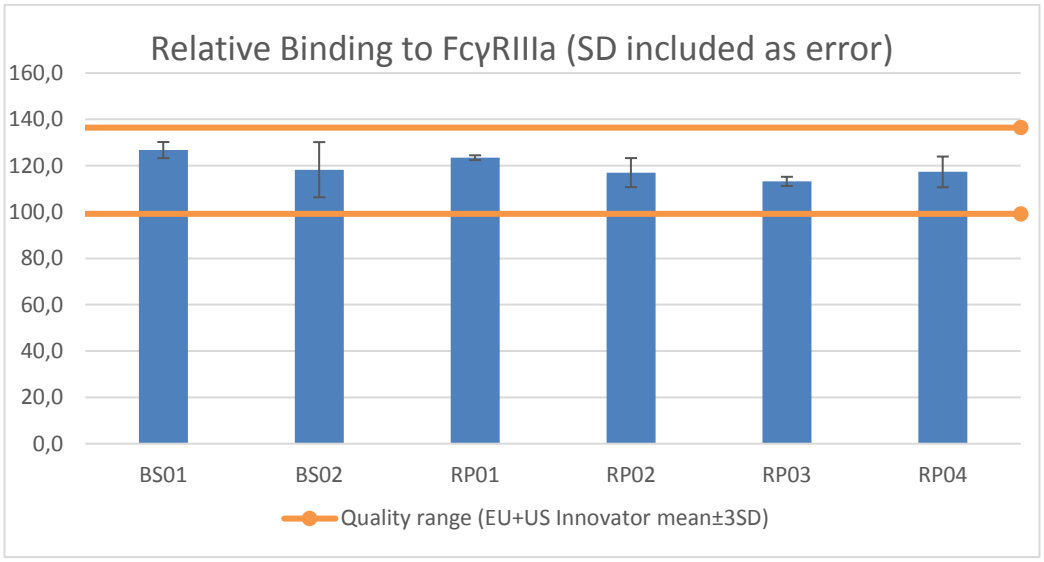


Figure 25. Relative binding to FcγRIIIa (%)

A single lot of each biosimilar and reference product was assessed for FcγR binding in the presence of soluble TNFα. The antibodies were incubated with antigens before the experiment. The antibody and antigen were incubated at 25°C and 37°C for 1 hour. The same methodology as applied for both FcγRI and FcγRIIIa binding for this assay.

Data collected from the experiment were double-referenced, and for the antibody-antigen and FcγRIa binding 1:1 binding model was fitted to generate the kinetic data (Table 11). For FcγRIIIa binding two-state binding model was fitted to generate the kinetic data (Table 12).

Table 11. FcγRIa binding with mAb and antigen binding kinetic data

| **Sample Name** | **ka (1/Ms)** | **kd (1/s)** | **KD (M)** | **Rmax (RU)** | **U-value** |
|---|---|---|---|---|---|
| Antibody | 3.01E+04 | 1,45E-03 | 4.82E-08 | 59.38 | 2 |
| Antibody -TNF25°C | 2.92E+04 | 7.86E-04 | 2.69E-08 | 62.65 | 2 |
| Antibody -TNF37°C | 2.92E+04 | 8.10E-04 | 2.77E-08 | 62.85 | 3 |

Table 12. FcγRIIIa binding with mAb and antigen binding kinetic data

| Sample Name | ka (1/Ms) | kd (1/s) | ka2 (1/Ms) | kd2 (1/s) | KD (M) | Rmax (RU) | Chi² (RU²) |
|---|---|---|---|---|---|---|---|
| Antibody | 2.13E+04 | 0.2268 | 0.0509 | 0.0194 | 2.94E-08 | 51.84 | 0.413 |
| Antibody -TNF25°C | 5.06E+04 | 0.0113 | 0.00415 | 7.60E-04 | 3.44E-08 | 138.7 | 22.0 |
| Antibody -TNF37°C | 7.11E+04 | 0.0126 | 0.00441 | 8.18E-04 | 2.78E-08 | 128.9 | 19.5 |

After mAb and antigen incubation ka level was not changed, but the kd level was significantly decreased. This decrease resulted in KD value decrease, which means that the affinity has increased.

### 4.1.2.3 FcRn binding analysis

The binding affinity value for the biosimilar and reference product to FcRn were determined in a single-cycle assay format using surface plasmon resonance (SPR). The steady-state fitting of the sensorgrams was performed to determine the binding affinity data. A relative binding affinity was calculated by comparing the values obtained for the biosimilar and reference products (Figure 26).

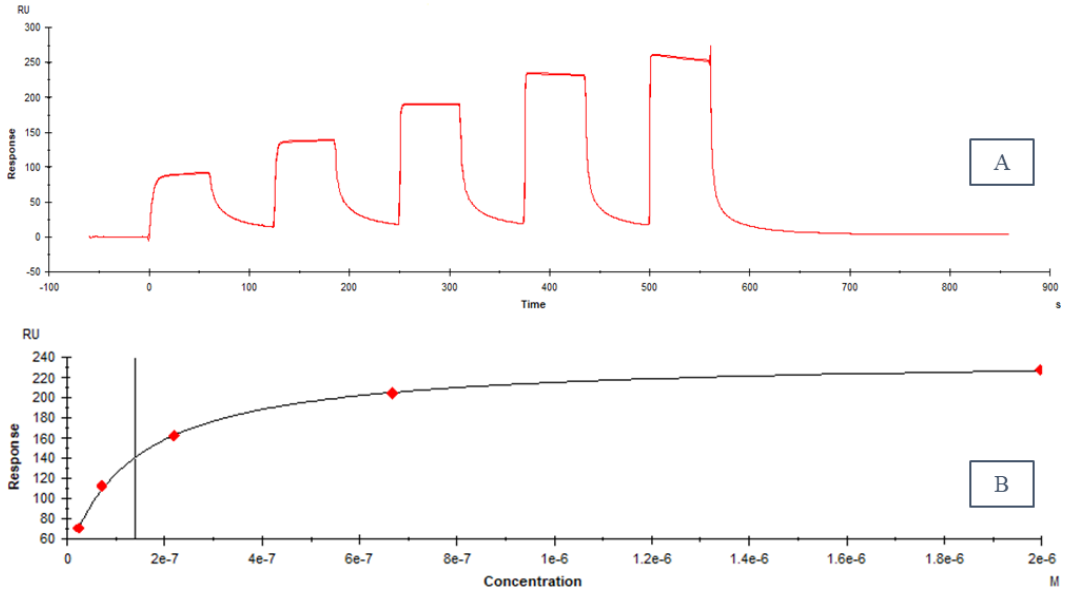


Figure 26. A: Sensorgram of Adalimumab binding to FcRn. B: Affinity graph of adalimumab binding to FcRn

For the antibody – FcRn binding steady-state binding model was fitted to generate the kinetic data. The quality range was defined as the mean of the reference product lots tested ± 3 standard deviations (Figure 27).

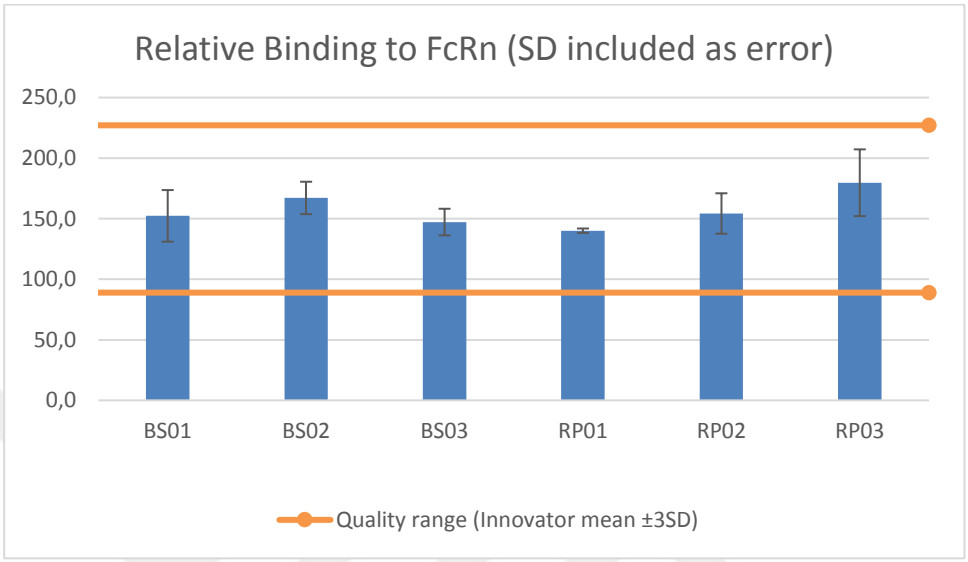


Figure 27. Relative binding to FcRn

The quality range limits were 88.9% to 227.1% relative potency, as shown in Figure 27. The biosimilar batches resulted between these quality ranges.

### 4.1.3 Cell-based Assay

#### 4.1.3.1 In vitro TNF-neutralizing activity

TNFα can bind to TNF receptors located on the L929 and U937 cell surface leading to TNF-mediated killing of these cells. Adalimumab binds to TNFα and prevents this interaction. Neutralizing activity by cell-based L929 and U937 assays was compared for the biosimilar and reference products. Assays were conducted in parallel.

Neutralizing of human TNF-α induced cytotoxicity on L929 cells were shown in Figure 28 where the percent viability was calculated based on viability of unstimulated cells. Both biosimilar and reference products had an overlapping sigmoidal log-dose-

response curve. The dose-response curve for biosimilar revealed that the half-maximum effective concentration ($EC_{50}$) value was similar to that of the reference product.

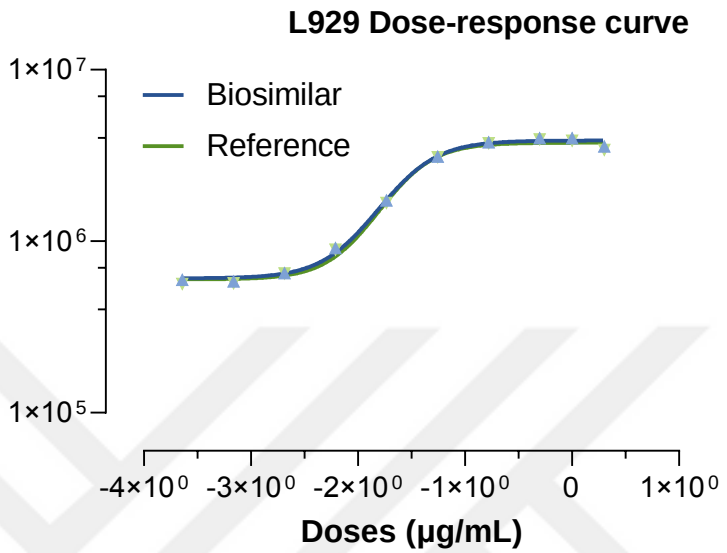


Figure 28. Neutralizing of human TNF-α induced cytotoxicity on L929 cells

TNF-α neutralizing activity of biosimilar and reference products was expressed as a relative potency compared to DRS. The $EC_{50}$ (half-maximum effective concentration) was calculated for each sample using sigmoidal dose-response-curve-fitting software, and the obtained data were tabulated in Table 13. Each experiment was carried out in triplicate, and an average value was reported.

Table 13. Comparison of Average $EC_{50}$ and relative potency for L929 cell line

| | **Relative potency (%)** | | **$EC_{50}$ (ng/mL)** | |
|---|---|---|---|---|
| | **Mean** | **SD** | **Mean** | **SD** |
| **BS01** | 98.8 | 22.7 | 0.024 | 0.004 |
| **BS02** | 105.6 | 11.2 | 0.024 | 0.005 |
| **RP01** | 93.5 | 17.2 | 0.024 | 0.004 |
| **RP02** | 117.1 | 25.7 | 0.027 | 0.005 |
| **RP03** | 104.8 | 20.8 | 0.029 | 0.006 |
| **RP04** | 86.3 | 13.7 | 0.026 | 0.010 |
| **RP05** | 89.0 | 2.0 | 0.027 | 0.007 |

The biosimilarity was concluded when the ± SD for the difference in means between the biosimilar is contained within an EAC of ± 2 times the SD of the dataset for the reference product lots tested. The quality range limits were 59.6% to 133.8% relative potency. The biosimilar batches resulted between these quality ranges (Figure 29).

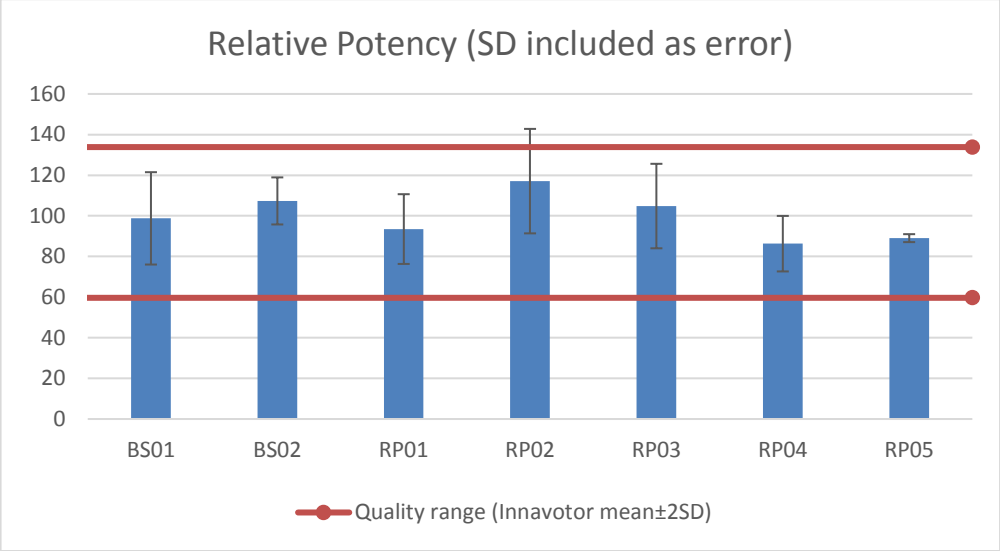


Figure 29. Relative potency results of cytotoxicity on L929 cells

Neutralizing of human TNF-α induced apoptosis in U937 cells was shown in Figure 30, where the percent viability was calculated based on the viability of unstimulated cells. Both biosimilar and reference products had an overlapping sigmoidal dose-response curve.

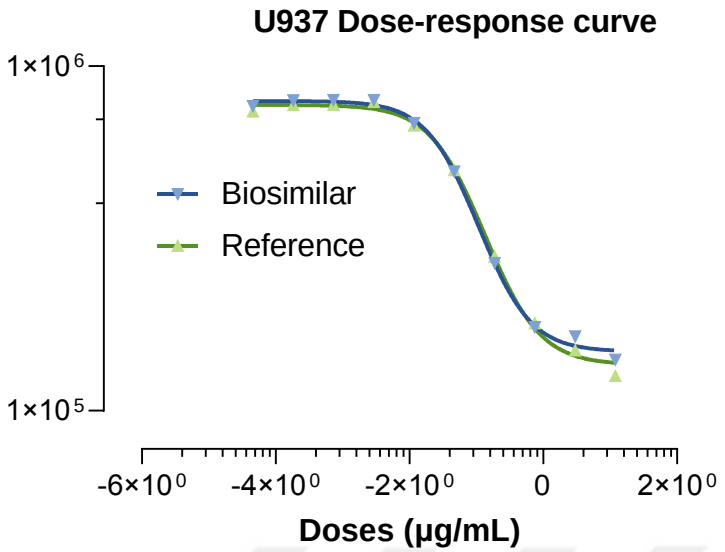


Figure 30. Neutralizing of human TNF-α induced apoptosis in U937 cells

The $EC_{50}$ (half-maximum effective concentration) was calculated for each sample using sigmoidal dose-response-curve-fitting software (GraphPad Prism), and the obtained data were tabulated in Table 14. TNF-α neutralizing activity of biosimilar and reference products was expressed as a relative potency compared to DRS.

Table 14. EC50 and Relative Potency Results

| | **Relative potency (%)** | | **$EC_{50}$ (µg/ml)** | |
|---|---|---|---|---|
| | **Mean** | **SD** | **Mean** | **SD** |
| **BS01** | 91.3 | 9.9 | 0.032 | 0.010 |
| **BS02** | 103.1 | 11.8 | 0.037 | 0.014 |
| **RP01** | 110.3 | 18.0 | 0.039 | 0.015 |

The quality range limits were 74.3% to 146.3% relative potency. The biosimilar batches resulted between these quality ranges (see Figure 31).

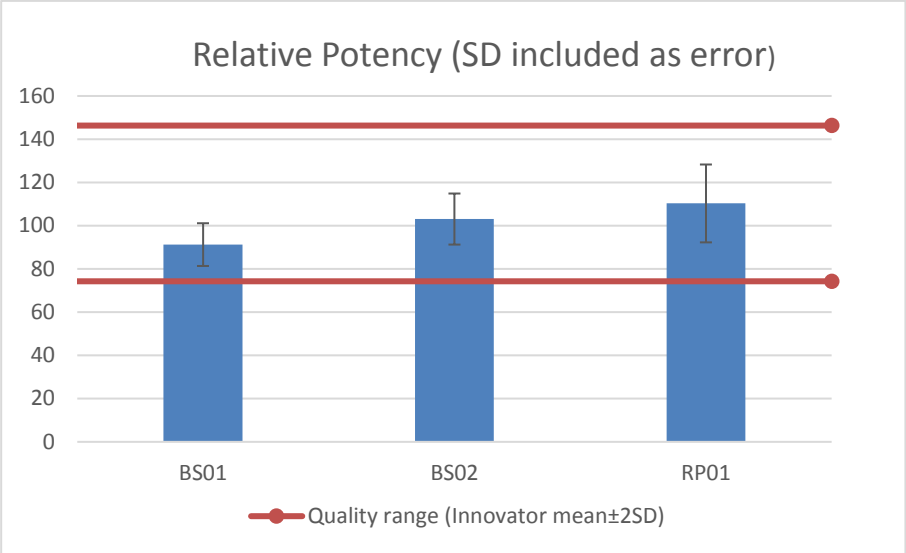


Figure 31. Relative potency results of cytotoxicity on U937 cells

The cell-based assays with L929 and U937, cell line findings, showed that the biosimilar has a similar TNF-neutralizing activity as the reference product.

#### 4.1.3.2 ADCC activity

Anti- TNFα antibodies run the risk of attaching to membrane-bound TNFα and activating effector processes like ADCC since TNF-alpha is created through the cleavage of a protein that is linked to membranes. Adalimumab can mediate ADCC activity, but the clinical efficacy is unclear because it is not a primary mechanism of action.

ADCC activity was conducted using Peripheral Blood Mononuclear cells (PBMCs), in which NK cells are the principal effectors of ADCC activity. NK cells were utilized as a whole blood preparation as an enriched NK fraction. This method utilizes an enriched NK preparation from donors of a V/F genotype.

Table 15. ADCC activity results

| | Relative Potency (%) | | Relative $EC_{50}$,(%) |
|---|---|---|---|
| | Mean | 95% CI | |
| **BS01** | 56.2 | 45.4 – 69.7 | 58.0 |
| **BS02** | 104.3 | 86.7 – 125.4 | 99.2 |
| **RP01** | 101.1 | 83.3 – 122.6 | 94.1 |
| **RP02** | 101.0 | 88.5 – 115.1 | 107.6 |

The relative potency of ADCC in this assay system seemed highly variable (Table 15, Figure 32). Reference product batches had a repeat result of approximately 100% followed by 115-120%; for the biosimilar batch (BS02), results in the range from 105 to 125% were observed, while for the biosimilar batch (BS01), relative potency reached a maximum of 70% with a mean value of 56%. Since there are no changes to adalimumab manufacturing between these two batches, these results are considered due to the assay variation.

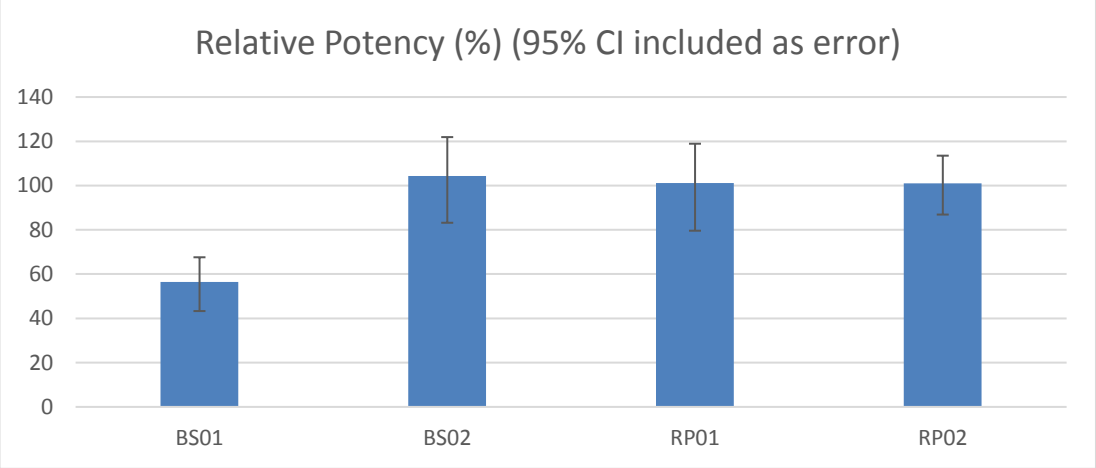


Figure 32. Relative potency results of ADCC assay

For reporter gene bioassay, ready-to-use engineered cells were used. By specifically expressing Firefly luciferase, ADCC Assay Ready Cells are engineered cells that make it possible to study antibody-dependent cell-mediated cytotoxicity (ADCC). The antibody can interact with the Fc receptors (FcγRIIIa) on the effector cell when they bind to the antigens on the target cell's surface. Multiple cross-linking of the two cell types occurs when the target-bound antibody's Fc-portion connects to the receptor. This can start a signaling cascade that causes the effector cell to express

firefly luciferase. The ability of the biosimilar and reference product to induce ADCC was assessed by the target and effector cell line, which are human cells (HEK293) engineered to overexpress mTNFα and human T lymphocyte cell line (Jurkat) optimized to express high levels of the low-affinity Fc receptor FcγRIIIa respectively.

Table 16. ADCC activity results from reporter gene bioassay

| | $EC_{50}$ (ng/mL) | |
|---|---|---|
| | **Mean** | **SD** |
| **BS01** | 15.81 | 8.28 |
| **RP01** | 14.52 | 1.35 |

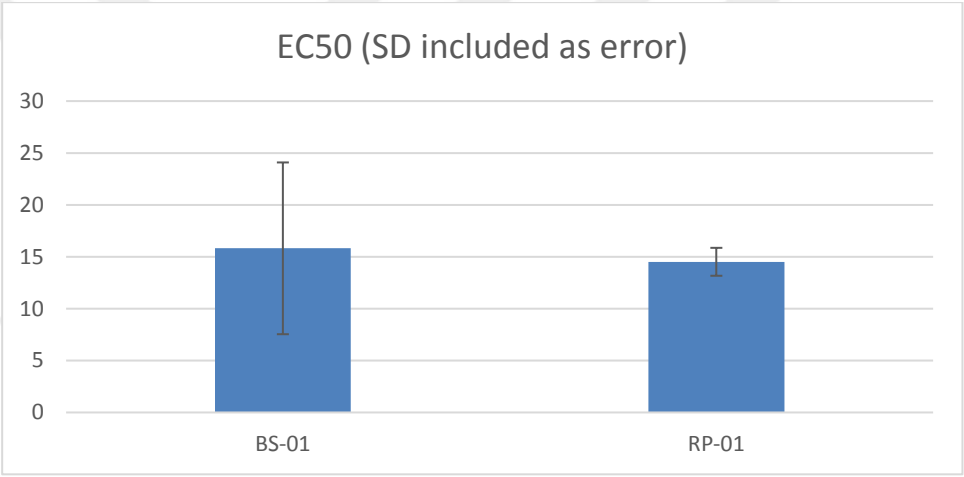


Figure 33. EC50 results of ADCC assay

The results of three replicate analysis were given in Table 16, Figure 33. Although the mean $EC_{50}$ result was similar to the biosimilar and reference products, the standard deviation of the biosimilar is very high.

### 4.2 Stress Analysis

In the stress study, lots of the biosimilar (BS) and reference products (RP) were analyzed in parallel. The biosimilar and reference products were subjected to chemical oxidation via different concentrations of hydrogen peroxide ($H_2O_2$). Under oxidative stress, the percentage of methionine oxidation, the binding kinetics of FcγR, and the

ADCC effects for biosimilar and reference products were compared. MS and SPR analyses show that oxidative stress similarly affects biosimilar and reference products.

### 4.2.1 Evaluation of MS/MS data under stress

MS/MS analysis is currently utilized to monitor post-translation modifications (PTMs) levels in biosimilar monoclonal antibody (mAb) characterization and comparison to reference products. The studied mAb sample comprises of totally five methionine (Met, M) residues, one Met on the light chain (LC-Met4) and four Met residues (HC-Met34, HC-Met83, HC-Met256, and HC-Met432) on the heavy chain. Met4, Met34, and Met83 are located in the Fab domain, whereas Met256 and HC-Met432 are positioned in the Fc domain.

For comparison under stress conditions, chemical oxidation was carried out by incubating biosimilar and reference product with different concentrations of $H_2O_2$ (0.1%, 0.5%, 1.0%, 3.0%) for 24h at 25 °C in darkness. After 24h, samples were buffer exchanged with ammonium bicarbonate solution, and then routine peptide mapping workflow followed. LC-MS/MS assays were used to identify and quantify Met oxidation under chemical oxidation stress. Oxidation of Met residue resulted in a +16 Da mass shift compared to the unoxidized counterpart. The oxidized peptides were confirmed by carefully interpreting their MS/MS spectra, *i.e.,* 16 Da mass increase in *b* and/or *y* ions. One sample preparation was performed for each sample, and two injections were done from each sample. The calculated Met oxidation levels (average of two injections) for biosimilar and reference product are listed in Table 17 and Table 18. Five tryptic peptides containing Met susceptible to oxidation were shown in the relevant tables. UNIFI software automatically calculates the percent oxidation level using XIC areas of the modified peptide divided by the sum of XIC areas of the modified and unmodified peptide. The modification sites were labeled with red color.

Table 17. Methionine Oxidation Level for Biosimilar Sample

| Biosimilar – Met Oxidation Level | | | | | | | |
|---|---|---|---|---|---|---|---|
| **Chain: Peptide No** | **Peptide** | **Position** | **Unstressed** | **0.1% $H_2O_2$** | **0.5% $H_2O_2$** | **1.0% $H_2O_2$** | **3.0% $H_2O_2$** |
| **LC:T1** | DIQMTQSPSSLSASVGDR | 4 | 0.67 | 1.21 | 4.64 | 10.3 | 22.9 |
| **HC:T3** | LSCAASGFTFDDYAMHWVR | 34 | 1.38 | 16.9 | 58.2 | 72.7 | 83.7 |
| **HC:T8** | NSLYLQMNSLR | 83 | 1.11 | 2.01 | 6.37 | 15.3 | 28.8 |
| **HC:T19** | DTLMISR | 256 | 4.17 | 93.4 | 100 | 100 | 100 |
| **HC:T39** | WQQGNVFSCSVMHEALHNHYTQK | 432 | 2.06 | 68.5 | 98.3 | 98.6 | 99.1 |

Table 18. Methionine Oxidation Level for Reference Product

| Reference – Met Oxidation Level | | | | | | | |
|---|---|---|---|---|---|---|---|
| **Chain: Peptide No** | **Peptide** | **Position** | **Unstressed** | **0.1% $H_2O_2$** | **0.5% $H_2O_2$** | **1.0% $H_2O_2$** | **3.0% $H_2O_2$** |
| **LC:T1** | DIQMTQSPSSLSASVGDR | 4 | 0.27 | 0.68 | 4.17 | 15.7 | 18.2 |
| **HC:T3** | LSCAASGFTFDDYAMHWVR | 34 | 1.28 | 10.1 | 38.6 | 74.2 | 83.5 |
| **HC:T8** | NSLYLQMNSLR | 83 | 0.40 | 1.15 | 4.61 | 20.8 | 20.8 |
| **HC:T19** | DTLMISR | 256 | 3.53 | 93.8 | 100 | 100 | 100 |
| **HC:T39** | WQQGNVFSCSVMHEALHNHYTQK | 432 | 1.07 | 67.9 | 98.3 | 98.4 | 98.5 |

The formation of oxidation was confirmed by careful interpretation of sequence informative *b*- and *y*-type ions via MS/MS spectra of modified and unmodified peptides. For example, MS/MS spectra of modified/unmodified T19 and T39 peptides are shown in Figure 34.

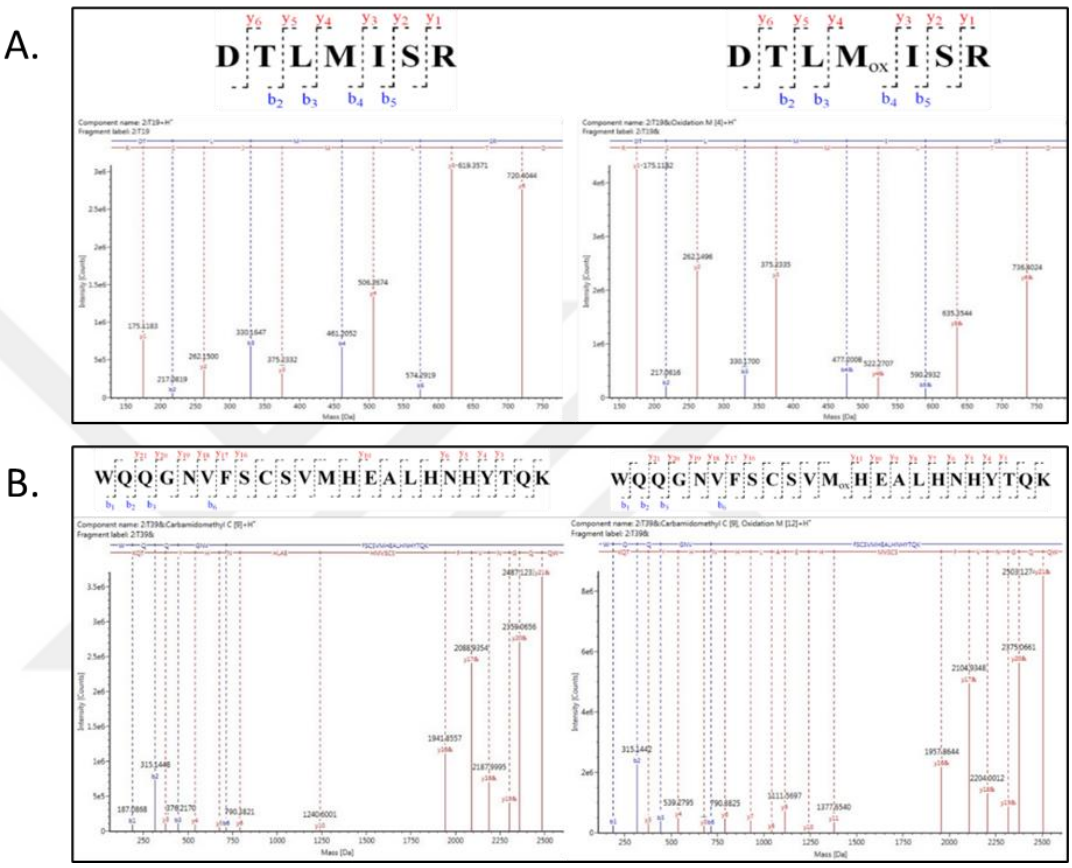


Figure 34. Comparison of MS/MS spectra for modified and unmodified peptide A: T19 T39 peptide B: T39 peptide

The data showed that increasing $H_2O_2$ concentration has nearly the same impact on Met34 oxidation for biosimilar and reference products. Moreover, Met4 and Met83 residues have shown nearly 20% oxidation under 3.0% $H_2O_2$ treatment for the two products. Incubation of biosimilar and reference product with 0.5% $H_2O_2$ for 24h at room temperature leads to completely oxidation of Met256 and Met432 residues (Figure 35).

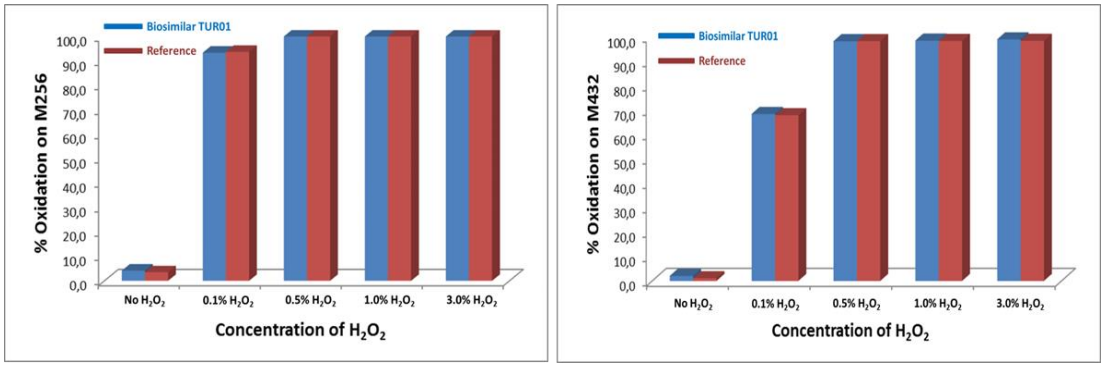


Figure 35. Oxidation profiles of Met256 and M493 under increasing H2O2 concentration

### 4.2.2 Evaluation of SPR data under stress

Surface plasmon resonance analysis is currently utilized to monitor FcγR binding kinetics for the biosimilar and reference products. According to the MS data, 0.1% and 1.0% $H_2O_2$ showed Met4 and Met83 oxidation and complete oxidation of Met256 and Met432 residues. Because of this, 0.1% and 1.0% $H_2O_2$ stress conditions were chosen for SPR analysis. The results of three different biosimilar and two different reference product lots are given below.

Overlayed SPR sensorgrams of oxidation-stressed samples for biosimilar and reference products are given below in Figure 36 and Figure 37, respectively. The oxidation stress binding kinetic data for FcɣRI binding with antibodies are given below in Table 19. The biosimilar and reference products gave similar KD values, but the Rmax level decreased with $H_2O_2$ exposure. However, the decrease in the Rmax level was not correlated with the concentration of $H_2O_2$. This decrease means that the total amount of mAb that binds to FcɣRI was decreased with oxidation stress.

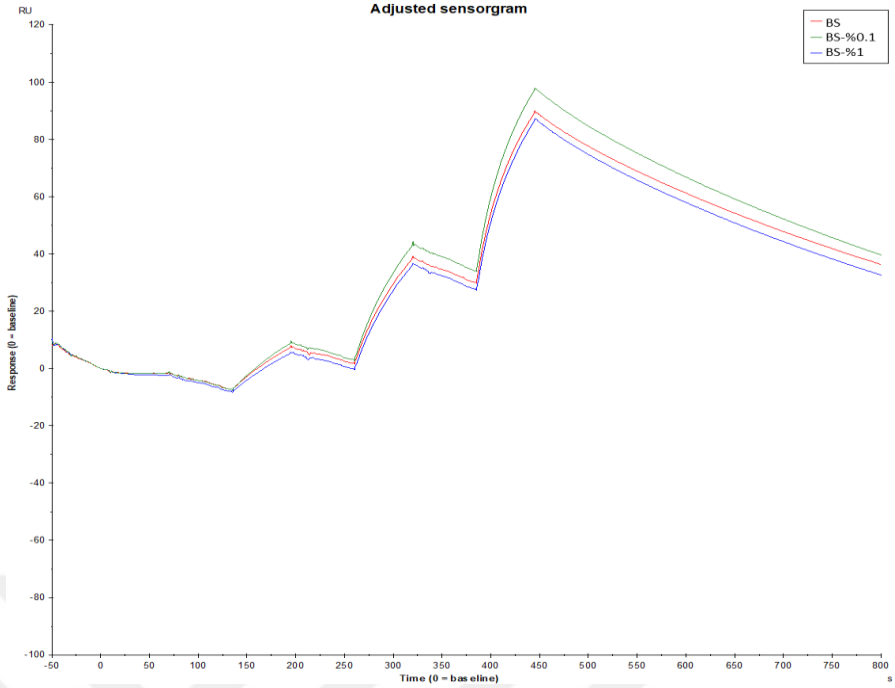


Figure 36. FcγRIa and oxidative stressed antibody binding sensorgrams for biosimilar

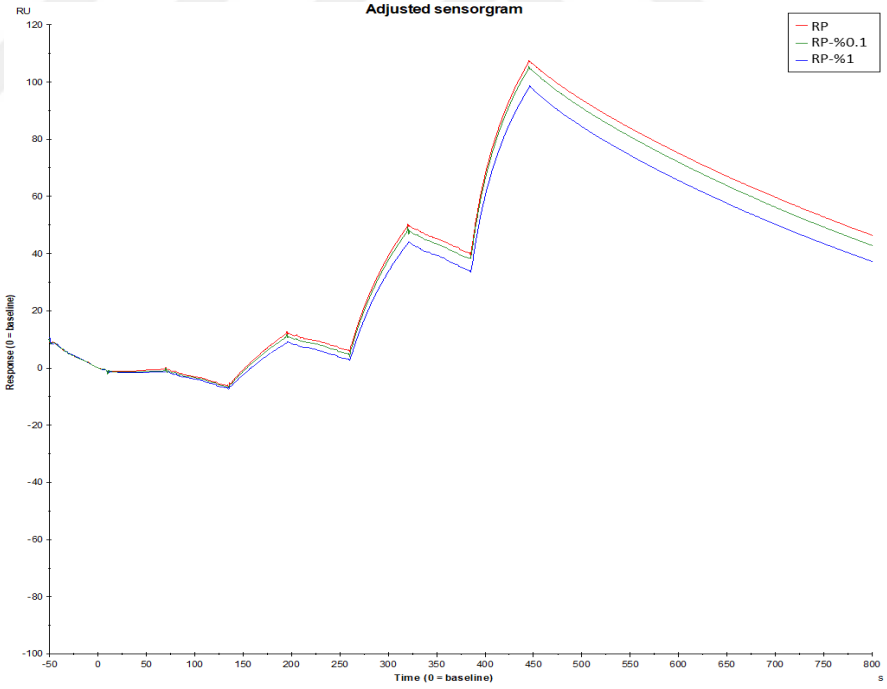


Figure 37. FcγRIa and oxidative stressed antibody binding sensorgrams for the reference product

Table 19. Oxidation stress results for FcγRI binding with mAb

| Sample Name | ka (1/Ms) | kd (1/s) | KD (M) | Rmax (RU) | U-value |
|---|---|---|---|---|---|
| **BS-01** | 2.618E+05 | 0.001311 | 5.009E-09 | 69.22 | 1 |
| **BS-01+0.1% $H_2O_2$** | 2.568E+05 | 0.001395 | 5.434E-09 | 64.50 | 1 |
| **BS-01+1.0% $H_2O_2$** | 2.483E+05 | 0.001489 | 5.998E-09 | 60.79 | 1 |
| **BS-02** | 2.797E+05 | 0.001307 | 4.674E-09 | 70.64 | 1 |
| **BS-02+0.1% $H_2O_2$** | 2.640E+05 | 0.001374 | 5.204E-09 | 61.19 | 1 |
| **BS-02+1.0% $H_2O_2$** | 2.480E+05 | 0.001406 | 5.669E-09 | 61.52 | 1 |
| **BS-03** | 2.797E+05 | 0.001305 | 4.667E-09 | 76.86 | 1 |
| **BS-03+0.1% $H_2O_2$** | 2.649E+05 | 0.001387 | 5.235E-09 | 69.70 | 1 |
| **BS-03+1.0% $H_2O_2$** | 2.622E+05 | 0.001403 | 5.353E-09 | 69.38 | 1 |
| **RP-01** | 3.09E+05 | 0.001368 | 4.471E-09 | 85.77 | 1 |
| **RP -01+0.1% $H_2O_2$** | 2.680E+05 | 0.001389 | 5.182E-09 | 74.31 | 1 |
| **RP -01+1.0% $H_2O_2$** | 2.778E+05 | 0.001436 | 5.168E-09 | 76.56 | 1 |
| **RP-02** | 3.364E+05 | 0.001290 | 3.835E-09 | 96.85 | 1 |
| **RP -02+0.1% $H_2O_2$** | 2.877E+05 | 0.001416 | 4.922E-09 | 82.62 | 1 |
| **RP -02+1.0% $H_2O_2$** | 2.961E+05 | 0.001454 | 4.910E-09 | 82.90 | 1 |

The oxidation stress results and sensorgrams for FcγRIIIa binding with antibodies are given below in Figure 38, Figure 39, and Table 20. The biosimilar and reference products gave similar KD values, but the Rmax level was slightly decreased with $H_2O_2$ exposure. This decrease means that the total amount of mAb that binds to FcγRIIIa was slightly decreased with oxidation stress.

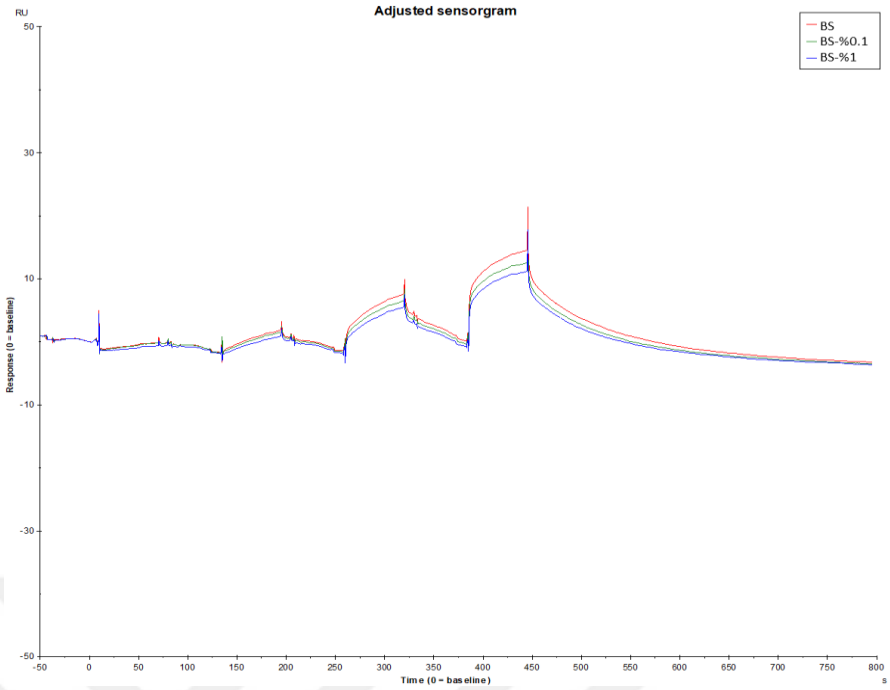


Figure 38. FcγRIIIa and oxidative stressed antibody binding sensorgrams for biosimilar

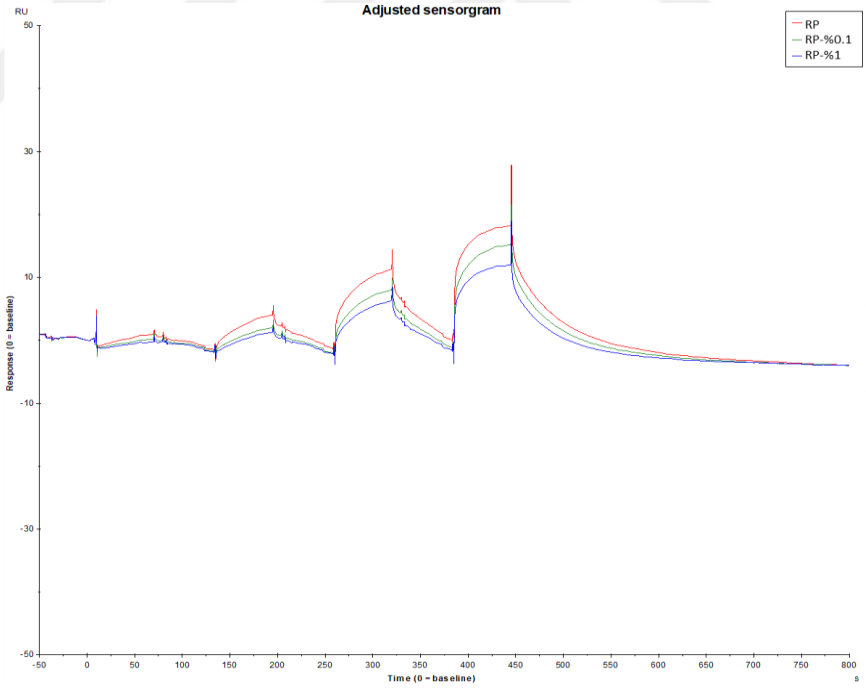


Figure 39. FcγRIIIa and oxidative stressed antibody binding sensorgrams for the reference product

Table 20. Oxidation stress results for FcγRIIIa binding with mAb

| Sample Name | ka (1/Ms) | kd (1/s) | ka2 (1/Ms) | kd2 (1/s) | KD (M) | Rmax (RU) | Chi² (RU²) |
|---|---|---|---|---|---|---|---|
| **BS-01** | 2,52E+05 | 0,4385 | 0,02292 | 0,01101 | 5,64E-07 | 25,74 | 0,0427 |
| **BS-01+0.1% $H_2O_2$** | 2,45E+05 | 0,5404 | 0,02649 | 0,01335 | 7,39E-07 | 24,36 | 0,0583 |
| **BS-01+1.0% $H_2O_2$** | 4,53E+05 | 0,5908 | 0,02881 | 0,01397 | 4,26E-07 | 19,49 | 0,0323 |
| **BS-02** | 2,59E+05 | 0,326 | 0,02589 | 0,01089 | 3,73E-07 | 23,65 | 0,1030 |
| **BS-02+0.1% $H_2O_2$** | 3,39E+05 | 0,4198 | 0,02966 | 0,01221 | 3,62E-07 | 21,03 | 0,0627 |
| **BS-02+1.0% $H_2O_2$** | 3,54E+05 | 0,5065 | 0,02931 | 0,01313 | 4,43E-07 | 20,85 | 0,0456 |
| **BS-03** | 3,28E+05 | 0,4782 | 0,02189 | 0,01091 | 4,85E-07 | 24,38 | 0,0474 |
| **BS-03+0.1% $H_2O_2$** | 3,68E+05 | 0,5615 | 0,02358 | 0,01252 | 5,29E-07 | 23,63 | 0,0275 |
| **BS-03+1.0% $H_2O_2$** | 3,78E+05 | 0,4772 | 0,02524 | 0,01239 | 4,16E-07 | 19,52 | 0,0268 |
| **RP-01** | 3,26E+05 | 0,3173 | 0,04815 | 0,02072 | 2,93E-07 | 23,45 | 0,1170 |
| **RP -01+0.1% $H_2O_2$** | 3,19E+05 | 0,3849 | 0,05932 | 0,02527 | 3,61E-07 | 22,45 | 0,0946 |
| **RP -01+1.0% $H_2O_2$** | 6,88E+04 | 0,0228 | 3,53E-04 | 0,00134 | 2,62E-07 | 16,23 | 0,1300 |
| **RP-02** | 3,02E+05 | 0,2645 | 0,03422 | 0,01746 | 2,96E-07 | 26,15 | 0,197 |
| **RP -02+0.1% $H_2O_2$** | 2,27E+05 | 0,3170 | 0,03949 | 0,02002 | 4,71E-07 | 24,63 | 0,1130 |
| **RP -02+1.0% $H_2O_2$** | 2,63E+05 | 0,3451 | 0,04504 | 0,02278 | 4,40E-07 | 20,25 | 0,0704 |

The oxidation stress-exposed samples showed no extraordinary binding properties to FcγRI or FcγRIII.

### 4.2.3 Evaluation of Cell-based assay data under stress

Cell-based assay currently utilized to monitor ADCC activity for the biosimilar and reference products. The same oxidation stress conditions as SPR analysis were chosen for cell-based assay in order to compare these two methods (0.1% and 1.0% $H_2O_2$ stress conditions). The results of biosimilar and reference product lots are given below.

Table 21 ADCC activity results from reporter gene bioassay under stress

| | **$EC_{50}$ (ng/mL)** | |
|---|---|---|
| | **Mean** | **SD** |
| **BS-01** | 15,81 | 8,28 |
| **BS-01+0.1% $H_2O_2$** | 27,81 | 8,25 |
| **BS-01+1.0% $H_2O_2$** | 25,77 | 4,66 |
| **RP-01** | 14,52 | 1,35 |
| **RP -01+0.1% $H_2O_2$** | 25,34 | 9,98 |
| **RP -01+1.0% $H_2O_2$** | 27,15 | 4,10 |

The results of three replicate analysis were given in Table 21. After oxidation stress the $EC_{50}$ has increased but the standard deviation of this assay is high. It could be concluded that although the standard deviation is high this assay resulted in the way as SPR analysis. After oxidation stress $EC_{50}$ values has increased and FcγR binding Rmax level has decreased.

# 5 DISCUSSION

Monoclonal antibodies are one of the most important biological molecules that have received much attention lately. In the discovery phase of mAbs, the mechanisms of action of antibodies are identified, which helps the emergence of biotherapeutic drugs. A crucial stage in the manufacturing process and drug release is the physicochemical characterization and functional comparability studies to provide a deep understanding of the structure and function relationship of the quality attributes.

This study aimed to understand the functional behaviors of the biosimilar and reference product, a therapeutic monoclonal antibody, and the binding characterization under different stress conditions. Anti-TNFα antibody in IgG1 structure is a biosimilar therapeutic product that Turgut İlaçları A.Ş develops, and it is produced from a new CHO cell line.

Biosimilar is a biological product that is very similar to a licensed reference product but not exactly the same, and there are "no clinically meaningful differences between the biosimilar and the reference product in terms of safety, purity, and potency," allowing for minor variations in inactive components (63). Due to different cell lines and manufacturing processes, minor differences between biosimilars and the reference product are already expected. Biologic products' multi-stage partly causes this complex production process (26). Although these minor variations, the amino acid sequence of biosimilar products should be identical to that of the reference product (30).

The peptide mapping test revealed that biosimilar and reference products shared identical amino acid sequences and almost similar post-translation modifications (PTM), including most PTM percentages, disulfide connections, and PTM locations. The comparing functional analysis results showed that biosimilar and reference products have similar properties.

It is known that adalimumab binds to TNFα and prevents it from interacting with TNF receptors. TNFα is found in soluble and transmembrane versions, each with different documented biological functions. Adalimumab and other licensed anti-TNF medicines have various reported action mechanisms (61,62). It has been established that the primary mechanism of action of Adalimumab is binding the circulating soluble TNFα (sTNFα). Adalimumab binds the sTNFα with high affinity and blocks the binding site to the TNF receptor (61). TNFα molecule has a homo-trimeric structure, a three-monomeric unit held together with noncovalent interactions. It has shown that adalimumab binds to two TNFα monomers, and all the subunits are together (64).

State-of-the-art SPR technique was performed for analyzing and comparing the antigen binding kinetics of biosimilar and reference product batches. It was crucial to compare the affinity of the biosimilar and reference product for binding to sTNFα because it is the primary mechanism of action of adalimumab. With antigen-antibody binding kinetic 1:1 binding model was the best model for kinetic data calculations.

The antigen and antibody binding was also investigated with biotinylated TNFα captured on the sensor chip flowed by antibody binding, and it found that the biosimilar and reference product has similar binding kinetics. Karlsson et al. have shown that applying the biotin capture method may obtain reproducible data. Biotin capture is reversible, and this method has the benefit of minimizing the need for assay development (65). It is necessary to design immobilization and regeneration conditions for assays based on covalent immobilization. But because they are incorporated into the biotin capture kit design, these procedures are not required with the current method.

IgG has two parts in the Fc region which are called $CH_2$ and $CH_3$ domains. According to the literature, Protein A/G interacts with the $CH_2$ and $CH_3$ domains of the Fc portion of the antibody (66). The high-affinity FcγRI has one active binding site at the $CH_2$ domain and can facilitate binding and signal transduction. On the other hand, the low-affinity FcγRIII has two specific binding sites, one on $CH_2$ and one on the $CH_3$ domain, which can also mediate binding and signaling. According to research, the $CH_3$ region impacts binding, whereas the $CH_2$ area affects both binding and the

signaling pathway (67–69). FcγRIII receptor has a low affinity for the Fc part of the IgG1 and binds only to aggregated antibodies. Adalimumab binding to FcγRIII was enhanced in the presence of TNFα. According to Arora et al., this binding enhancement was due to the formation of large antibody-antigen complexes (70).

The Fab and Fc mediated binding analysis can also be determined by solid phase enzyme-linked immunosorbent assay (ELISA), but the SPR technique gives more detail about the binding characteristics. Both techniques give similar results, according to Vaisocherová et al., and SPR is a perfect alternative to the ELISA technique. ELISA technique uses a tagged antibody and substrate to measure the binding, the SPR technique provides a direct label-free alternative because it uses the refractive index change to measure binding kinetics. (71). ELISAs have some difficulties with low-affinity interactions; they can either have a weak signal which falls outside the standard curve, or the protein lost during the wash steps. On the other hand, SPR can effectively quantify low-affinity interaction with real-time sensitive measurement (72).

TNFα is likely the most efficacious inducer of apoptosis out of the members of the TNF superfamily. TNFα simultaneously triggers cell-survival and cell-death pathways. The survival and proliferative effects of TNFα are regulated by the activation of Nuclear Factor kappa B -dependent genes, whereas the activation of caspases regulates the apoptotic effects. TNF-induced apoptosis is mediated by binding TNFα to type I receptors and activating the apoptotic cascade (73). TNFα can also induce non-apoptotic cell death (74). Since adalimumab binds to TNFα, it can inhibit cell death. Therefore, biosimilarity was also investigated for TNFα induced apoptotic and non-apoptotic cell death were compared with cell-based assays. The biosimilar and reference product has similar bioactivity inhibiting TNFα induced cell death.

The antigen binding activity, Fc receptor binding affinity, inhibiting TNFα induced cell death, and tmTNF transfected cell line binding of biosimilar and the reference product were highly comparable. The Fc-effector function (ADCC) has shown a slight difference due to the assay variability.

The clinical relevance of ADCC-mediated cytotoxicity, which has only been observed significantly in cells expressing artificially high densities of tmTNFα, has not been established to date. A literature search has found no published evidence of ADCC induction by adalimumab in non-transfected, non-stimulated human cells. A study by Van den Brande et al. demonstrated that infliximab, which presents similar ADCC activity as adalimumab in tmTNFα transfected cells, failed to mediate ADCC activity in normal human PBMC (75). ADCC is unlikely to play a role in the therapeutic response in the non-IBD indications since both etanercept, which shows reduced ADCC activity, and certolizumab pegol, which possesses no ADCC activity, are effective in these indications (76,77). ADCC is also unlikely to play a role in the IBD indications since cell depletion via ADCC is not a requisite for efficacy in IBD of anti-TNF agents. Certolizumab pegol has shown positive clinical data in treating subjects with Crohn's disease (78,79).

The first FDA-approved infliximab biosimilar, CT-P13, showed slightly lower levels of ADCC activity in cell lines overexpressing tmTNF-α compared to the infliximab reference product. The clinical trials confirmed the comparability of CT-P13 and the reference product (80).

Minor differences between the biosimilar and reference products should have an impact on the antibody efficacy, safety, or immunogenicity. According to Tu et al., reference biological products originating from different manufacturing sites have nearly identical clinical outcomes (81). Based on these findings, if the biosimilar has physicochemical and functional similarities, they are expected to give similar clinical trial results.

When an antibody is exposed to oxidative stress, several possible outcomes can occur depending on the severity and duration of the stress condition. Oxidation stress can oxidize specific amino acid residues within the antibody. In particular, oxidation of the methionine (Met) side chains can alter the antibody structure, which may result in an affected antibody binding to an antigen or Fc receptors. All these modifications can change the stability and half-life of the antibodies. Methionine (Met, M) oxidation

is accepted as one of the most commonly observed PTM during the manufacturing, formulation, and storage stages. It may affect the protein's biological function, structure, and stability (53,82–84).

Different oxidation stress conditions were applied as a part of forced degradation studies to understand the antibodies' molecular binding properties. Biosimilar and reference product samples were left to incubate with $H_2O_2$ for oxidation stress. Incubation of biosimilar and reference product with 0.5% $H_2O_2$ for 24h at room temperature leads to completely oxidation of Met256 and Met432 residues. Those residues are located in the Fc region ($CH_2$–$CH_3$ interface) and exposed to the protein surface. These Met residues are more prone to oxidation compared to the others. On the other hand, Met34 is located on the complementarity-determining region (CDR), which may impact antigen binding kinetics.

It was observed that oxidation stress affected the FcγR binding kinetics and ADCC activity. In the peptide mapping analysis, this situation becomes significant with the more oxidation of methionine amino acids in the Fc region. As a result of oxidation stress applied at two different $H_2O_2$ levels, no significant difference was observed in KD and Rmax values in antigen binding kinetic analyzes. Although no significant difference was observed in the KD values in the FcγR binding kinetic analyses performed due to the same stress, the Rmax values decreased in connection with the $H_2O_2$ level. With these results, it is understood that the oxidation of methionine amino acid is effective on FcγR binding.

# 6 CONCLUSION

According to this study's findings, functional analysis showed that biosimilar and reference products have similar functional properties. The biosimilar of adalimumab has a similar structure and function to that of the reference product. Importantly, there is a relationship between the physicochemical and biological characteristics of the antibodies.

The peptide mapping test revealed that biosimilar and reference products shared identical amino acid sequences and remarkably similar post-translation modifications (PTM), including most PTM percentages, disulfide connections, and PTM locations. High-level similarities in oxidation profiles for LC-Met4, HC-Met34, HC-Met83, HC-Met256, and HC-Met432 residues were observed. Out of 5 Met residues, HC-Met256 and HC-Met432 are more prone to oxidation due to solvent exposure. Conformational dynamics were affected at the same level for biosimilar and reference products under chemical oxidation stress. SPR data shows that the relative FcγRs binding of biosimilar and reference products are affected similarly under the same oxidative stress conditions.

As recommended by guidelines on biosimilars, a step-wise approach was followed in the characterization of biosimilar biological properties in nonclinical studies. In vitro assays were performed to assess biosimilarity in binding to the antigens and Fc receptors (FcγRI, FcγRIII). Fab-mediated activities on a cellular level were assessed, such as inhibition of the sTNFα-mediated apoptosis process in L929 and in U937 cell lines. Finally, Fc-mediated activities such as ADCC and CDC activities were compared in vitro. All assays included several reference batches to ensure high assay sensitivity for an assessed parameter. All in vitro studies have confirmed the similarity of the biosimilar and reference products and did not detect any clinically relevant differences. Since the ADCC assay presents high variability, the conclusion from this assay does not contribute to similarity discussion.

The antigen binding activity, Fc receptor binding affinity, and potency assay of biosimilar and the reference product were comparable. The Fc-effector function (ADCC) was slightly different. Since the ADCC assay presents high variability, the conclusion from this assay does not contribute to the similarity discussion. ADCC activity has not shown a clear clinical relevance for reference product-approved indications. In light of comparable Fab- and Fc- mediated and especially considering FcγR binding that mediates ADCC did not reveal any differences, a biosimilar is still considered highly similar to the reference product. We have also demonstrated that biosimilar and reference products behave similarly under stress conditions. These findings showed that the biosimilar and the reference product had analytical and functional similarities, providing essential data for additional nonclinical and clinical similarity assessments.

It is intended to broaden the scope of this study in future studies. Expanding the data collection, analyzing the products under more demanding stress conditions, and replicating the results with other biosimilar mAb manufactured batches and reference product batches will provide crucial information before upcoming clinical trials.

# 7 REFERENCES


1. Lu RM, Hwang YC, Liu IJ, Lee CC, Tsai HZ, Li HJ, et al. Development of therapeutic antibodies for the treatment of diseases. Journal of Biomedical Science 2020 27:1. 2020 Jan 2;27(1):1–30.
2. Morrison SL, Oi VT. Genetically Engineered Antibody Molecules. In 1989. p. 65–92.
3. Kaplon H, Muralidharan M, Schneider Z, Reichert JM. Antibodies to watch in 2020. MAbs. 2020;12(1):1703531.
4. Shan L, Mody N, Sormani P, Rosenthal KL, Damschroder MM, Esfandiary R. Developability Assessment of Engineered Monoclonal Antibody Variants with a Complex Self-Association Behavior Using Complementary Analytical and in Silico Tools. Mol Pharm. 2018 Dec 3;15(12):5697–710.
5. Wang X, An Z, Luo W, Xia N, Zhao Q. Molecular and functional analysis of monoclonal antibodies in support of biologics development. Protein Cell. 2018 Jan 21;9(1):74–85.
6. Knezevic I, Griffiths E. Biosimilars – Global issues, national solutions. Biologicals. 2011 Sep;39(5):252–5.
7. Kim YS, Choi BW, Yang SW, Shin SM, Nam SW, Roh YS, et al. Biosimilars: Challenges and path forward. Biotechnology and Bioprocess Engineering. 2014 Nov 20;19(5):755–65.
8. Schroeder HW, Cavacini L. Structure and function of immunoglobulins. Journal of Allergy and Clinical Immunology. 2010 Feb;125(2):S41–52.
9. Brandtzaeg P. Secretory immunity with special reference to the oral cavity. J Oral Microbiol. 2013 Jan 1;5(1):20401.
10. Charles A Janeway J, Travers P, Walport M, Shlomchik MJ. The structure of a typical antibody molecule. 2001;
11. Chiu ML, Goulet DR, Teplyakov A, Gilliland GL. Antibody Structure and Function: The Basis for Engineering Therapeutics. Antibodies. 2019 Dec 3;8(4):55.
12. Painter RH. IgG. Encyclopedia of Immunology. 1998;1208–11.
13. Palmeira P, Quinello C, Silveira-Lessa AL, Zago CA, Carneiro-Sampaio M. IgG Placental Transfer in Healthy and Pathological Pregnancies. Clin Dev Immunol. 2012;2012:1–13.
14. Vidarsson G, Dekkers G, Rispens T, Klinman D. IgG subclasses and allotypes: from structure to effector functions. 2014;
15. Köhler G, Milstein C. Continuous cultures of fused cells secreting antibody of predefined specificity. Nature. 1975;256(5517):495–7.
16. Mitra S, Chaudhary Tomar P. Hybridoma technology; advancements, clinical significance, and future aspects. 2021;19:159.
17. Pandey S. Hybridoma Technology for Production of Monoclonal Antibodies. Int J Pharm Sci Rev Res. 1(2).

18. Safdari Y, Farajnia S, Asgharzadeh M, Khalili M. Antibody humanization methods – a review and update. Biotechnol Genet Eng Rev. 2013 Oct;29(2):175–86.
19. Morrison SL, Johnson MJ, Herzenberg LA, Oi VT. Chimeric human antibody molecules: mouse antigen-binding domains with human constant region domains. Proceedings of the National Academy of Sciences. 1984 Nov;81(21):6851–5.
20. Boulianne GL, Hozumi N, Shulman MJ. Production of functional chimaeric mouse/human antibody. Nature 1984 312:5995. 1984;312(5995):643–6.
21. Kim JY, Kim YG, Lee GM. CHO cells in biotechnology for production of recombinant proteins: current state and further potential. Appl Microbiol Biotechnol. 2012 Feb;93(3):917–30.
22. Li Y mei, Tian Z wei, Xu D hua, Wang X yin, Wang T yun. Construction strategies for developing expression vectors for recombinant monoclonal antibody production in CHO cells. Mol Biol Rep. 2018 Dec 1;45(6):2907–12.
23. Dyson MR, Masters E, Pazeraitis D, Perera RL, Syrjanen JL, Surade S, et al. Beyond affinity: selection of antibody variants with optimal biophysical properties and reduced immunogenicity from mammalian display libraries. MAbs. 2020;12(1):1829335.
24. Monoclonal Antibodies (MAbS) Global Market Report 2023 [Internet]. [cited 2023 May 16]. Available from: https://www.researchandmarkets.com/reports/5733858/monoclonal-antibodies-mabs-global-market-report
25. Dal OH, Karadoğan M, Sezer AD. Biyobenzerler: Kavramlar ve Ruhsatlandırma Süreçleri. MARMARA PHARMACEUTCAL JOURNAL. 2015 Apr 20;19(3).
26. Kirchhoff CF, Wang XZM, Conlon HD, Anderson S, Ryan AM, Bose A. Biosimilars: Key regulatory considerations and similarity assessment tools. Biotechnol Bioeng. 2017 Dec;114(12):2696–705.
27. Berghout A. Clinical programs in the development of similar biotherapeutic products: Rationale and general principles. Biologicals. 2011 Sep;39(5):293–6.
28. Alt N, Zhang TY, Motchnik P, Taticek R, Quarmby V, Schlothauer T, et al. Determination of critical quality attributes for monoclonal antibodies using quality by design principles. Biologicals. 2016 Sep;44(5):291–305.
29. Goetze AM, Schenauer MR, Flynn GC. Assessing monoclonal antibody product quality attribute criticality through clinical studies. MAbs. 2010;2(5):500–7.
30. Kwon O, Joung J, Park Y, Kim CW, Hong SH. Considerations of critical quality attributes in the analytical comparability assessment of biosimilar products. Biologicals. 2017 Jul;48:101–8.
31. Alt N, Zhang TY, Motchnik P, Taticek R, Quarmby V, Schlothauer T, et al. Determination of critical quality attributes for monoclonal antibodies using quality by design principles. Biologicals. 2016 Sep;44(5):291–305.
32. Medicines Agency E. Committee for Medicinal Products for Human Use (CHMP) Guideline on similar biological medicinal products containing monoclonal antibodies-non-clinical and clinical issues. 2012;

33. Schweppe RE, Haydon CE, Lewis TS, Resing KA, Ahn NG. The characterization of protein post-translational modifications by mass spectrometry. Acc Chem Res. 2003 Jun;36(6):453–61.
34. Alhazmi HA, Albratty M. Analytical Techniques for the Characterization and Quantification of Monoclonal Antibodies. Pharmaceuticals. 2023 Feb 14;16(2):291.
35. Rustandi RR, Wang Y. Use of CE-SDS gel for characterization of monoclonal antibody hinge region clipping due to copper and high pH stress. Electrophoresis. 2011 Nov;32(21):3078–84.
36. Hong P, Koza S, Bouvier ESP. Size-Exclusion Chromatography for the Analysis of Protein Biotherapeutics and their Aggregates. J Liq Chromatogr Relat Technol. 2012 Nov;35(20):2923–50.
37. Suba D, Urbányi Z, Salgó A. Capillary isoelectric focusing method development and validation for investigation of recombinant therapeutic monoclonal antibody. J Pharm Biomed Anal. 2015 Oct;114:53–61.
38. Joshi V, Shivach T, Yadav N, Rathore AS. Circular Dichroism Spectroscopy as a Tool for Monitoring Aggregation in Monoclonal Antibody Therapeutics. Anal Chem. 2014 Dec 2;86(23):11606–13.
39. Calvaresi V, Redsted A, Norais N, Rand KD. Hydrogen–Deuterium Exchange Mass Spectrometry with Integrated Size-Exclusion Chromatography for Analysis of Complex Protein Samples. Anal Chem. 2021 Aug 24;93(33):11406–14.
40. Weise M, Bielsky MC, De Smet K, Ehmann F, Ekman N, Giezen TJ, et al. Biosimilars: what clinicians should know. Blood. 2012 Dec 20;120(26):5111–7.
41. Chames P, Van Regenmortel M, Weiss E, Baty D. Therapeutic antibodies: successes, limitations and hopes for the future. Br J Pharmacol. 2009 May;157(2):220–33.
42. Fda, Cder, Purdie, Florine P. Scientific Considerations in Demonstrating Biosimilarity to a Reference Product Guidance for Industry [Internet]. 2015. Available from: http://www.fda.gov/Drugs/GuidanceComplianceRegulatoryInformation/Guidances/default.htmand/orhttp://www.fda.gov/BiologicsBloodVaccines/GuidanceComplianceRegulatoryInformation/Guidances/default.htm
43. Medicines Agency E. Committee for Medicinal Products for Human Use (CHMP) Guideline on similar biological medicinal products containing monoclonal antibodies-non-clinical and clinical issues [Internet]. 2012. Available from: www.ema.europa.eu
44. Drake AW, Myszka DG, Klakamp SL. Characterizing high-affinity antigen/antibody complexes by kinetic- and equilibrium-based methods. Anal Biochem. 2004 May 1;328(1):35–43.
45. Fekete S, Gassner AL, Rudaz S, Schappler J, Guillarme D. Analytical strategies for the characterization of therapeutic monoclonal antibodies. TrAC Trends in Analytical Chemistry. 2013 Jan;42:74–83.
46. Albini A. Tumor and endothelial cell invasion of basement membranes. Pathology & Oncology Research. 1998 Sep;4(3):230–41.

47. Stengl A, Hörl D, Leonhardt H, Helma J. A Simple and Sensitive High-Content Assay for the Characterization of Antiproliferative Therapeutic Antibodies. SLAS Discov. 2017 Mar;22(3):309–15.
48. Gómez Román VR, Murray JC, Weiner LM. Antibody-Dependent Cellular Cytotoxicity (ADCC). In: Antibody Fc. Elsevier; 2014. p. 1–27.
49. Tay MZ, Wiehe K, Pollara J. Antibody-Dependent Cellular Phagocytosis in Antiviral Immune Responses. Front Immunol. 2019 Feb 28;10.
50. Kellner C, Otte A, Cappuzzello E, Klausz K, Peipp M. Modulating Cytotoxic Effector Functions by Fc Engineering to Improve Cancer Therapy. Transfus Med Hemother. 2017 Sep;44(5):327–36.
51. Hendriks D, Choi G, de Bruyn M, Wiersma VR, Bremer E. Antibody-Based Cancer Therapy. In 2017. p. 289–383.
52. Das TK, Narhi LO, Sreedhara A, Menzen T, Grapentin C, Chou DK, et al. Stress Factors in mAb Drug Substance Production Processes: Critical Assessment of Impact on Product Quality and Control Strategy. J Pharm Sci. 2020 Jan;109(1):116–33.
53. Solomon TL, Delaglio F, Giddens JP, Marino JP, Yu YB, Taraban MB, et al. Correlated analytical and functional evaluation of higher order structure perturbations from oxidation of NISTmAb. MAbs. 2023 Dec 31;15(1).
54. Gaza-Bulseco G, Faldu S, Hurkmans K, Chumsae C, Liu H. Effect of methionine oxidation of a recombinant monoclonal antibody on the binding affinity to protein A and protein G. J Chromatogr B Analyt Technol Biomed Life Sci. 2008 Jul 1;870(1):55–62.
55. Li X, Xu W, Wang Y, Zhao J, Liu YH, Richardson D, et al. High throughput peptide mapping method for analysis of site specific monoclonal antibody oxidation. J Chromatogr A. 2016 Aug;1460:51–60.
56. Sokolowska I, Mo J, Dong J, Lewis MJ, Hu P. Subunit mass analysis for monitoring antibody oxidation. MAbs. 2017 Apr 3;9(3):498–505.
57. Vena GA, Cassano N. Drug focus: adalimumab in the treatment of moderate to severe psoriasis. Biologics. 2007;(2):93–103.
58. Schreiber S, Yamamoto K, Muniz R, Iwura T. Physicochemical analysis and biological characterization of FKB327 as a biosimilar to adalimumab. Pharmacol Res Perspect. 2020 Jun;8(3):e00604.
59. Arora T, Padaki R, Liu L, Hamburger AE, Ellison AR, Stevens SR, et al. Differences in binding and effector functions between classes of TNF antagonists. Cytokine. 2009 Feb;45(2):124–31.
60. Ellis CR, Azmat CE. Adalimumab. 2023.
61. Billmeier U, Dieterich W, Neurath MF, Atreya R. Molecular mechanism of action of anti-tumor necrosis factor antibodies in inflammatory bowel diseases. World J Gastroenterol. 2016 Nov 11;22(42):9300.
62. Tracey D, Klareskog L, Sasso EH, Salfeld JG, Tak PP. Tumor necrosis factor antagonist mechanisms of action: A comprehensive review. Pharmacol Ther. 2008 Feb;117(2):244–79.

63. Scientific Considerations in Demonstrating Biosimilarity to a Reference Product | FDA [Internet]. [cited 2023 May 17]. Available from: https://www.fda.gov/regulatory-information/search-fda-guidance-documents/scientific-considerations-demonstrating-biosimilarity-reference-product
64. van Schie KA, Ooijevaar-de Heer P, Dijk L, Kruithof S, Wolbink G, Rispens T. Therapeutic TNF Inhibitors can Differentially Stabilize Trimeric TNF by Inhibiting Monomer Exchange. Sci Rep. 2016 Sep 8;6(1):32747.
65. Karlsson R, Fridh V, Frostell Å. Surrogate potency assays: Comparison of binding profiles complements dose response curves for unambiguous assessment of relative potencies. J Pharm Anal. 2018 Apr;8(2):138–46.
66. Yang H, Gurgel P V, Williams DK, Bobay BG, Cavanagh J, Muddiman DC, et al. Binding site on human immunoglobulin G for the affinity ligand HWRGWV. J Mol Recognit. 2010;23(3):271–82.
67. Ashoor DN, Ben Khalaf N, Bourguiba-Hachemi S, Marzouq MH, Fathallah MD. Engineering of the upper hinge region of human IgG1 Fc enhances the binding affinity to FcγIIIa (CD16a) receptor isoform. Protein Eng Des Sel. 2018 Jun 1;31(6):205–12.
68. Wines BD, Powell MS, Parren PWHI, Barnes N, Hogarth PM. The IgG Fc Contains Distinct Fc Receptor (FcR) Binding Sites: The Leukocyte Receptors FcγRI and FcγRIIa Bind to a Region in the Fc Distinct from That Recognized by Neonatal FcR and Protein A. The Journal of Immunology. 2000 May 15;164(10):5313–8.
69. Gergely J, Sarmay G. The two binding- site models of human IgG binding Fcγ receptors. The FASEB Journal. 1990 Dec;4(15):3275–83.
70. Arora T, Padaki R, Liu L, Hamburger AE, Ellison AR, Stevens SR, et al. Differences in binding and effector functions between classes of TNF antagonists. Cytokine. 2009 Feb;45(2):124–31.
71. Vaisocherová H, Faca VM, Taylor AD, Hanash S, Jiang S. Comparative study of SPR and ELISA methods based on analysis of CD166/ALCAM levels in cancer and control human sera. Biosens Bioelectron. 2009 Mar;24(7):2143–8.
72. Nechansky A. HAHA – nothing to laugh about. Measuring the immunogenicity (human anti-human antibody response) induced by humanized monoclonal antibodies applying ELISA and SPR technology. J Pharm Biomed Anal. 2010 Jan;51(1):252–4.
73. Rath PC, Aggarwal BB. TNF-induced signaling in apoptosis. J Clin Immunol. 1999 Nov;19(6):350–64.
74. Trost LC, Lemasters JJ. A Cytotoxicity Assay for Tumor Necrosis Factor Employing a Multiwell Fluorescence Scanner. Anal Biochem. 1994 Jul;220(1):149–53.
75. Van den Brande JMH, Braat H, van den Brink GR, Versteeg HH, Bauer CA, Hoedemaeker I, et al. Infliximab but not etanercept induces apoptosis in lamina propria T-lymphocytes from patients with Crohn's disease. Gastroenterology. 2003 Jun;124(7):1774–85.
76. Mitoma H, Horiuchi T, Tsukamoto H, Tamimoto Y, Kimoto Y, Uchino A, et al. Mechanisms for cytotoxic effects of anti–tumor necrosis factor agents on transmembrane tumor necrosis

factor α–expressing cells: Comparison among infliximab, etanercept, and adalimumab. Arthritis Rheum. 2008 May;58(5):1248–57.

77. Fossati G, Nesbitt AM. Effect of the Anti-TNF Agents, Adalimumab, Etanercept, Infli... : Official journal of the American College of Gastroenterology | ACG.

78. Schreiber S. Certolizumab pegol for the treatment of Crohn's disease. Therap Adv Gastroenterol. 2011 Nov;4(6):375–89.

79. Schreiber S, Rutgeerts P, Fedorak RN, Khaliq-Kareemi M, Kamm MA, Boivin M, et al. A randomized, placebo-controlled trial of certolizumab pegol (CDP870) for treatment of Crohn's disease. Gastroenterology. 2005 Sep;129(3):807–18.

80. Gabbani T, Deiana S, Annese V. CT-P13: design, development, and place in therapy. Drug Des Devel Ther. 2017;11:1653–61.

81. Tu CL, Wang YL, Hu TM, Hsu LF. Analysis of Pharmacokinetic and Pharmacodynamic Parameters in EU- Versus US-Licensed Reference Biological Products: Are In Vivo Bridging Studies Justified for Biosimilar Development? BioDrugs. 2019 Aug;33(4):437–46.

82. Gupta S, Jiskoot W, Schöneich C, Rathore AS. Oxidation and Deamidation of Monoclonal Antibody Products: Potential Impact on Stability, Biological Activity, and Efficacy. J Pharm Sci. 2022 Apr;111(4):903–18.

83. Bertolotti-Ciarlet A, Wang W, Lownes R, Pristatsky P, Fang Y, McKelvey T, et al. Impact of methionine oxidation on the binding of human IgG1 to FcRn and Fcγ receptors. Mol Immunol. 2009 May;46(8–9):1878–82.

84. Mo J, Yan Q, So CK, Soden T, Lewis MJ, Hu P. Understanding the Impact of Methionine Oxidation on the Biological Functions of IgG1 Antibodies Using Hydrogen/Deuterium Exchange Mass Spectrometry. Anal Chem. 2016 Oct 4;88(19):9495–502.

# 8 APPENDIX

**APPENDIX 1: Antigen and Antibody Binding Kinetic Data**

| Sample ID | ka (1/Ms) | kd (1/s) | KD (M) | Rmax (RU) | tc | Chi² (RU²) | U-value | Relative % KD | Mean Capture Level |
|---|---|---|---|---|---|---|---|---|---|
| **DRS-01** | 4,41E+05 | 6,94E-05 | 1,58E-10 | 28,63 | 9,04E+19 | 0,0683 | 1 | 100,0 | 65,5 |
| **RP03** | 4,51E+05 | 6,42E-05 | 1,43E-10 | 32,65 | 4,14E+21 | 0,0927 | 1 | 90,5 | 76,4 |
| **BS03** | 4,49E+05 | 6,62E-05 | 1,48E-10 | 31,91 | 6,07E+19 | 0,141 | 1 | 93,8 | 74,3 |
| **RP02** | 4,41E+05 | 6,28E-05 | 1,43E-10 | 30,8 | 4,52E+14 | 0,121 | 1 | 90,5 | 66,9 |
| **DRS-02** | 4,45E+05 | 6,82E-05 | 1,53E-10 | 28,8 | 3,30E+14 | 0,0745 | 1 | 97,2 | 65,0 |
| **DRS-01** | 5,35E+05 | 5,80E-05 | 1,08E-10 | 27,2 | 7,27E+21 | 0,0838 | 1 | 100,0 | 69,2 |
| **BS03** | 5,38E+05 | 5,60E-05 | 1,04E-10 | 27,82 | 4,58E+14 | 0,0799 | 1 | 96,0 | 71,5 |
| **RP03** | 5,29E+05 | 6,17E-05 | 1,17E-10 | 28,06 | 1,80E+16 | 0,113 | 1 | 107,6 | 67,8 |
| **DRS-02** | 5,29E+05 | 5,58E-05 | 1,06E-10 | 28,6 | 4,89E+14 | 0,0962 | 1 | 97,3 | 69,7 |
| **DRS-01** | 5,785E+05 | 6,190E-05 | 1,070E-10 | 25,58 | 2,61E+07 | 0,0443 | 1 | 100,0 | 72,0 |
| **RP02** | 5,536E+05 | 5,546E-05 | 1,002E-10 | 28,18 | 3,61E+07 | 0,0537 | 1 | 93,6 | 79,7 |
| **BS03** | 5,441E+05 | 5,814E-05 | 1,069E-10 | 24,63 | 6,14E+07 | 0,0351 | 1 | 99,9 | 67,3 |

**APPENDIX 1: Antigen and Antibody Binding Kinetic Data (continue)**

| Sample ID | ka (1/Ms) | kd (1/s) | KD (M) | Rmax (RU) | tc | Chi² (RU²) | U-value | Relative % KD | Mean Capture Level |
|---|---|---|---|---|---|---|---|---|---|
| **DRS-02** | 5,546E+05 | 5,887E-05 | 1,062E-10 | 25,67 | 3,78E+07 | 0,141 | 2 | 99,3 | 72,0 |
| **DRS-01** | 6,86E+05 | 1,04E-04 | 1,52E-10 | 15,49 | 3,42E+06 | 0,0745 | 2 | 100,0 | 77,5 |
| **RP01** | 7,69E+05 | 1,15E-04 | 1,50E-10 | 12,96 | 2,81E+06 | 0,0332 | 1 | 98,4 | 65,5 |
| **BS01** | 7,56E+05 | 1,27E-04 | 1,68E-10 | 15,36 | 2,96E+06 | 0,0977 | 2 | 110,5 | 81,7 |
| **BS02** | 1,06E+06 | 1,45E-04 | 1,37E-10 | 12,38 | 1,89E+06 | 0,0235 | 1 | 90,1 | 66,9 |
| **DRS-02** | 1,34E+06 | 1,63E-04 | 1,22E-10 | 13,42 | 1,63E+06 | 0,151 | 3 | 80,3 | 79,1 |
| **DRS-01** | 3,22E+05 | 6,15E-05 | 1,91E-10 | 34,8 | 4,74E+21 | 0,0889 | 1 | 100,0 | 100,8 |
| **RP03** | 3,41E+05 | 6,76E-05 | 1,99E-10 | 25,42 | 4,35E+14 | 0,0983 | 1 | 103,8 | 74,1 |
| **BS03** | 3,03E+05 | 5,24E-05 | 1,73E-10 | 28,72 | 3,61E+14 | 0,0661 | 1 | 90,3 | 70,1 |
| **DRS-02** | 3,32E+05 | 6,91E-05 | 2,08E-10 | 31,08 | 3,16E+14 | 0,062 | 1 | 108,6 | 103,9 |
| **DRS-01** | 3,104E+05 | 6,548E-05 | 2,109E-10 | 30,87 | 4,51E+17 | 0,0393 | 1 | 100,0 | 85,3 |
| **RP01** | 3,083E+05 | 7,162E-05 | 2,323E-10 | 29,26 | 2,22E+17 | 0,0414 | 1 | 94,8 | 86,8 |
| **BS01** | 3,095E+05 | 6,832E-05 | 2,207E-10 | 28,43 | 6,85E+15 | 0,111 | 1 | 92,1 | 86,1 |

**APPENDIX 1: Antigen and Antibody Binding Kinetic Data (continue)**

| Sample ID | ka (1/Ms) | kd (1/s) | KD (M) | Rmax (RU) | tc | Chi² (RU²) | U-value | Relative % KD | Mean Capture Level |
|---|---|---|---|---|---|---|---|---|---|
| **DRS-02** | 3,118E+05 | 6,535E-05 | 2,096E-10 | 32,06 | 1,49E+14 | 0,0415 | 1 | 103,9 | 76,7 |
| **DRS-01** | 3,48E+05 | 8,40E-05 | 2,42E-10 | 18,81 | 1,03E+08 | 0,0782 | 2 | 100,0 | 79,9 |
| **RP01** | 3,67E+05 | 9,02E-05 | 2,46E-10 | 18,27 | 1,49E+19 | 0,0206 | 1 | 101,6 | 76,5 |
| **BS02** | 3,86E+05 | 8,48E-05 | 2,20E-10 | 19,47 | 1,62E+19 | 0,0261 | 1 | 92,5 | 81,2 |
| **DRS-02** | 3,84E+05 | 8,30E-05 | 2,17E-10 | 20,1 | 5,32E+13 | 0,0224 | 1 | 82,8 | 83,4 |
| **DRS-01** | 2,87E+05 | 7,01E-05 | 2,44E-10 | 24,53 | 3,44E+18 | 0,0602 | 1 | 100,0 | 85,3 |
| **RP01** | 2,86E+05 | 7,35E-05 | 2,57E-10 | 23,38 | 8,30E+15 | 0,0619 | 1 | 105,2 | 86,8 |
| **BS01** | 2,86E+05 | 7,54E-05 | 2,64E-10 | 22,69 | 1,35E+14 | 0,055 | 1 | 108,1 | 86,1 |
| **DRS-02** | 2,85E+05 | 7,38E-05 | 2,59E-10 | 24,41 | 6,93E+16 | 0,0401 | 1 | 106,1 | 76,7 |
| **DRS-01** | 2,84E+05 | 8,32E-05 | 2,93E-10 | 19,52 | 7,48E+06 | 0,0638 | 1 | 100,0 | 51,6 |
| **BS01** | 2,82E+05 | 7,84E-05 | 2,78E-10 | 23,39 | 1,46E+15 | 0,0569 | 1 | 94,9 | 60,1 |
| **BS02** | 2,87E+05 | 7,56E-05 | 2,64E-10 | 25,18 | 4,74E+07 | 0,0402 | 1 | 90,0 | 67,7 |
| **DRS-02** | 2,73E+05 | 8,00E-05 | 2,93E-10 | 20,68 | 8,28E+07 | 0,0577 | 1 | 100,1 | 51,2 |

**APPENDIX 2: FcγRI and Antibody Binding Kinetic Data**

| Sample ID | ka (1/Ms) | kd (1/s) | KD (M) | Rmax (RU) | tc | Chi² (RU²) | U-value | Relative % KD | Mean Capture level |
|---|---|---|---|---|---|---|---|---|---|
| **DRS-01** | 2,39E+05 | 1,48E-03 | 6,19E-09 | 252,4 | 8,49E+17 | 6,91 | 1 | 100,0 | 189,13 |
| **RP01** | 2,82E+05 | 1,46E-03 | 5,18E-09 | 255 | 3,93E+18 | 3,31 | 1 | 83,7 | 253,55 |
| **RP03** | 3,00E+05 | 1,48E-03 | 4,93E-09 | 249 | 2,08E+21 | 3,41 | 1 | 79,6 | 245,02 |
| **RP02** | 3,23E+05 | 1,32E-03 | 4,10E-09 | 247,5 | 7,45E+17 | 4,03 | 1 | 66,2 | 244,33 |
| **RP04** | 3,27E+05 | 1,37E-03 | 4,19E-09 | 248,6 | 3,72E+16 | 5,09 | 1 | 67,8 | 244,78 |
| **BS02** | 2,61E+05 | 1,48E-03 | 5,66E-09 | 240,1 | 5,55E+17 | 3,09 | 1 | 91,5 | 249,35 |
| **BS03** | 3,11E+05 | 1,44E-03 | 4,62E-09 | 256,7 | 2,92E+18 | 3,87 | 1 | 74,7 | 247,00 |
| **BS01** | 2,81E+05 | 1,46E-03 | 5,18E-09 | 253,1 | 5,56E+18 | 3,4 | 1 | 83,7 | 250,78 |
| **DRS-02** | 2,36E+05 | 1,51E-03 | 6,41E-09 | 243,2 | 9,81E+18 | 7,95 | 1 | 103,6 | 246,19 |
| **DRS-03** | 2,50E+05 | 1,35E-03 | 5,41E-09 | 225,8 | 2,36E+08 | 7,5 | 1 | 87,5 | 243,39 |
| **DRS-01** | 2,72E+05 | 8,55E-04 | 3,14E-09 | 41,51 | 7,19E+19 | 0,124 | 1 | 100,0 | 69,925 |
| **RP01** | 2,74E+05 | 9,00E-04 | 3,29E-09 | 43,83 | 9,22E+15 | 1,2 | 1 | 104,6 | 74,525 |
| **RP03** | 3,14E+05 | 8,92E-04 | 2,84E-09 | 30,3 | 6,14E+20 | 0,371 | 1 | 90,3 | 67,925 |
| **RP02** | 3,01E+05 | 8,95E-04 | 2,97E-09 | 29,97 | 5,49E+15 | 0,132 | 1 | 94,6 | 67,05 |
| **RP04** | 2,81E+05 | 8,90E-04 | 3,17E-09 | 28,63 | 3,36E+15 | 0,25 | 1 | 101,0 | 67,275 |

**APPENDIX 2: FcγRI and Antibody Binding Kinetic Data (continue)**

| Sample ID | ka (1/Ms) | kd (1/s) | KD (M) | Rmax (RU) | tc | Chi² (RU²) | U-value | Relative % KD | Mean Capture level |
|---|---|---|---|---|---|---|---|---|---|
| **BS02** | 2,83E+05 | 8,52E-04 | 3,01E-09 | 35,47 | 8,54E+15 | 0,432 | 1 | 95,9 | 70,15 |
| **BS01** | 2,88E+05 | 8,66E-04 | 3,01E-09 | 40,77 | 3,76E+19 | 0,785 | 1 | 95,9 | 72,65 |
| **DRS-02** | 3,06E+05 | 8,45E-04 | 2,76E-09 | 30,98 | 1,89E+20 | 0,149 | 1 | 87,9 | 67,15 |
| **DRS-03** | 3,08E+05 | 8,77E-04 | 2,84E-09 | 28,51 | 3,82E+15 | 0,331 | 1 | 90,5 | 65,875 |
| **DRS-01** | 2,87E+05 | 1,19E-03 | 4,14E-09 | 55,12 | 7,50E+15 | 0,321 | 1 | 100 | 80,55 |
| **RP01** | 2,89E+05 | 1,17E-03 | 4,03E-09 | 48,59 | 3,40E+15 | 0,887 | 1 | 97,5 | 78,25 |
| **RP03** | 3,07E+05 | 1,01E-03 | 3,30E-09 | 44,22 | 3,83E+16 | 0,527 | 1 | 79,7 | 71,025 |
| **RP02** | 2,70E+05 | 0,001271 | 4,71E-09 | 68,88 | 2,24E+20 | 0,362 | 1 | 113,9 | 57,15 |
| **RP04** | 2,95E+05 | 1,11E-03 | 3,77E-09 | 41,8 | 2,37E+15 | 0,298 | 1 | 91,2 | 69,95 |
| **BS02** | 3,23E+05 | 1,08E-03 | 3,34E-09 | 50,07 | 5,71E+19 | 0,753 | 1 | 80,8 | 74 |
| **BS03** | 3,02E+05 | 1,07E-03 | 3,52E-09 | 45,46 | 3,84E+15 | 0,485 | 1 | 85,2 | 73,025 |
| **BS01** | 2,82E+05 | 1,02E-03 | 3,60E-09 | 47,18 | 5,50E+15 | 1,11 | 1 | 87,0 | 75,475 |
| **DRS-02** | 2,97E+05 | 1,06E-03 | 3,57E-09 | 44,29 | 7,24E+15 | 0,495 | 1 | 86,3 | 72,225 |
| **DRS-03** | 2,97E+05 | 8,01E-04 | 2,70E-09 | 70,06 | 1,75E+16 | 0,981 | 1 | 65,2 | 44,65 |

**APPENDIX 3: FcγRIII and Antibody Binding Kinetic Data**

| Sample ID | ka1 (1/Ms) | kd1 (1/s) | ka2 (1/Ms) | kd2 (1/s) | KD (M) | Rmax (RU) | Chi² ($RU^2$) | Relative KD (%) | Mean Capture Level |
|---|---|---|---|---|---|---|---|---|---|
| **RP01** | 7.21E+04 | 2.51E-02 | 2.22E-03 | 8.46E-03 | 2.76E-07 | 30.87 | 0.274 | 122.3 | 30.65 |
| **RP03** | 7.15E+04 | 2.16E-02 | 8.60E-04 | 4.10E-03 | 2.49E-07 | 26.16 | 0.241 | 110.5 | 27.85 |
| **RP02** | 1.68E+05 | 1.29E-01 | 3.68E-02 | 2.08E-02 | 2.78E-07 | 31.2 | 0.17 | 123.3 | 27.3 |
| **RP04** | 6.30E+04 | 2.17E-02 | 8.39E-04 | 3.16E-03 | 2.72E-07 | 27.48 | 0.201 | 120.5 | 55.5 |
| **BS02** | 1.95E+05 | 1.94E-01 | 2.57E-02 | 1.08E-02 | 2.94E-07 | 32.12 | 0.185 | 130.2 | 29.1 |
| **BS01** | 1.65E+05 | 1.44E-01 | 2.18E-02 | 1.00E-02 | 2.75E-07 | 32.46 | 0.269 | 121.9 | 29.65 |
| **T01-DRS-1** | 1.09E+05 | 6.75E-02 | 1.91E-02 | 1.09E-02 | 2.26E-07 | 31.84 | 0.277 | 100.0 | 29.55 |
| **T01-DRS-2** | 1.74E+05 | 1.32E-01 | 2.62E-02 | 1.11E-02 | 2.26E-07 | 31.32 | 0.235 | 100.2 | 28.1 |
| **T01-DRS-3** | 1.51E+05 | 1.05E-01 | 2.35E-02 | 1.11E-02 | 2.23E-07 | 28.63 | 0.228 | 98.8 | 26.9 |
| **RP01** | 1.44E+05 | 1.27E-01 | 4.01E-02 | 2.23E-02 | 3.16E-07 | 16.73 | 0.122 | 124.8 | 15.55 |
| **RP03** | 1.92E+05 | 1.90E-01 | 5.28E-02 | 2.20E-02 | 2.92E-07 | 15.88 | 0.0748 | 115.1 | 15 |
| **RP02** | 1.68E+05 | 1.45E-01 | 5.02E-02 | 2.42E-02 | 2.81E-07 | 15.84 | 0.0869 | 110.8 | 14.8 |
| **RP04** | 1.69E+05 | 1.75E-01 | 5.63E-02 | 2.44E-02 | 3.12E-07 | 16.11 | 0.0652 | 123.4 | 15 |
| **BS02** | 9.37E+04 | 6.87E-02 | 2.17E-02 | 1.26E-02 | 2.70E-07 | 14.14 | 0.0814 | 106.4 | 15.2 |

**APPENDIX 3: FcγRIII and Antibody Binding Kinetic Data (continue)**

| Sample ID | ka1 (1/Ms) | kd1 (1/s) | ka2 (1/Ms) | kd2 (1/s) | KD (M) | Rmax (RU) | Chi² (RU²) | Relative KD (%) | Mean Capture Level |
|---|---|---|---|---|---|---|---|---|---|
| **BS01** | 2.04E+05 | 2.35E-01 | 3.01E-02 | 1.21E-02 | 3.29E-07 | 16.39 | 0.0522 | 129.9 | 15.35 |
| **T01-DRS-1** | 4.83E+04 | 1.22E-02 | 9.30E-06 | 2.22E-02 | 2.53E-07 | 13.09 | 0.179 | 100.0 | 15.2 |
| **T01-DRS-2** | 1.50E+05 | 1.30E-01 | 3.13E-02 | 1.27E-02 | 2.51E-07 | 15.48 | 0.0991 | 99.1 | 15.05 |
| **T01-DRS-3** | 5.15E+04 | 1.40E-02 | 8.59E-04 | 9.15E-06 | 2.87E-09 | 12.81 | 0.131 | 1.1 | 14.65 |
| **RP01** | 2.43E+05 | 2.70E-01 | 4.59E-02 | 2.00E-02 | 3.37E-07 | 20.59 | 0.16 | 123.31 | 19 |
| **RP03** | 2.70E+05 | 2.82E-01 | 4.65E-02 | 1.98E-02 | 3.12E-07 | 19.91 | 0.135 | 114.14 | 18.55 |
| **RP04** | 2.79E+05 | 2.93E-01 | 5.53E-02 | 2.16E-02 | 2.95E-07 | 19.47 | 0.0943 | 108.13 | 18.35 |
| **BS01** | 3.39E+05 | 3.87E-01 | 2.72E-02 | 1.20E-02 | 3.51E-07 | 20.86 | 0.0644 | 128.47 | 18.8 |
| **T01-DRS-1** | 2.82E+05 | 2.80E-01 | 3.28E-02 | 1.24E-02 | 2.73E-07 | 20.18 | 0.0881 | 100 | 18.8 |
| **T01-DRS-2** | 2.91E+05 | 2.75E-01 | 3.30E-02 | 1.22E-02 | 2.55E-07 | 19.71 | 0.0803 | 93.44 | 18.6 |
| **T01-DRS-3** | 2.86E+05 | 2.80E-01 | 3.51E-02 | 1.26E-02 | 2.59E-07 | 18.96 | 0.0875 | 94.87 | 18.3 |

**APPENDIX 4: FcRn and Antibody Binding Affinity Data**

| Sample ID | KD (M) | SE(KD) | Rmax (RU) | SE(Rmax) | offset (RU) | SE(offset) | Mean Capture level |
|---|---|---|---|---|---|---|---|
| **DRS-01** | 9.21E-08 | 5.70E-09 | 202.9 | 3.3 | 42.6 | 3.7 | 100 |
| **RP01** | 1.28E-07 | 5.80E-09 | 205.1 | 2.1 | 51.1 | 2.4 | 138.8 |
| **RP03** | 1.48E-07 | 8.80E-09 | 199.9 | 2.6 | 47.5 | 2.9 | 160.2 |
| **RP02** | 1.31E-07 | 5.20E-09 | 194 | 1.8 | 42.9 | 2 | 142.5 |
| **BS02** | 1.45E-07 | 8.90E-09 | 203.9 | 2.8 | 49.1 | 3 | 157.7 |
| **BS03** | 1.29E-07 | 6.70E-09 | 203.1 | 2.4 | 49.4 | 2.7 | 139.5 |
| **BS01** | 1.27E-07 | 7.30E-09 | 207 | 2.8 | 52.4 | 3.1 | 137.3 |
| **DRS-02** | 8.87E-08 | 7.20E-09 | 194.6 | 4.2 | 36.8 | 4.8 | 96.3 |
| **DRS-03** | 9.03E-08 | 7.50E-09 | 190.2 | 4.2 | 35.5 | 4.7 | 98 |

**APPENDIX 4: FcRn and Antibody Binding Affinity Data (continue)**

| Sample ID | KD (M) | SE(KD) | Rmax (RU) | SE(Rmax) | offset (RU) | SE(offset) | Mean Capture level |
|---|---|---|---|---|---|---|---|
| **DRS-01** | 8.37E-08 | 6.60E-09 | 204 | 4.4 | 45.7 | 5 | 100 |
| **RP01** | 1.18E-07 | 5.70E-09 | 206.5 | 2.4 | 57.2 | 2.7 | 141.4 |
| **RP03** | 1.67E-07 | 1.00E-08 | 201.1 | 2.7 | 49.7 | 2.9 | 199.2 |
| **RP02** | 1.39E-07 | 5.60E-09 | 196.8 | 1.8 | 42.1 | 2 | 166.1 |
| **BS02** | 1.48E-07 | 1.00E-08 | 207.8 | 3.2 | 54.1 | 3.5 | 176.6 |
| **BS03** | 1.30E-07 | 6.60E-09 | 207.7 | 2.4 | 50.2 | 2.7 | 155 |
| **BS01** | 1.40E-07 | 9.60E-09 | 215.8 | 3.3 | 55 | 3.6 | 167.4 |
| **DRS-02** | 8.20E-08 | 7.30E-09 | 191.5 | 4.7 | 38.6 | 5.3 | 97.9 |
| **DRS-03** | 8.18E-08 | 7.20E-09 | 186.3 | 4.5 | 36.3 | 5.1 | 97.6 |

# 9 CURRICULUM VITAE